



**HAL**  
open science

## **Storm-induced marine flooding: Lessons from a multidisciplinary approach**

Eric Chaumillon, Xavier Bertin, André B. Fortunato, Marco Bajo, Jean-Luc Schneider, Laurent Dezileau, John Patrick Walsh, Agnès Michelot, Etienne Chauveau, Axel Créach, et al.

### ► To cite this version:

Eric Chaumillon, Xavier Bertin, André B. Fortunato, Marco Bajo, Jean-Luc Schneider, et al.. Storm-induced marine flooding: Lessons from a multidisciplinary approach. *Earth-Science Reviews*, 2017, 165, pp.151 - 184. 10.1016/j.earscirev.2016.12.005 . hal-01671832

**HAL Id: hal-01671832**

**<https://univ-rochelle.hal.science/hal-01671832v1>**

Submitted on 26 Mar 2021

**HAL** is a multi-disciplinary open access archive for the deposit and dissemination of scientific research documents, whether they are published or not. The documents may come from teaching and research institutions in France or abroad, or from public or private research centers.

L'archive ouverte pluridisciplinaire **HAL**, est destinée au dépôt et à la diffusion de documents scientifiques de niveau recherche, publiés ou non, émanant des établissements d'enseignement et de recherche français ou étrangers, des laboratoires publics ou privés.

## Accepted Manuscript

Storm-induced marine flooding: lessons from a multidisciplinary approach

Eric Chaumillon, Xavier Bertin, André Fortunato, Marco Bajo, Jean-Luc Schneider, Laurent Dezileau, John Patrick Walsh, Agnès Michelot, Etienne Chauveau, Axel Créach, Alain Hénaff, Thierry Sauzeau, Benoit Waeles, Bruno Gervais, Gwenaële Jan, Juliette Baumann, Jean-François Breilh, Rodrigo Pedreros

PII: S0012-8252(16)30459-7  
DOI: doi:[10.1016/j.earscirev.2016.12.005](https://doi.org/10.1016/j.earscirev.2016.12.005)  
Reference: EARTH 2355

To appear in: *Earth Science Reviews*

Received date: 26 May 2016  
Revised date: 30 November 2016  
Accepted date: 6 December 2016



Please cite this article as: Chaumillon, Eric, Bertin, Xavier, Fortunato, André, Bajo, Marco, Schneider, Jean-Luc, Dezileau, Laurent, Walsh, John Patrick, Michelot, Agnès, Chauveau, Etienne, Créach, Axel, Hénaff, Alain, Sauzeau, Thierry, Waeles, Benoit, Gervais, Bruno, Jan, Gwenaële, Baumann, Juliette, Breilh, Jean-François, Pedreros, Rodrigo, Storm-induced marine flooding: lessons from a multidisciplinary approach, *Earth Science Reviews* (2016), doi:[10.1016/j.earscirev.2016.12.005](https://doi.org/10.1016/j.earscirev.2016.12.005)

This is a PDF file of an unedited manuscript that has been accepted for publication. As a service to our customers we are providing this early version of the manuscript. The manuscript will undergo copyediting, typesetting, and review of the resulting proof before it is published in its final form. Please note that during the production process errors may be discovered which could affect the content, and all legal disclaimers that apply to the journal pertain.

## Storm-induced marine flooding: lessons from a multidisciplinary approach

Eric Chaumillon<sup>1</sup>, Xavier Bertin<sup>1</sup>, André Fortunato<sup>2</sup>, Marco Bajo<sup>3</sup>, Jean-Luc Schneider<sup>4</sup>, Laurent Dezileau<sup>5</sup>, John Patrick Walsh<sup>6</sup>, Agnès Michelot<sup>7</sup>, Etienne Chauveau<sup>8</sup>, Axel Créach<sup>8</sup>, Alain Hénaff<sup>9</sup>, Thierry Sauzeau<sup>10</sup>, Benoit Waeles<sup>11</sup>, Bruno Gervais<sup>12</sup>, Gwenaële Jan<sup>13</sup>, Juliette Baumann<sup>1</sup>, Jean-François Breilh<sup>14</sup>, Rodrigo Pedreros<sup>15</sup>.

<sup>1</sup>UMR 7266 LIENSs, CNRS-Université de La Rochelle, La Rochelle, France

<sup>2</sup>Laboratório Nacional de Engenharia Civil, Lisboa, Portugal

<sup>3</sup>ISMAR-CNR, Venice, Italy

<sup>4</sup>UMR 5805 EPOC, CNRS-Université de Bordeaux, Pessac, France

<sup>5</sup>UMR 5243 Géosciences Montpellier, CNRS-Université de Montpellier, France

<sup>6</sup>Department of Geological Sciences, East Carolina University of East Carolina, Greenville, USA

<sup>7</sup>CEJEP EA 3170, Université de La Rochelle, La Rochelle, France

<sup>8</sup>UMR 6554 LETG/Géolittomer-Nantes, CNRS-Université de Nantes, Nantes, France

<sup>9</sup>UMR 6554 LETG, Université de Bretagne Occidentale, Brest, France

<sup>10</sup>CRIHAM, EA 4270, Université de Poitiers, Poitiers

<sup>11</sup>Consultant in Coastal Engineering, Brest, France

<sup>12</sup>SDIS Charente Maritime, La Rochelle, France

<sup>13</sup>SHOM, Brest, France

<sup>14</sup>UNIMA, rue Jacques de Vaucanson, 17180, Périgny, France

<sup>15</sup>BRGM-DRP, Orléans, France

**PLAN****1- Introduction****2- State of the knowledge of marine submersions from a disciplinary viewpoint****2.1- Physical processes governing storm surges and marine flooding**

2.1.1- Storm surges

2.1.2- Storm-induced marine flooding

2.1.2.1- Overflowing over dikes and sedimentary barriers

2.1.2.2- Wave overtopping

2.1.2.3- Sedimentary barrier breaching

**2.2- Past marine floods**

2.2.1- Past marine floods in historical archives

2.2.1.1- Worldwide examples of long-term historical documentary records

2.2.1.2- Past storm surge events in France

2.2.1.2.1- Brittany

2.2.1.2.2- Charente-Maritime

2.2.1.2.3- Languedoc

2.2.2- Past marine flooding from sediment records

2.2.2.1- Washover fans

2.2.2.2- Backbarrier sedimentation (marshes, coastal lakes)

2.2.2.3- Beach ridges

2.2.2.4- Offshore submarine deposits related to storm and storm surge flooding

2.2.2.5- Strengths and limits of sedimentary records

2.2.2.5.1- Preservation potential of the paleostorm records

2.2.2.5.2- Dating of the paleostorm records

2.2.2.5.3- Storm paleointensities

**2.3- Vulnerability studies from old and recent and well-documented marine submersions****3- Relevance of multidisciplinary approaches in coastal flooding knowledge**

3.1- Variability and intensities of marine floods and potential climate connections revealed by combination of historical and sedimentological archives

3.2- Physical approaches improve the interpretation of historical and sedimentological archives

3.3- Combining historical data and numerical hindcast to determine extreme water level return periods

**4- From new knowledge to adaptation**

4.1- Marine Submersions forecast

4.2- From the knowledge of flooding risk to the development decision support tool (The central French Atlantic coast example)

4.3- Managing realignment of coastal defenses

4.4- Sea flooding in the context of climate change: which legal perspectives for adaptation?

**5- Conclusions**

**Abstract:** There is a growing interest for marine flooding related to recent catastrophic events and their unintended consequences in terms of casualties and damages, and to the increasing population and issues along the coasts in a context of changing climate. Consequently, the knowledge on marine flooding has progressed significantly for the last years and this review, focused on storm-induced marine submersions, responds to the need for a synthesis. Three main components are presented in the review: (1) a state-of-the-art on marine submersions from the viewpoint of several scientific disciplines; (2) a selection of examples demonstrating the added value of interdisciplinary approaches to improve our knowledge of marine submersions; (3) a selection of examples showing how the management of future crises or the planning efforts to adapt to marine submersions can be supported by new results or techniques from the research community.

From a disciplinary perspective, recent progress were achieved with respect to physical processes, numerical modeling, the knowledge of past marine floods and vulnerability assessment. At a global scale, the most vulnerable coastal areas to marine flooding with high population density are deltas and estuaries. Recent and well-documented floods allow analyzing the vulnerability parameters of different coastal zones. While storm surges can nowadays be reproduced accurately, the modeling of coastal flooding is more challenging, particularly when barrier breaches and wave overtopping have to be accounted for. The chronology of past marine floods can be reconstructed combining historical archives and sediment records. Sediment records of past marine floods localized in back barrier depressions are more adequate to reconstruct past flooding chronology. For the two last centuries, quantitative and descriptive historical data can be used to characterize past marine floods. Beyond providing a chronology of events, sediment records combined with geochronology, statistic analysis and climatology, can be used to reconstruct millennial-scale climate variability and enable a better understanding of the possible regional and local long-term trends in storm activity. Sediment records can also reveal forgotten flooding of exceptional intensity, much more intense than those of the last few decades. Sedimentological and historical archives, combined with high-resolution topographic data or numerical hindcast of storms can provide quantitative information and explanations for marine flooding processes. From these approaches, extreme past sea levels height can be determined and are very useful to complete time series provided by the instrumental measurements on shorter time scales. In particular, historical data can improve the determination of the return periods associated with extreme water levels, which are often inaccurate when computed based on instrumental data, due to the presence of gaps and too short time-series. Long-term numerical hindcast of tides and surges can also be used to provide the required time series for statistical analysis. Worst-case scenarios, used to define coastal management plans and strategies, can be obtained from realistic atmospheric settings with different tidal ranges and by shifting the trajectory of storms.

Management of future crises and planning efforts to adapt to marine submersions are optimized by predictions of water levels from hydrodynamic models. Such predictions combined with in situ measurements and analysis of human stakes can be used to define a vulnerability index. Then, the efficiency of adaptation measures can be evaluated with respect to the number of lives that could be potentially saved. Numerical experiments also showed that the realignment of coastal defenses could result in water level reduction up to 1 m in the case where large marshes are flooded. Such managed realignment of coastal defenses may constitute a promising adaptation to storm-induced flooding and future sea level rise. From a legal perspective, only a few texts pay specific attention to the risk of marine flooding whether nationally or globally. Recent catastrophic events and their unintended consequences in terms of death and damages have triggered political decisions, like in USA after hurricane Katrina, and in France after catastrophic floods that occurred in 2010.

**Keywords:** Marine flooding; Storm Surge; Climate change; Past marine floods; Historical archives; storm flood deposits; Risk; vulnerability; Numerical model; Overflowing; Overtopping; Barrier breaching; Submersions forecast; Coastal realignment; Public policies

## 1- Introduction

Marine floods, or submersions, are related to water-level rises often induced by a storm. In unfortunate cases, these may be major natural disasters, sometimes affecting densely populated coastal regions of the world such as the Bay of Bengal. Taking into account the expected sea-level rise at the end of century (IPCC, 2014), together with regionally increased storm activity (Gönnert et al., 2001; von Storch and Reichardt, 1997; Vousdoukas et al., 2016) and the expected population increase in coastal zones in the next decades (Lutz and Samir, 2010), marine-submersion frequency and associated damages are expected to increase. Anticipating and managing future marine submersions is thus a priority. To improve our preparedness, a holistic approach is needed because the causes and consequences of these disasters involve both complex natural processes and societal factors, and it is a concern that the research is fragmented as many disciplines are involved.

Significant flooding of coastal areas results mainly from storm surges and tsunamis, although large or “king” tides can also produce problems for many communities (e.g., Theuerkauf et al., 2014). This article focuses on storm-related marine submersions, and some key points about storm tides and surges are summarized below. Storm surges correspond to short-term non-astronomic variations in the ocean free surface driven by meteo-oceanic forcing, and are usually related to tropical and extratropical cyclones (Pugh, 1987). Coasts threatened by tropical cyclones are located mainly in North America, south and southeast Asia, and Oceania. Coasts threatened by extratropical cyclones are primarily in North America, South America and northern and southern Europe. Several studies also make reference to “storm tides”, which in this case corresponds the combined water level from the astronomical tide and a storm surge.

Extreme storm surge heights can reach several meters at the coastline. For example, storm surges close to or larger than 9 m were reported in the Gulf of Mexico during hurricane Katrina in 2005 (Blake, 2007; Dietrich et al., 2010) and in the Bay of Bengal in 1970 during cyclone Bhola (Das, 1972; Karim and Mimura, 2008). Both of these locations are known to have a great potential for major storm surges and coastal flooding; this is related to the surrounding shelf bathymetry and the regional propensity for strong cyclones. Other recent examples include Hurricane Sandy, which made landfall in the New York area in 2012 with surges reaching 4 m (Valle-Levinson et al., 2013) and typhoon Haiyan in the Philippines (2013), which produced storm surges of 3-6 m (Shimozono et al., 2015). These events and many others illustrate that large storm surges and subsequent damages can occur in many regions of the world. In Europe, the most dramatic catastrophe in the modern history

occurred in the southern part of the North Sea in January 1953, during an historical storm tide. More specifically, a strong extra-tropical storm produced a surge locally larger than 3 m in phase with spring tides (Wolf and Flather, 2005), and this combination caused extensive flooding of low-lying coastal zones of the Netherlands, Belgium and United Kingdom.

The main objective of this paper is to synthesize knowledge about storm-induced marine submersions using contributions from a broad representation of researchers from different disciplines (e.g., physical oceanographers, geomorphologists, geographers, historians, sedimentologists, lawyers). First, we present a state-of-the-art on marine submersions from the viewpoint of several scientific disciplines. In the following section, we argue, based on selected examples, how an interdisciplinary approach allows for a better understanding of the problem. Finally, we show how new insights or techniques, whether of disciplinary or multi-disciplinary origin, are useful for the management of future crises. This work is especially important in planning efforts by policymakers, coastal managers, civil protection managers and the general public to adapt to sea-level rise and marine submersions.

## **2- State of the knowledge of marine submersions from a disciplinary viewpoint**

In this section we will successively present a synthesis about physical processes leading to marine floods, past marine floods and vulnerability of coasts to marine flooding.

### **2.1- Physical processes governing storm surges and marine flooding**

#### **2.1.1- Storm surges**

In the absence of density gradients, due to temperature and salinity variations, and/or stratification, the coastal circulation is well described by the depth-averaged shallow water equations (also called Saint-Venant equations). These equations are obtained by the general Navier-Stokes equations by using the Boussinesq approximation for the water density, the hydrostatic approximation and the Reynolds formulation for the turbulent viscosity (Gill, 1982). This simplification is only more questionable for estuaries where the water column is not well mixed, in deeper water depths where the fast moving upper layer of the ocean is not represented by depth-integrated velocities, or in surf zones where the flow is sheared due to the development of a bed return current. The governing equations, which represent the horizontal momentum conservation and the mass conservation (i.e., the continuity equation), read:

$$\begin{aligned}
& \frac{\partial \zeta}{\partial t} + \frac{\partial}{\partial x} \left( \frac{1}{\rho_w} \frac{\partial \tau_{bx}}{\partial x} + \frac{1}{\rho_w} \frac{\partial \tau_{sx}}{\partial y} \right) + \frac{\partial}{\partial y} \left( \frac{1}{\rho_w} \frac{\partial \tau_{by}}{\partial y} + \frac{1}{\rho_w} \frac{\partial \tau_{sy}}{\partial x} \right) + \frac{\partial}{\partial x} \left( \frac{1}{\rho_w} \frac{\partial \tau_{bx}}{\partial x} + \frac{1}{\rho_w} \frac{\partial \tau_{sx}}{\partial y} \right) + \frac{\partial}{\partial y} \left( \frac{1}{\rho_w} \frac{\partial \tau_{by}}{\partial y} + \frac{1}{\rho_w} \frac{\partial \tau_{sy}}{\partial x} \right) \\
& + \frac{\partial}{\partial x} \left( \frac{1}{\rho_w} \frac{\partial \tau_{bx}}{\partial x} + \frac{1}{\rho_w} \frac{\partial \tau_{sx}}{\partial y} \right) + \frac{\partial}{\partial y} \left( \frac{1}{\rho_w} \frac{\partial \tau_{by}}{\partial y} + \frac{1}{\rho_w} \frac{\partial \tau_{sy}}{\partial x} \right) + \frac{\partial}{\partial x} \left( \frac{1}{\rho_w} \frac{\partial \tau_{bx}}{\partial x} + \frac{1}{\rho_w} \frac{\partial \tau_{sx}}{\partial y} \right) + \frac{\partial}{\partial y} \left( \frac{1}{\rho_w} \frac{\partial \tau_{by}}{\partial y} + \frac{1}{\rho_w} \frac{\partial \tau_{sy}}{\partial x} \right) \\
& + \frac{\partial}{\partial x} \left( \frac{1}{\rho_w} \frac{\partial \tau_{bx}}{\partial x} + \frac{1}{\rho_w} \frac{\partial \tau_{sx}}{\partial y} \right) + \frac{\partial}{\partial y} \left( \frac{1}{\rho_w} \frac{\partial \tau_{by}}{\partial y} + \frac{1}{\rho_w} \frac{\partial \tau_{sy}}{\partial x} \right) + \frac{\partial}{\partial x} \left( \frac{1}{\rho_w} \frac{\partial \tau_{bx}}{\partial x} + \frac{1}{\rho_w} \frac{\partial \tau_{sx}}{\partial y} \right) + \frac{\partial}{\partial y} \left( \frac{1}{\rho_w} \frac{\partial \tau_{by}}{\partial y} + \frac{1}{\rho_w} \frac{\partial \tau_{sy}}{\partial x} \right)
\end{aligned}$$

(1-3)

Where  $t$  is the time,  $x$  and  $y$  are the zonal and meridional coordinates,  $\zeta$  is the free surface elevation,  $u$  and  $v$  are the zonal and meridional components of the depth-averaged velocity,  $H$  is the water level, sum of the undisturbed water level and the surface perturbation  $\zeta$ . The sea water density is  $\rho_w$ ,  $g$  is the gravity acceleration,  $f$  is the Coriolis parameter,  $P_a$  is the surface atmospheric pressure, and  $\tau_{bx}$  and  $\tau_{sx}$  are the bottom and surface stresses in the  $x$  direction and similar ones in  $y$ .  $A_H$  is the horizontal turbulent viscosity coefficient. Finally,  $S_{xx}$ ,  $S_{xy}$  and  $S_{yy}$  are the components of the wave radiation stress tensor, which correspond to the momentum flux associated with the short gravity waves.

Three physical processes lead to the formation of storm surges. First, the *Inverse Barometer Effect* (IBE) is due to atmospheric pressure gradients (Doodson, 1924). In steady conditions, the associated rule of thumb states that a decrease/increase of 1 hPa with respect to the mean sea level atmospheric pressure (1013 hPa) causes a 1 cm increase/decrease of the sea level. For extreme tropical hurricanes, where the minimum sea-level pressure can reach 900 mbar or less, the contribution of this effect in the storm surge can thus exceed 1.0 m. However, steady conditions are never perfectly reached, especially when the low pressure associated to the storm is moving fast. Indeed, the IBE implies the development of barotropic currents, which are restrained by bottom friction. Therefore the deviation from the rule of thumb can be consistent. The IBE contribution to the total storm surge is often dominant in deep water, offshore or near coastlines where the shelf is restricted or absent.

Second, the wind stress is a major contribution to the storm surges. The wind stress depends on the wind speed but also on the sea surface roughness. For moderate winds, measurements suggest that the sea surface roughness increases linearly with the wind speed but under extreme wind conditions ( $> 35$ - $40$  m/s), the sea surface roughness can reach a maximum or even decrease due to wave-induced streaks of foam and sprays (Powell et al., 2003; Takagaki et al., 2012). For a given wind speed, the sea roughness also depends on the conditions of the sea and, in particular, on the wave age (Charnock, 1955;



Stewart, 1974; Mastenbroek et al., 1993; Moon, 2005; Brown and Wolf, 2009; Bertin et al., 2012; Olabarrieta et al., 2012). The Xynthia storm, which hit the south west coast of France (central part of the Bay of Biscay), is a good example of the importance of the wave age on the storm surge generation (Bertin et al., 2012; Bertin et al., 2015). The storm surge associated with Xynthia reached 1.6 m in La Rochelle Harbor (Fig. 1), and was the largest value ever recorded since the installation of a permanent tide gauge (1997). However, the average wind during this storm was not very strong (25 to 30 m/s) and this exceptional storm surge was explained by the presence of steep and young wind-waves that increased the sea roughness and thereby the surface stress (Bertin et al., 2012, 2015).

It is well known that due to the Earth's rotation and the subsequent Coriolis effect, the wind-driven flow is deviated to the right in the Northern Hemisphere (left in the Southern Hemisphere). Under steady conditions, this deviation is theoretically  $45^\circ$  at the surface and the net water transport is oriented at  $90^\circ$  of the wind direction in deep water. In shallow water, this deviation decreases due to the increase in bottom stress (Rego and Li, 2010). When a storm approaches the coast, the alongshore component of the wind stress drives an "Ekman setup" (Kennedy et al., 2011) at the coast located to the right-hand side of the wind (to left-hand side in the Southern Hemisphere). An important consequence is that the coastal region located to the right-hand side of the storm track (resp. to the left in the Southern Hemisphere) usually suffers larger storm surge and damages than the coastal region located on the left side (resp. to the right, Kennedy et al., 2011).

Finally, short gravity waves can also contribute to storm surges close to the shoreline. In shallow waters, wave dissipation causes gradients of radiation stress (Longuet Higgins and Stewart, 1964), which result in the development of a *wave setup* along the coast. Under storm waves, this setup can easily reach tens of centimeters and contribute to the storm surge significantly (Roland et al., 2009). This contribution can even be dominant in coastal zones bordered by narrow continental shelves, such as volcanic islands, where the wind contribution is limited (e.g. Kennedy et al., 2012). Recent studies also have shown that wave setup can even propagate outside the surf zones and contribute to the storm surge in areas sheltered from wave breaking such as coastal lagoons (e.g. Bertin et al., 2009; Dodet et al. 2013), estuaries (Bertin et al., 2015) and tropical lagoons bordered by coral reefs (Aucan et al., 2012; Kennedy et al., 2012). However, it should be noted that wave setup is not predicted correctly with 2DH models for storm waves, mostly due the vertical circulation that takes place in the surf zones (e.g. Apotsos et al., 2007). In addition to this phase-averaged mechanism, short waves also induce other phenomena such as the wave run-up and the overtopping/overwash, which can yield significant flooding even in areas protected by barriers (dune or dike) and crests (Le Roy et al., 2015). Finally, infra-gravity waves, which

correspond to long waves associated to the presence of groups in incident short waves, can also contribute to flooding during storms. For example, Roeber and Bricker (2015) showed that this process was dominant in the flooding of the city of Tacloban during super-typhoon Haiyan (2013).

In regions where the tidal range is large, coastal flooding occurs when a large storm surge is in phase with the spring tide. On the contrary, under a storm inducing a surge of several meters, the tidal phase is negligible in micro-tidal areas, such as in the Gulf of Mexico. Conversely, in the macrotidal central part of the Bay of Biscay, a major flooding can only occur if a large surge is in phase with a high spring tide (Breilh et al., 2014). Also, for a given storm, the associated surge can vary along the tidal phase due to tide-surge interactions. Such interactions are explained by the non-linear terms in the governing shallow water equations (eqs. 2-3): bottom and surface stresses, and advection in the momentum equations and the finite amplitude term ( $Hu$ ,  $Hv$ ) in the continuity equation. For instance, a storm surge propagates faster at high tide than at low tide, since the wave celerity increases with the total water depth (Horsburgh and Wilson, 2007). Non-linear interactions particularly are relevant in shallow coastal areas where tidal ranges are large, such as in the English Channel (Idier et al., 2012) or the East Coast of England (Wolf, 1978). Finally, in low-lying environments such as estuaries or coastal lagoons, heavy precipitations that are usually associated with storms can contribute to extreme water levels together with storm surges. Wahl et al. (2015) reviewed the importance of rain fall during storms for the major cities located along the coastlines of the USA and revealed that the risk of such “compound flooding” was higher for the Atlantic and Gulf of Mexico coasts relative to the Pacific coast.

### **2.1.2- Storm-induced marine flooding**

Storm-induced flooding usually occurs through three main processes, which can be combined: (1) overflowing (or “inundation” following Sallenger, 2000), when the still water level is above the barrier crest; (2) wave overtopping, when the still water level is close or below the barrier crest and flooding intermittently occurs because of the runup from waves and (3) barrier breaching. This section will present three examples of coastal flooding associated with these mechanisms, where the flooding is adequately reproduced numerically.

#### **2.1.2.1- Overflowing over dikes and sedimentary barriers**

Bertin et al. (2014) performed a fully coupled high-resolution hindcast of the coastal flooding associated with Xynthia, a mid-latitude storm that severely hit the central part of the Bay of Biscay in February 2010. These authors implemented a numerical modeling system that couples the circulation model SELFE (Zhang and Baptista, 2008) and the wind wave model WWMII (Roland et al., 2012). This hindcast used an unstructured grid covering the whole NE Atlantic Ocean, with a spatial resolution ranging from more than 10,000 m offshore to locally less than 5 m along the dikes and dunes in the study area.

Figure 2 shows the comparison between the maximum modeled inundation and the extension of the inundation observed after Xynthia. This figure reveals firstly that the maximum water depth in flooded areas ranges from about 1 m over a large part of the study area, to locally more than 3 m. The comparison with observations reveals that, at regional scale, the model is able to reproduce the extent of the flooding quite reasonably (Fig. 2). The agreement is particularly good in large marshes where the inundation exceeds several tens of km<sup>2</sup> (Fig. 2A). In more details, the model fails to reproduce the flooding of small areas (i.e. less than 1 km<sup>2</sup>) along the coastline affected by wave-overtopping-related flooding (Fig. 2B). This problem is explained by the use of a phase-averaged wave model, which does not allow for the representation of wave runup or infra-gravity phenomena. Model results suggest that waves in the range 2-3 m were breaking in front of these areas during Xynthia. The representation of wave-runup and infra-gravity phenomena at regional scale poses a serious challenge in terms of computational time and is thus a needed focus for mid- to long-term research. The next section shows that today it is possible to account for wave overtopping at a scale of the order of 1 km.

#### **2.1.2.2- Wave overtopping**

Le Roy et al. (2015) performed a high-resolution hindcast of the flooding induced by storm Johanna (10 March 2008) in Gâvres, a small coastal city located to the North of the Bay of Biscay. These authors first used a suite of nested wave and tide/storm surge models to compute wave and water level conditions in front of Gâvres Bay. From these quantities, they reconstructed a time series of water level representing short waves in order to force a local very high-resolution shallow water model implemented over area of Gâvres. This model corresponds to SURF-WB (Marche et al., 2007), which solves for the non-linear shallow water equations combining shock-capturing and well-balanced numerical schemes. The geographical space was discretized using a regular grid with 1m x 1m spatial resolution, built based on LIDAR data. Such a fine spatial resolution allowed for an explicit representation of buildings and houses. The comparison with the available data revealed that their model was

capable of reproducing the extension of the flooding quite reasonably (Fig. 3). The analysis of model results demonstrated that the flooding occurred mainly due to wave overtopping along the oceanfront dikes and this lasted about three hours around high tide.

Among their findings, Le Roy et al. (2015) also compared their baseline simulation with a simulation where houses and building areas are represented implicitly through a larger bottom friction. This comparison showed that, although the extension of the flooding is comparable in both cases, current velocities are much higher in the streets when houses are represented explicitly, with differences locally exceeding 2 m/s.

### **2.1.2.3- Sedimentary barrier breaching**

McCall et al. (2010) performed a numerical hindcast of the barrier breaching and the flooding of Santa Rosa Island during Hurricane Ivan, which severely impacted the Gulf of Mexico coast in September 2004. These authors used the X-Beach morphodynamic modeling system (Roelvink et al., 2009) to simulate the coastal circulation, the wave propagation and the resulting sediment transport and bottom changes. Compared to other process-based modeling systems, X-Beach offers the possibility of accounting for infragravity waves and sediment avalanching and was designed to simulate the erosion of dunes during storms. Starting from a LIDAR-derived high-resolution topography (Fig. 4A), their model was able to reproduce the flooding and the breaching of Santa Rosa Barrier Island (Fig. 4B). Comparison with a LIDAR survey carried out after Hurricane Ivan (not shown) revealed that the modeling system performed well in predicting morphological changes, including the development of overwash fans in back-barrier areas. Once X-Beach was validated, McCall et al. (2010) performed a sensitivity analysis of the model from which they gained interesting knowledge about dune breaching during storms. Insights included: (1) the start of overwash was determined more by wave conditions (wave period and wave height) than the overall surge level, (2) the overall surge level affected the amount of overwash deposition, and (3) a time lag of the surge level in the back-barrier bay compared to the open ocean increased the amount of deposition in the back barrier. These observations should also be relevant to other localities.

## **2.2- Past marine floods**

Marine floods have occurred throughout time, and concern has heightened with climate change. It has been clearly established that our planet has been warming since pre-industrial times and that this can increase local storm frequency and magnitude (Solomon et al., 2007; IPCC, 2014). However, the effects of climate change on extreme events are

difficult to assess because of the decadal and interannual variability of the climate, the limited length of meteorological and oceanographic records and the short memory of humans. Several storms and floods have hit France and Europe in recent years but the link between these events (number and intensity) and climate change is difficult to deduce. As a result of greater coastal populations and public infrastructure, communities are at increased (and increasing) risk and are more likely to be severely impacted from the destructive influence of intense climate episodes. Given these extreme events are inherently rare and therefore difficult to observe in the period of a human life (Dezileau et al., 2011), it is essential to place such events in a broader context of time, over several centuries and millennia.

Estimates of the largest marine floods are required for the design of coastal defenses and coastal planning, even if their probability is low. For example, in the Netherlands, coastal defenses are designed to withstand extreme water levels with probabilities of 1-5 per 10,000 years (Baart et al., 2011). Like any natural hazard, marine floods can be defined based on five parameters (Alcántara-Ayala, 2002; Leone et al., 2011): magnitude, spatial influence, duration of immediate and deferred action, intensity of the observed or potential damage, and probability of occurrence. For reasonable planning and consideration of low probability events, these parameters must be known over the long term, i.e., longer than the last few decades as is typically the case (Fanthou and Kaiser, 1990; Garnier et al., 2012). To reach these goals, historical archives and sedimentological records are essential.

### **2.2.1- Past marine floods in historical archives**

Historic inventories of marine floods are based on information about their consequences (damages) registered in many archives.

#### **2.2.1.1- Worldwide examples of long-term historical documentary records**

Information about past storms provides an important historical context for storms at shorter timescales. Historical documents from China have provided tremendous data on typhoon landfalls. Such data are particularly important as the northwest Pacific basin is characterized by the highest frequency and intensity of tropical cyclone occurrence in the world (Liu et al., 2001). Coastal areas of China were hit by 380 tropical cyclone landfalls from 1949 to 1988 (Liu et al., 2001), and 158 of these cyclones struck the Guangdong area (Fig. 1). Chinese records provide exceptional documentation of typhoons spanning over 1,000 years. The earliest unequivocally recorded typhoon occurred in AD 975 (Liu et al., 2001).

Chinese records of typhoons include two groups of historical documents: “official History” and “local gazettes”. Lee and Hsu (1989) made an inventory of 571 typhoon strikes from AD 975 to 1909 (935 years) by excluding sea surges caused by tsunamis and winter storms. By combining historical and instrumental datasets, Liu et al (2001) were able to conduct statistical analyses and compare the data with paleoclimatic proxies in China. First, it appeared that the historic record was incomplete before AD 1400 with lower typhoon frequency (about 6 per decade) compared to the period from 1400 to 1909 (frequency of about 10 per decade) and to the last century (frequency of 4 per year). But, the discrepancy between historical and instrumental data was explained by the fact that historical documents only recorded strong tropical cyclones (typhoons) and not tropical storms. The periods of highest frequency of typhoons landfalls (AD 1660-1689 and 1850-1880) coincide with the coldest and driest periods of the Little Ice Age in China. An apparent return period of 50 years in typhoon frequency suggested an external forcing mechanism.

Japan also has a long documented history of floods related to tsunamis and storms. Tsuchiya and Kawata (1986) studied changes in storm surge disasters in the Osaka area from historical documents, for about the last 1200 years. They showed that storm surge disasters occurred 53 times since AD 700 and estimated the mean interval between major storm surge disasters to be about 150 years. Huge storms, in which a thousand or more people were killed, have occurred seven times during the past 1200 years in the Osaka area. In this study, the authors point out the lack of document describing storm surge disasters between AD 900 and 1400. Sawai et al. (2008) used a compilation of storms and storm-related floods from 380 old documents, since AD 701, for the Sendai area (Arakawa et al., 1961). A reduction in the amount of storms is also evident for the period from the tenth through to the sixteenth centuries. Six large storms were reported between AD 701 and 1865, among which only one produced an important storm surge in 1648 (Sawai et al., 2008).

Historical documents from North America have also provided data on hurricane landfalls, but over a more recent period of time, compared to China and Japan. In particular, historical documents are available in New England for the last 400 years since early European settlement (Boose et al., 2001, Ludlum, 1963, Neumann et al., 1993). The first historical record of an intense hurricane striking New England was for an event on 25 August 1635 (Donnelly et al., 2001b). Three other major hurricanes (> Category 3) with associated storm surges from 2 to 5 m and 27 minor (Category 1 and 2) hurricanes with associated storm surges of generally less than 2 m have been reported in historical documents.

### 2.2.1.2- Past storm surge events in France

Analysis of the historical documentation of past extreme storms and storm surges in France is under way and may bring new knowledge on the amplitude and frequency of past surges. Insights will add to recent, well-documented extreme water-level events that have been used to develop disaster risk reduction plans. Historical documentation is also essential to develop the "memory" of marine floods, a fundamental element of the knowledge of coastal risks as the "culture of the risk" remains insufficient (Beucher et al., 2004; Bonnot-Courtois et al., 2008; Garnier, 2010).

Historical archives found in France include: public and French naval archives, local newspapers, academic reports and scientific publications. Following their collection, those historical archives are processed both spatially (using a GIS) and chronologically. Marine flooding consequences are described in terms of impacts and damages, which constitute representative indicators of the processes involved (Breilh et al, 2014, Douglas, 2007). Despite biases and inaccuracies associated with non-scientific sources, historical archives are very useful for characterizing past marine floods (Breilh et al, 2014, Peeters et al., 2009; Garnier and Surville, 2010; Rilo et al., 2015). Focusing on French historical documents, two periods can be identified regarding the types of information reported. First, before the 19th century, personal accounts are important. A witness who wrote about a marine flooding seemed to be either personally concerned or interested for monetary purposes. If personally concerned, the event was described in general terms, and often the storm was viewed as punishment from god (Barriendos, 2010; Desarthe, 2011). If interested from a business or financial perspective, the event was described in detail with the goal of a tax exemption or some type of reparation. Before the mid-20<sup>th</sup> century, accountings of past marine floods were generally limited to the chronology of events. This information only enables researchers to draw insights about potential vulnerability in an area. In more recent times, since about the end of the 18<sup>th</sup> century, atmospheric pressure, temperature, wind speed and direction began to be measured, and scientific data and analysis were more common. Later, in the 19<sup>th</sup> century, the French maritime administration was officially registered to study the sky and the sea state. Thus, since data collection began, historical research can help provide quantitative and descriptive data to characterize past marine floods.

Results of historical investigations for three different coastal areas of France (i.e., Brittany, the central part of the Bay of Biscay, and in Languedoc; Fig. 1) are presented below, providing a contrasted view of impacts for different geomorphologic settings. Brittany is a typical Ria-type coast characterized by pocket beaches, headlands, cliffs, and rocky

shores. This region in general has limited lowland areas in the backshore, with the exception of around Mont Saint-Michel Bay, located at the northeastern border of Brittany. In contrast, the coast located in the central part of the Bay of Biscay is a low elevation mixed rocky and sedimentary coast (Breilh et al., 2013; Chaumillon et al., 2004). This region is characterized by extensive lowlands, reaching tens of kilometers inland, corresponding to Holocene incised valley-fills (Weber et al., 2004a and b). These coastal lowlands are a result of rapid shoreline regression within estuaries related to large sediment supply and extensive land reclamation (Chaumillon et al., 2004; Breilh et al., 2013).

Finally, The coast of Languedoc (northwestern Mediterranean Sea) is characterized by ~kilometre-wide lagoons separated from the sea by emerged sandy barriers that are a few hundreds of meters wide (Dezileau et al., 2011). This specific morphology results from a well-known process of shore construction by waves and currents in a microtidal environment (Barousseau et al., 1996). Tidal range is modest (with a mean range of 0.30 m), which minimizes the influence of dynamic tidal currents. This coast is located along the southeastern-facing shoreline, and is extremely vulnerable to intense Mediterranean storms coming from south and southeast.

#### **2.2.1.2.1- Brittany**

Historical investigations in Brittany have not focused on defining the number of marine floods but rather on understanding the damage associated with specific hazard events. Damage is often defined as the number of structures and properties including human construction (e.g., houses, buildings, dikes, roads), agricultural parcels, plots of land and natural coasts (beaches, aeolian dunes, sediment barriers, rocky cliffs) affected by coastal hazards, including marine floods and erosion. Along the 4,000 km of coastlines of the Brittany peninsula, 4,000 damages were reported between 1800 and 2010 (Fig. 5). Among those damages, 20% were related to marine floods, giving an average of four flood-related damages per year. It is noteworthy that no deaths due to floods were reported. The relatively low number of damages associated with marine flooding along the Brittany coast can be explained by the small surface areas of coastal lowlands and land reclamation zones and also because most of those areas were developed in the last decades (i.e. after most of the historical floods). Of the documented flood-related damages, 25% occurred by overflowing; 13% resulted by overflowing and failure of dikes; 2% occurred though barrier breaching; 15% were caused by wave overtopping, and 44% were not specified. In most of the cases, flooding occurred in areas where sea defenses were already present, indicating that this hazard was already known. Higher numbers of damages related to marine floods occurred in 1877, 1904, 1924, 1937, 1967, 1996, 2008 and 2010 (Fig. 5). Although developed properties



likely increased continuously during the studied period, it is noteworthy that the flood-related damages remained relatively constant. Most of the flood-related damages occurred during winter, i.e., December (18%), January (16%), February (22%) and March (21%), which is the storm season in Western Europe. Most of the flood-related damages (40%) occurred during storm conditions; 20% resulted from gale wind events; 15% occurred during storm or gale periods associated with high tide levels, and 7% were produced without a pronounced atmospheric event. Years with high numbers of flood-related damages corresponded to years when tide levels were elevated (Fig. 5), especially during the Chaldean tides cycle of 18.6 years (Gratiot et al., 2008; Weill et al., 2012).

#### **2.2.1.2.2- Charente-Maritime**

Along the 460 km of coastlines of Charente-Maritime (between La Faute-sur-mer and the Gironde Estuary, Fig. 1), 46 coastal floods were reported for the last 500 years. This corresponds to one event every 11 years on average (Breilh et al., 2014). Most of the marine floods (89%) occurred during the boreal winter (October to March). According to marine meteorological records during the 19th century, about 80% of the marine floods along the Charente-Maritime coast were linked to southwest storm winds. The highest frequency of coastal floods was during the 20th century with a total of 16 coastal floods. This increase in the number of recorded floods with time can be explained by the increase of the number of historical archives from 1500 AD to present time (Breilh et al., 2014). Since the early 19th century, the recording is believed to be exhaustive. The spatial distribution of marine floods shows important variations from one coastal area to another, which is also related to the quality of the archive (e.g., based on size of records, Breilh et al., 2014). During earlier periods, damages were not always reported because human activities near the coastline were reduced compared to that of today.

In order to quantify the intensity of each flooding, Breilh et al. (2014) arbitrarily subdivided the Charente-Maritime coast into six domains of similar length. A coastal flood was considered to be "major" if at least four of these six domains were flooded. By using this criterion, nine major marine floods were identified for the last 500 years: 29 January 1645, 17 January 1784, 11 February 1895, 9 January 1924, 16 November 1940, 16 February 1941, 15 February 1957, 27 December 1999 (Martin) and 28 February 2010 (Xynthia). For the oldest marine flood (1645), no measurements of sea level or wind strength are available, but four long texts, written by different witnesses, provide a similar description. Samuel Robert, a justice officer, wrote that the wind blew from the west/south-west and that hundreds of kms of coastlines were flooded. Another witness wrote that 35 vessels, waiting in the fore-port of La Rochelle were wrecked by the sea storm, and one of them was transported about 4 meters

above sea level. Although the reference level was not explicitly mentioned for this witness, it is very likely that, “sea level” referred to the level of the highest tides in March, because this reference level (in French: “le flot de mars”) was systematically used during the 17th and 18th centuries, and it was the standard specified in the royal ordinances of the time (Grande Ordonnance de la Marine, 1681). Thus, 12 feet would be about 4 meters higher than the level of the high tide during the equinox. Such height suggests that the vessel was transported by both the storm surge and wave action. A tidal prediction for this date using the T\_Tide program (Pawlovicz et al., 2002) fed with contemporaneous water level data acquired in La Rochelle reveals that this storm occurred under spring tides (tidal range of 5.5 m). Despite the unavailability of instrumental data for this storm, the historical analysis of this example reveals that this marine flooding occurred under southwest storm winds in phase with high spring tide. Such a combination has also been shown for recent better-documented storms including Xynthia and the storms of 1940, 1941 and 1957 (Péret and Sauzeau, 2014, Breilh et al., 2014).

#### **2.2.1.2.3- Languedoc**

In communal archives, intense storm events were mentioned because they caused damage in the vicinity of different coastal cities on the French Mediterranean coast (Dezileau et al., 2011, Sabatier et al., 2012). For the last 400 years, eighteen intense storms occurred in Languedoc. Among all of these, some seem to be more intense. The storm of December 4th, 1742, recorded in many city archives around the Aigues-Mortes Gulf, is considered as the most catastrophic event. This storm, probably due to S to SE winds, submerged some local cultivated lands which had been gained at the expense of the older parts of the Palavasian lagoon. The lagoon was covered with a sand layer over “300 toises”, i.e. 500 m. One of the main consequences was the creation of a large inlet, near Maguelone, which remained open until 1761. The storm of 23 November 1848 associated with strong SSE winds induced the wreckage of a few ships in the Sète Harbor, the biggest port in the region. The sea completely submerged defense barriers in the Harbor. This storm caused the death of numerous people. Certified by many engraved illustrations, the storm of September 21, 1893 also resulted in devastation around Sète Harbor and the wreckage of a few ships. The winter storm of 1982, with 46 m/s wind (category 2 in the Saffir-Simpson scale) caused the death of 15 people and economic losses estimated at 400 million Euros. This storm caused a partial devastation of the new Palavas and Carnon harbors.

Historical archives provide valuable information for understanding marine flooding risks. From these historical examples, a few generic points arise. First, they show that marine

floods are not rare events. Although qualitative, historical descriptions of marine floods show similarities with modern examples. When quantitative meteorological data (such as atmospheric pressure, wind speeds, or tide gauge measurements) are available, they allow more accurate comparisons with recent floods (Liu et al., 2001), and they allow outlining the main meteorological conditions leading to marine floods. Nevertheless, historical archives have limitations, mainly because they are less complete (Breilh et al., 2014; Liu et al., 2001; Sawai et al., 2008; Tsuchiya and Kawata, 1986). From a general point of view, these limitations may prevent concluding a change in storminess over the last few centuries in terms of frequency and intensity. Although some historical studies have suggested an increase in storminess such as during the second half of the 16th century (de Kraker, 1999), the Little Ice Age (Liu et al., 2001, Dezileau et al., 2011, Shah-Hosseini et al., 2011) and the Spörer Minimum (Camuffo et al., 2000).

### **2.2.2- Past marine floods from sediment records**

Given that historical archives are limited in description and time and are unavailable for many coastal areas, the analysis of sediment records is invaluable to better understanding. Seminal works by Liu and Fearn (1993, 2000a,b) and Donnelly et al. (2001a,b) have provided the demonstration that sedimentary archives are very important to reconstruct past storm surge events. Although previous works identified the presence of storm event deposits in coastal sedimentary records, the sedimentary analysis combined with dating allowed the reconstruction of past storm frequencies and the emergence of a new discipline: paleotempestology (Liu, 2004). Indeed, sediment records allow investigation further back into the past compared to historical archives and can help demonstrate change in storm surge frequency (Nott et al., 2009, Mann et al., 2009) or intensity (Dezileau et al., 2011) for a given coast. Another advantage of sedimentary archives of marine submersions is that they result from the total inundation, including contributions from the tide, surge and wave runup, while tide gauges, often located in harbors sheltered from wave activity, typically only record water levels from tides and storm surge. The purpose of this section is to present the characteristics of storm-surge-related deposits. Then, a discussion concerning the limitations of their sedimentary interpretation is made to address questions of their utility in paleotempestology studies.

The first studies devoted to the analysis of surge deposits were related to tropical cyclones; these events often lead to the emplacement of thick and large volume washover fan deposits, mainly in back-barrier environments (Blumenstock, 1958; Hayes, 1967a, b;

Leatherman, 1976). They have been mostly studied along the Gulf of Mexico and Atlantic Ocean coasts of the United States and around Australia (e.g., Buynevich et al., 2004, 2006; Coch, 1994; Collins et al., 1999; Donnelly et al., 2001a,b; Fisher and Stauble, 1977; Fritz et al., 2007; Froede, 2006; Horton et al., 2009; Kiage et al., 2011; Nelson and Leclair, 2006; Nott, 1997, 2004a; Nott et al., 2013, Scott et al., 2003; Switzer and Jones, 2008; Wang and Horwitz, 2007), but also along other coasts (Haslett and Bryant, 2007). Most of these studies focused on the overwash strata and processes of barrier systems. Works in some areas have given valuable information on less severe events (Sabatier et al., 2008, 2012; Dezileau et al., 2011, 2016; Raji et al., 2015; Degeai et al., 2015).

#### **2.2.2.1- Washover fans**

In most instances, overwash deposition (note: overwash is synonymous with washover) results from the overtopping or breaching of the foredune of a littoral barrier and the associated reworking of eroded sediment (typically, sand; e.g., Pierce, 1970; Morton and Sallenger, 2003; Nott, 2004b; Buynevich and Donnelly, 2006). Washover fans (Fig. 6A) are typically sand-dominated sediment bodies of various sizes and shapes (Hudock et al., 2014) that form on the landward-facing slopes behind the beach berm (or coastal dune, depending on the morphology) and commonly extend into back-barrier marshes and potentially beyond (discussed in next section). Overwashing ocean water typically becomes channelized producing a relatively narrow throat that corresponds to a developing breach channel across the barrier system (Leatherman, 1976, 1979; Andrade et al., 2004). Washover fans are event depositional bodies, and deposits (potentially expansive) are often reported along microtidal storm-dominated coastlines (Schwartz, 1982). However, they can also form along macrotidal coasts during strong events. Like other sedimentary deposits, the preservation of washover fans in the geological record is presumably favored by both high sediment supply and subsidence conditions, enabling burial and precluding erosion. Overwash processes are major agents of the natural morphological evolution of barrier islands, a key driver of accretion landward that compensates for erosion seaward in the barrier “rollover” process (e.g., Donnelly et al., 2006; Tillmann and Wunderlich, 2013). Washover fans differ from estuary-sourced storm surge deposits that spread over marshes in that washovers have a direct connection with the dune or beach system. Their edges almost never coincide with the inundation limit as clear water can flow further inland because of settling of the transported sediment. Washover fan deposits usually correspond to sandy sedimentary prisms that thin landwards and have planar landward-dipping surfaces. Deposit edges typically do not coincide with the inundation limit as sandy sediment settles during transport. Shell-rich washover fans are frequent along some coasts (Aigner, 1985). Rare gravel-rich deposits are

also known (Carter and Orford, 1981; Buckley et al., 2012). The constituting sediment largely corresponds to eroded material reworked from the foredune, beach or nearshore of the barrier system. Morphologically, overwash deposits may be single sedimentary layer (i.e., a washover fan), or may be an amalgamation of multiple sediment bodies to form a washover terrace. These typically sand-dominated deposits often display planar laminations with numerous discontinuities (Fig. 7A) and some foreset lamina dipping landwards when the washover enters ponds (Schwartz, 1975; Eipert, 2007; Fig. 7B). Individual laminations often include elevated concentrations of heavy minerals reworked from the beach. The planar bedding suggests the important role of sediment traction (bedload) during emplacement. Individual depositional intervals can display a normal grading. Reverse graded intervals are rare but may dominate the deposits within the throat channel (Leatherman et al., 1977). This result from density segregation of small heavy mineral particles that have a hydraulic equivalence of larger siliciclastic particles, so less dense shell fragments can concentrate at the top of a reverse-graded layer. Cross-laminated intervals, indicative of ripple formation, also can be observed. Reactivation surfaces are present and attest to rapid variations in the flow energy during a single event or recurrent flooding surges through the same throat over multiple high tides or subsequent storms. Washover fans typically show a general progressive inland reduction of the mean grain size distribution. Figure 8 illustrates an example of deposits of a washover fan that has been emplaced during the cluster of storms of the 2013-2014 winter along the southwest coast of Oléron Island (southwest France). These deposits display typical features of washover deposits, dominated by planar laminations including heavy mineral concentrations and landward-dipping foreset strata.

#### **2.2.2.2- Backbarrier sedimentation (e.g., marshes, coastal lakes)**

Landward of the foredune or the coastal barrier (Fig. 6B and D), sediment deposits in response to storm surge can form along the back side of dunes or in barrier flats, marshes, coastal lakes or other water bodies (e.g., Liu and Fearn, 1993; 2000a,b, Donnelly et al., 2001a,b). Discrete storm layers can often be identified although aeolian sediment influx cannot be neglected (de Groot et al., 2011; Rodriguez et al., 2013). The distinction of surge- versus aeolian-sourced sediment may be difficult but made by the presence of biogenic material of marine origin (e.g. foraminifera) within the sandy/silty surge deposits (Hippensteel et al., 2013). It is important to note that sediment may be transported to the backbarrier areas through landward overwash or through estuarine surge (potentially seaward) (Fig. 6B). Deposits may consist of discontinuous layers of sandy to muddy sediments that fine and thin away from the shoreline (depending on transport direction; e.g. Goodbred and Hine, 1995; Donnelly et al., 2004; Williams and Flanagan, 2009), and microfossils may inform the storm

deposition (e.g. Hippensteel et al., 2013 and references therein). Event layers may be normally graded (Fig. 7C) and display a mud drape on top as a result of settling of fine-grained particles in suspension at the end of the flooding event (Williams, 2011a). The edge of sand deposition in estuarine inundations is unlikely to coincide with the inundation limit due to settling of the coarse-grained fraction of the transported sediment, and in sediment-limited cases, a lithologic or micropaleontologic deposit may not be produced (Mulligan et al., 2014; Hippensteel et al., 2013). But with major events and appropriate conditions, fairly continuous sand layers by overwash may be produced and preserved in marshes (e.g., Donnelly et al., 2004), and storm-supplied sediment can help marsh accretion (Turner et al., 2006; Fitzgerald et al., 2008). In estuarine areas with reoccurring storm-driven flooding and bank erosion, backbarrier berms may form from sedimentation over time (e.g., Lagomasino et al., 2013). Also, organic materials floating on the surge can form high-water “wrack” deposits along estuarine shorelines, especially where much material (e.g., detrital marsh grass) is available (Mulligan et al., 2014). Event deposits on barriers and in coastal lakes have allowed reconstructions of storm activity (Liu and Fearn, 1993, 2000a and b; Donnelly et al., 2001a,b; Das et al., 2013; Sabatier et al., 2008, 2012; Dezileau et al., 2011, 2016; Raji et al., 2015; Degeai et al., 2015).

If a coastal sandy barrier is present and extreme inundation occurs (from the ocean or the estuarine shore), breaching can allow the deposition of sand/silt sheets and potentially the development of a new inlet with associated strata (not reviewed here; see Fitzgerald et al., 2008). In western France, large coastal marshes are often located below the mean sea level (Breilh et al., 2013). The absence of an adjacent coastal sandy barrier reduces the likelihood for the formation of an identifiable coarse event layer deposited on backbarrier marshes. Numerous surges, like during the Xynthia storm in 2010 (Lumbroso and Vinet, 2011; Breilh et al., 2013) over some parts of the coast of western France and Hurricane Irene along the North Carolina, U.S.A. coast (Hippensteel et al., 2013; Mulligan et al., 2014), for example, have not mobilized a sufficient volume of sediment to form an identifiable widespread deposit. In these situations, only water with low amounts of fine-grained sediment or biogenic material in suspension flooded the coastal plain. Inundation can potentially be identified by enhanced marine biogenic material mixed within the background terrestrial sedimentary record or thick (many cm to m) wrack layers. Moreover, the shearing induced by storm surge flow over the preexisting sediment surface can induce an abnormal compaction or erosion with the formation of a sedimentary hiatus (Fig. 7D) as recognized for instance after hurricane storm surges along the coast of South Carolina, U.S.A. (Scott et al., 2003).

### 2.2.2.3- Beach ridges

Beach ridges (Fig. 6C) are usually wave-built and occasionally wind-built relict strandplain ridges originated in the inter- and supratidal zones (Otvos, 2000). Many examples of beach ridges are built during storm events at or above the normal spring high tide level (Taylor and Stone, 1996; Hesp, 2006). They are generally aligned parallel to the swash zone in regressive coastal settings and can be constituted of various types of sediment (sand, gravel, shell or coral fragments). Gravelly beach ridges display landward clast imbrications (Fig. 7E). Ridges are separated from each other by swales filled with mud, sand and/or organic material. One coarse-grained beach ridge of several meters in height and hundreds of meters in length can be emplaced during a single storm event (Maragos et al., 1973; Baines and McLean, 1976; Nott, 2003). Thus, accretion of successive storm ridges occurs as the consequence of several storm events (Haynes and Chappel, 2001; Nott et al., 2013). One positive sedimentary aspect of beach ridges is that they record the elevation of the marine inundation. Thus, they can be used to document episodes of higher than normal wave or tide conditions, such as associated with marine flood events (Reineck and Singh, 1978; Mason and Jordan, 1993).

Cheniers are a particular type of transgressive beach ridges emplaced within a regressive facies framework (Otvos and Price, 1979, Otvos, 2000). These wave-built shore-aligned ridges are often constituted of marine shells and shell fragments (Williams, 2011b; Fig. 7F), and become isolated from the shore by a band of prograding intertidal flat deposits. Chenier internal architecture is almost exclusively composed of landward-dipping planar and foreset lamina attributed to washover sedimentation, covered on the seaward side by a thin veneer of beach deposits. A study on modern chenier ridges in a macrotidal setting (Weill et al., 2012) revealed that the transition between landward-dipping planar laminations and landward-dipping foreset laminations is controlled by the level of flooding in the backbarrier area. These observations are supported by experimental evidence (Weill et al., 2013). In this particular low-wave / high-tidal-range environment, the level of flooding generally corresponds to the spring-high-tide water level, modulated by low magnitude storm surges. The study also suggests that the elevation and altitude of chenier ridges may be influenced by the 4.4 and 18.6-year tidal cycles.

Beach ridges (including cheniers) can occur along coasts affected by tropical cyclones and can be used to reconstruct the chronology of those events (e.g., Nott et al., 2009, 2013, Nott, 2015). An example is given at Cowley Beach (NE Australia) where most of the beach ridges have been dated using the optically stimulated luminescence technique and record extreme intensity tropical cyclones over the past 6000 years (Nott et al., 2009). Beach ridge deposits typically display alternation of beach and soil intervals (Nott et al., 2013) and

attest to beach sediment being carried landward over soil-covered areas during a storm event.

Sedimentary impacts of storm-surges have been described within coastal dune complexes (Cunningham et al., 2011). Coastal dunes can preserve high-magnitude storm surge deposits at elevated locations. In this case, deposits display basal erosional surfaces and shell-rich graded sediments (Fig. 7G).

#### **2.2.2.4- Offshore submarine deposits related to storm and storm surge flooding**

Storm deposits have long been studied in shallow offshore submarine settings (Aigner, 1985 and references therein); however in the last two decades, more process measurements and models have been conducted. In particular, the submarine sedimentary record of storm-related transport has been hypothesized to play an important role on inner-shelf stratigraphy, and there is an extensive literature on hummocky cross-stratification (HCS, Dumas and Arnott, 2006). Indeed, storms can cause substantial and widespread erosion along a coast, and transport may be landward (e.g., into marshes, Turner et al., 2006) or seaward to the open sea (Fig. 6E, Reineck and Singh, 1972; Allison et al., 2010). This provides a potential new source of sediment for offshore areas, in addition to sediment inputs from runoff. But, while some sediment from land or nearshore may be advected offshore, it is important to remember that on the shelf overall, much (possibly most, depending on the location and circulation) subaqueous sediment is material eroded from and redeposited on the shelf. Therefore, shelf-sediment remobilization by non-surge processes may be most important, as suggested by modeling (Xu et al., 2016) and organic and foraminifera for Katrina deposits (Goni et al., 2007; Rabien et al., in press). Hurricane-related offshore deposits have been identified for several events in the Gulf of Mexico (Keen et al., 2004; Allison et al., 2005; Walsh et al., 2006; Goni et al., 2007; Allison et al., 2010; Goff et al., 2010). Many factors control event sedimentation on the shelf including waves, currents and sediment input or local availability (see Nittrouer et al., 2007; Corbett et al., 2014 and papers therein). More specifically, storm surge ebb transport of coastal sediment can be key for to the inner shelf (Goff et al., 2010). Where inner shelf materials are transported seaward, sandy deposits may be recognized over muddy strata (Fig. 7H), with erosional contacts beneath normally or reverse graded layers (Allison et al., 2005; Fan et al., 2004). However, the stratigraphy of shelf event layers is spatially and temporally complex (Goff et al., 2002; Walsh et al., 2014), and these deposits can be confused with tsunami deposit layers that display very similar features (Sakuna-Schwartz et al., 2015). Bioturbation does not favor the preservation of submarine storm or flood layers (Dott, 1983; Keen et al., 2004; Bentley and Nittrouer, 2003; Tesi et al., 2012). For example, Walsh et al. (2014) and references therein



indicate physical and biological reworking of event layers over many centimeters to decimeters of the upper seabed.

#### **2.2.2.5- Strengths and limits of sedimentary records**

##### **2.2.2.5.1- Preservation potential of the paleostorm records**

Except for proximal washover fan areas, the sedimentary record of storm surge flooding both inland and offshore usually corresponds to thin (less than a few centimeters) sediment layers (e.g. sand/silt sheets within marshes and coastal water bodies). However, these thin sedimentary intervals provide crucial information about the frequency past storm activity (Liu, 2004; Liu and Fearn, 1993, 2001a,b; Donnelly et al., 2001b; Mann et al., 2009) and potentially about storm paleointensities (Donnelly et al., 2001a; Liu and Fearn, 1993; Nott, 2004a; Woodruff et al., 2008a).

The preservation potential of the paleostorm record is very important to constraining paleotempestological studies and is essential for the construction of past events (Nott and Hayne, 2001; Bentley et al., 2002, 2006; Nott, 2003; Dezileau et al., 2011). Coastal sedimentary environments are very dynamic and are prone to severe erosion and reworking, e.g., because of barrier island migration. Moreover, anthropic control, biologic activity (bioturbation by animals and plant roots) and subsequent storms can strongly modify the original textures of primary deposits or even erase them. First, to be preserved, a storm event must produce a sedimentary deposit. Consequently, it is necessary to that the associated processes (e.g., surge and waves) reach a minimum threshold to erode material somewhere allowing the formation of a related deposit (Dott, 1983; Einsele et al., 1996; Shiki, 1996). This threshold depends on the physical conditions of the storm but also the nature (e.g., availability and texture of sediment) that will potentially constitute a resulting event layer. To be identifiable, an event layer must be composed of a sediment that texturally and/or compositionally differs from the ambient sediment in the sedimentation area. The study of modern events and the processes governing preservation (or non-preservation) of event layers indicates that the main controlling factors are the thickness of the event deposit, the local hydrodynamic conditions, background sedimentation rate and biological activity (see review in Nittrouer et al., 2007). In submarine environments, sedimentation and bioturbation are competing processes in the formation and preservation of primary sedimentary fabric, respectively (see examples in Bentley et al., 2002, 2006; Bentley and Nittrouer, 2003; Bentley and Sheremet, 2003; Wheatcroft and Drake, 2003). The preservation of event layers is relatively short, depending on their thickness, unless there is rapid advection of the layer through the surface mixing layer. Interested readers are urged to

see Wheatcroft et al. (2007) and references therein. Although this text focuses on margin sedimentation, the theory presented is broadly relevant. To our knowledge, the preservation issue has not been well addressed for coastal (e.g., salt marsh) environments, and this is an important topic deserving further research. Nevertheless, because of the relatively poor preservation potential of coastal storm event layers, the incompleteness of the sedimentary record must never be neglected.

At first glance, washover fans appear to be the most voluminous and potentially best defined and thus easiest to examine relative to other sedimentary storm records. However, they do not appear to be optimal targets for the reconstruction of the storm chronologies as they, in many areas, correspond to composite and/or spatially isolated deposits that may be reworked during subsequent storms. Moreover, as the mobilized sediment from the dune, beach or nearshore source always displays similar sedimentological properties, the superimposed deposits can preclude identification of sequential events because of stratigraphic homogeneity. Consequently, apart from the presence of reactivation surfaces, that can also form during a single event, it is difficult to distinguish deposits related to independent events. Finally, the preservation potential of washover fans may suffer from erosion related to island migration or post-storm winds (Sedgwick and Davis, 2003) that can transport washover sand elsewhere (Leatherman, 1976). Processes of washover healing have been discussed by Matias et al. (2010). For these reasons, the storm sedimentary record is likely best captured and preserved within protected, accreting areas (e.g., marshes, embayments, coastal lakes and beach ridges). Thus, overwash sand layers preserved in backbarrier environments are considered to be one of the most useful possibilities for the reconstruction of past hurricane strikes (Liu and Fearn, 1993, 2000a,b; Donnelly et al., 2001a,b; Scott et al., 2003; Liu, 2004; Woodruff et al., 2008a and b). Nevertheless, bioturbation by plants and animals (Sedgwick and Davis, 2003) as well as dissolution of biogenic particles (Jonasson and Patterson, 1992) may affect and preclude the sedimentary record. Moreover, agricultural practices and road clearing of overwash sediment complicate the preservation of storm surge deposits. Additionally, specific local conditions affecting storm deposit thickness, grass density or even anoxia may contribute to better preservation (Otvos, 2011). In the coastal woodlands and marshes of Louisiana, U.S.A., Williams and Flanagan (2009) determined that the thickness of some storm deposits was reduced by 50% only two years after the event (Hurricane Rita). Further complicating the matter, human modifications (e.g., dune development) can modify the amount and character of overwash (Rogers et al., 2015)

#### **2.2.2.5.2- Dating of the paleostorm records**

Accurate dating to establish the chronology of events is one of the major challenges and concerns when sedimentological records of past marine floods are preserved and identifiable.

Stratigraphic dating is frequently carried out using  $^{14}\text{C}$  on shell or wood fragments. Age uncertainties can vary widely, from a few decades to hundreds of years depending on method, corrections and the material used (Taylor et al., 1992, Duller, 2004). A major concern is potential reworking as shells are easily remobilized during storms. Consequently, efforts to date a specific event with radiocarbon may be speculative. When the  $^{14}\text{C}$  method is used to date samples equilibrated in marine or continental bodies of water, a reservoir age correction is required. This reservoir age may change with time and is very difficult to estimate. For example, the modern reservoir  $^{14}\text{C}$  age was estimated by Sabatier et al., 2010 by comparing AMS  $^{14}\text{C}$  ages of recent mollusk shells found in sediment cores sampled in the Palavasian Lagoon system (southern France) with ages derived from  $^{210}\text{Pb}$  and  $^{137}\text{Cs}$  data and historical accounts of identifiable storm events. The calculated modern  $R(t)$  value of  $943 \pm 25$   $^{14}\text{C}$  years was about 600 years higher than the global mean sea surface reservoir age. This high value, probably due to the relative isolation of the lagoon from marine inputs, was in good agreement with other  $R(t)$  estimates in Mediterranean Lagoon systems.  $^{14}\text{C}$  ages were also obtained on a series of Holocene mollusk shells sampled at different depths of the ~8-m-long core. Careful examination of the  $^{14}\text{C}$  ages versus depth relationships suggest that  $R(t)$  in the past was lower and similar to the value presently measured in the Gulf of Lion ( $618 \pm 30$   $^{14}\text{C}$  yrs). The change in  $R(t)$  from 618 to 943 yrs is thought to result from final closure of the coastal lagoon by the sandy barrier, due to the along-shore sediment transfer (Sabatier et al., 2010). In some particular cases, absolute chronology of storm events dated by AMS  $^{14}\text{C}$  age model can be reinforced with annual couplets. Such sedimentation pattern is found in the blue hole, in the lagoon of Lighthouse Reef Atoll, Belize, where annually layered biogenic carbonate mud and silts are intercalated with coarser grained storm beds (Gischler et al., 2008). Such robust age/depth framework allowed the documentation of increased tropical cyclone activity between AD 800 and 1350, corresponding to Medieval Warm Period and conversely decreased cyclone activity during the Little Ice Age (Denommee et al., 2014).

In ideal water-clarity and transport conditions, dating by optically stimulated luminescence (OSL) is possible. This is the case, for instance, where relict scarps are buried under prograding barriers and beach and dune sequences during large-magnitude storm-related erosional events (Buynevich et al., 2007; Clemmensen et al., 2013). Briefly, OSL measures sediment particle burial time using amount of electrons stored in “electron traps” of mineral grains, which result of natural radiation over time. Energy release (light emission) is

used to quantify the time since last pre-burial exposure considering the local radiation. Error in the method is related to the analysis as well as assumptions (e.g., about radiation over time) and potential incomplete resetting of the OSL clock during exposure.

For the last century, dating is also possible using  $^{210}\text{Pb}$ ,  $^{137}\text{Cs}$ , and  $^{241}\text{Am}$ . Dating with  $^{210}\text{Pb}$  is based on the rate of decay of the radioisotope (half-life: 22.2 years), which is produced in the atmosphere or water-column and subsequently adsorbed on sedimentary particles accumulating over time, particularly clay minerals. Since Goldberg (1963) first established a method based on  $^{210}\text{Pb}$  chronology, this procedure has provided a very useful tool for dating recent sediments; see Corbett and Walsh (2015) for a review of coastal application. While these isotopes are invaluable, their use requires models with specific assumptions, and in general, these assumptions can be problematic for locations experiencing episodic event deposition. But under ideal conditions, e.g., relatively steady sedimentation,  $^{210}\text{Pb}$  can provide robust temporal constraints and potentially a detailed chronology.

Storm layers can also be age dated with  $^{137}\text{Cs}$  and  $^{241}\text{Am}$  in marsh and estuarine deposits (Wheeler et al., 1999; Donnelly et al., 2007; 2015; Dezileau et al., 2005, 2016; Dezileau and Castaing, 2014; Sabatier et al., 2008; Castaings et al., 2011; Brandon et al., 2013; Raji et al., 2015).  $^{137}\text{Cs}$  and  $^{241}\text{Am}$  are human-derived isotopes, which can be found worldwide. The peak in the activity of  $^{137}\text{Cs}$  is typically associated with the date of maximum atmospheric nuclear weapons tests fallout in 1963. Another smaller peak of  $^{137}\text{Cs}$  may be visible in Europe and Asia as a consequence of fallout from the Chernobyl disaster that occurred in 1986. The most common dating approach based on  $^{137}\text{Cs}$  assumes that the depth of maximum  $^{137}\text{Cs}$  activity in the sediment corresponds to the maximum atmospheric production in 1963 (Robbins and Edgington, 1975; see Corbett and Walsh, 2015 for review). In areas near Chernobyl, two  $^{137}\text{Cs}$  peaks may be associated with 1963 and 1986 layers; the latter can be differentiated with measurable  $^{241}\text{Am}$ . A property of Cs is its high mobility in marine sediments, with a preferential downward diffusive transport in porewater (Radakovitch et al., 1999). Despite potential Cs mobility,  $^{137}\text{Cs}$  activity is a generally good time-marker, and often is also used to validate sedimentation rates derived from  $^{210}\text{Pb}$  models.

Radiometric dating methods have proved their reliability as a dating tool in different studies of estuarine and continental margin areas (see Nittrouer et al., 2007; Corbett et al., 2014; Corbett and Walsh, 2015 and references therein), although where sedimentation is absent or non-steady their application is more problematic. For example, the agreement between dating methods was found in the lagoon of Venice (Ciavola et al., 2002). This site recorded the extreme flood event of 1966 as a characteristic break in the  $^{210}\text{Pb}_{\text{ex}}$  profile and

the position of the  $^{137}\text{Cs}$  peak marker. Comparison of  $^{137}\text{Cs}$ ,  $^{210}\text{Pb}$ ,  $^{14}\text{C}$  chronology and historical accounts have permitted the identification of deposits from three extreme storm events in 1742, 1848 and 1893 A.D., respectively, in the Pierre Blanche and the Prevost lagoons located near Palavas (Fig. 1), and on the French Mediterranean coast (Dezileau et al., 2005, 2011; Sabatier et al., 2008). These dating tools also permitted the quantification of hurricane strikes to Vieques, Puerto Rico (Donnelly and Woodruff, 2007). The accuracy of the radiometric dating methods discussed above is highly variable depending on the sediments, scavenging and model, but where able to be used, radioisotopes can allow better precision, but exclusively for deposits less than  $\sim 100$  years.

#### **2.2.2.5.3- Storm paleointensities**

As described above, various dating methods can be successfully applied to storm deposits, particularly in marsh and estuarine (e.g., lagoonal) areas where organic-rich muddy deposits are accumulating. These data are crucial for the construction of the chronology past events. However, very few studies have been devoted to understanding the magnitude/intensity of stratigraphically recorded storms. In a few well-constrained sedimentary settings, attempts based on grain-size distributions have hypothesized the relative intensities (Woodruff et al., 2008a; Brandon et al., 2013; Toomey et al., 2013). The used methods are based on various approaches among which, (1) the grain-size variations with distance from the source (Woodruff et al, 2008a), (2) the sediment transport competency by the surge, empirically determined from grain size data and maximum wind speeds relationships (Brandon et al., 2013), and (3) by the recognition of intervals enriched in coarser sediment ( $D > 250 \mu\text{m}$ ) among the ambient sedimentation within the sedimentary successions (Toomey et al., 2013).

In sum, the analysis of sedimentary successions potentially recording storm events provides useful insights. However, dating of storm/surge-related sedimentary intervals is crucial for the construction of calendars of past events. Preservation is a potential problem for all coastal storm deposits, and more work is needed to examine known events in different settings. In any case, researchers must remember that the sedimentary record of past storm events is typically incomplete and highly site dependent. Consequently, it appears always necessary to analyze various environments and sedimentation areas, if possible, to connect the sedimentary record with historical data to verify and potentially improve the completeness of the record.

### 2.3- Vulnerability studies from old and recent and well-documented marine submersions

Studies of recent and past coastal floods from both historical archives and sediment records show that vulnerability to coastal flooding is related to the presence of low-lying coasts exposed to tropical or extra tropical storms leading to extreme water levels. Low-lying coastal areas include deltas and estuaries, and these often are heavily populated coastal zones. At a global scale, deltas and estuaries are the most vulnerable to coastal flooding, and some of these locations have substantial development. In addition, anthropogenic development along the coast, such as land reclamation, can seriously increase the surface area of the low lands and thus augment the vulnerability to marine submersion.

Deltas are areas where the vulnerability to marine flooding is the highest as extensive areas of low-lying land are present and human populations are high. In 2010, deltas concentrated about 500 million people in less than 2% of the land surface, including twelve megacities with a total of >150 million inhabitants (Syvitski and Saito, 2007; Syvitski et al., 2012). One of the main reasons for the flooding risk in deltas is related to their subsidence. Delta subsidence includes tectonics, compaction sedimentation and anthropogenic causes, such as oil and water pumping (Brown and Nichols, 2015; Syvitski et al., 2009; Giosan et al., 2014). In addition, dams are responsible for sediment trapping upstream and have substantially decreased sediment supply to many river mouths around the world (Syvitski et al., 2005). Studies have shown that among the 33 largest deltas in the world, 24 are experiencing strong erosion, potentially a response to accelerated subsidence and elevated relative sea-level rise (Brown and Nichols, 2015; Syvitski and Saito, 2007; Syvitski et al., 2012). However, satellite-imagery based analysis of five systems (Ganges-Brahmaputra, Fly, Irrawaddy, Mekong, Kikori-Purari deltas) demonstrates inconsistent trends (Shearman et al., 2013). Nevertheless, flooding is a major concern. A study of 33 representative deltas (Syvitski et al., 2009) shows that 26,000 km<sup>2</sup> of deltaic areas have average elevations below present-day sea level, protected from inundation by sediment barriers or engineered structures, and 100,000 km<sup>2</sup> of deltaic areas have elevations less than two meters above present-day sea level, and are therefore directly exposed to storm surge. Subsidence can be compensated by sediment supply, a major parameter of delta's morphodynamics, but fluvial loads delivered to many deltas have plummeted (Syvitski and Saito, 2007; Giosan et al., 2014).

Regarding estuaries, inundation risk is partly a result from the same mechanisms, although natural subsidence in estuaries is usually lower. However, several mechanisms may increase the importance of storm surges, including the funneling effect created by the geometry of the estuaries and the deepening of navigation channels. Moreover, large estuaries have in many cases become areas of important harbors (e.g., Hudson River

estuary, New York City), and now host extensive industrial and port facilities around in the world. The growth of these sites over the last half a century has increased technological risks because of the concentration of central power generation and other heavy industry (Zhao et al., 2014).

Finally, exceptional human densities occur on the coasts and deltas of southern and southeastern Asia, where the cyclogenesis areas are observed. This puts many territories at great risk to coastal flooding, particularly if shallow waters and/or extensive continental shelves border them. This risk is further accentuated by the vulnerability of the societies in these areas, which are in some cases poorly prepared to respond to these dramatic episodes. Urbanization adds to this vulnerability, because in many places uncontrolled development has occurred, adding economic risk. Consequently the deadliest disasters related to marine flooding are regularly observed in this geographical area. Outside of urban centers, the infrastructure and population at risk is lower, but nevertheless still critical, especially in societies which are less resilient, because of socioeconomic conditions (e.g. developing countries) or where damages to coastal infrastructure are catastrophic.

The number of victims is an important indicator of vulnerability. Since Hurricane Katrina in 2005, whose heavy human toll was unexpected (1800 victims), four cyclones generated higher death tolls (largely from storm surge): Sidr in Bangladesh (4100 victims, November 2007, Rahman and Rahman, 2015), Haiyan, which recorded wind speed of 315 km/h and minimum pressure estimated at less than 880 hPa in the Philippines, (7350 victims, November 2013, Lapidez et al., 2015), and above all, Nargis in Myanmar in May 2008, with its frightening human toll of 138,000 victims. Incredibly, the storm surge of Cyclone Nardis was lower less than 4 meters, but it swept across the entire Irrawaddy delta upon which the capital Yangon is built (Pelling and Dill, 2010).

Evaluating flooding risk emphasizes the contrast between countries with a high development level, where the economic damages may be high, and emerging countries, where the number of victims is usually larger. For example, Hurricane Sandy, which impacted the New York metropolitan area (October 2012, 200 victims), and Katrina (August 2005), which affected the area around New Orleans, cost respectively \$52 and \$108 billion (Mikami et al., 2015), over 10 times more than the major Asian disasters whose human toll was much heavier.

Europe is less affected by massive coastal flooding; nevertheless it includes very vulnerable territories, mainly because the morphology of the Atlantic coastline of Europe is dominated by estuaries (Perillo, 1995), which include large land reclaimed areas. The central part of the Bay of Biscay, which was severely flooded during the storm Xynthia in February

2010 (Bertin et al., 2014; Breilh et al., 2013), is a recent and well-documented example illustrating this vulnerability (Breilh et al., 2013). The French coastal population density is above national average: 281 inhabitants/km<sup>2</sup>, versus 114 inhabitants/km<sup>2</sup> for metropolitan France. However, compared to the Mediterranean coast, population density is lower along the Atlantic coast with a population density of 198 inhabitants/km<sup>2</sup> (ONML, 2013). A study of the flooding vulnerability of the French Atlantic coasts (CETMEF and western CETEs, 2009), performed before the Xynthia Storm, showed that the most vulnerable coasts were those between the Gironde and the Loire Estuaries (Fig. 1).

The flood associated with Xynthia was one of the costliest and deadliest to strike France in modern history. More than 50,000 ha of land were flooded, and 55 towns were affected by the flooding. Tragically, 46 people died, 41 by drowning (Chauveau et al., 2011; Vinet et al., 2012; Breilh et al., 2013; Chadenas et al., 2013; Kolen et al., 2013; Bertin et al., 2014; Creach et al., 2015). Such a heavy toll reveals the vulnerability of the central part of the Bay of Biscay in contrast with the Brittany coast (see above). Below, we present explanatory elements of this tragedy and propose a vulnerability analysis. Both physical and human parameters explain the vulnerability of the southwest French coast to marine flooding. First, the vulnerability of the coast located in central part of the Bay of Biscay is related to its exposure to extratropical cyclones, its extensive low-lying coastal zones and the presence of extensive shallow waters and wide continental shelf. For example, within the Pertuis Charentais, the coastal area which was the most severely hit by floods during Xynthia (2010-02) and Martin (1999-12), more than 50% of the surface area of the 10 km wide coastal band is below sea level during the highest astronomical tides (Breilh et al., 2013). In addition to this vulnerable physical setting, human parameters help explain such a toll.

The first factor, a structural one, is the growth of the suburbanization in coastal low-lying areas. This growth is related to widespread construction of residential houses since the 50's (INSEE, 2014) in land reclamation areas, originally used for agriculture. Development in coastal low-lying areas was facilitated by the presence of old dikes (Péret and Sauzeau, 2014) and a lack of regulation (Chadenas et al., 2013). During Xynthia, 100 % of the drowning took place at distances of less than 400 m from the dikes (Vinet et al., 2012). The second factor is related to the concentration of elderly persons in coastal towns. For example, in La Faute-sur-Mer where 29 inhabitants died, more than 45% of people were older than 60, while the national percentage is 18%. As a consequence, 75% of drowned persons were older than 60 (Vinet et al., 2012). Furthermore, elderly persons are most exposed to side effects like heart attack (Jonkman and Kelman, 2005). The third factor is related to the massive development of seaside tourism since the late 1950s that took place during an uncommon period characterized by the absence of major marine flooding (1957-



1999, Breilh et al., 2014). Consequently, most of the low-lying building areas were occupied by new inhabitants who were unaware of the flooding risk (Péret and Sauzeau, 2014). The last factor is the predominance of traditional single storey-houses in those low-lying areas. 78% of the deaths in La Faute-sur-Mer occurred in single storey-houses (Vinet et al., 2012). They acted as a trap for people who were unable to evacuate (Lumbroso and Vinet, 2011; Vinet et al., 2012) when 2.5 meters of water was reached in some houses (Creach et al., 2015). Nevertheless, this flooding vulnerability was pointed out before Xynthia, in the Preliminary Flood Risk Assessments (EPRI, 2011), the first step in the implementation of Flood Risk Management Plans from the EU Flood Directive 2007. In those EPRI, the percentage of single storey-constructions in low-lying coastal areas was estimated, and it was revealed that the coastal area between the Noirmoutier Island and the Pertuis Charentais concentrates the largest number of units of this type exposed to marine submersion.

### **3- Relevance of multidisciplinary approaches in coastal flooding knowledge**

In this section, we show, from selected examples, how the multidisciplinary emphasis allows the cross-fertilization of individual disciplines.

#### **3.1- Variability and intensities of marine floods and potential climate connections revealed by combination of historical and sedimentological archives**

In this section, we show how a combination of historical and sedimentological archives provide critical information about past storms and marine floods and enhance our understanding about the variability of marine floods over geologic time.

At time scale of centuries, both sedimentological and historical data provide key information about the past. When available, historical documents can be used to accurately reconstruct the chronology of storm surges deposits (Donnelly et al., 2001b, Sawai et al., 2008). Typically, the chronology of major storm surges established from historical records can be reasonably linked with dated successive event layers (e.g., overwash deposits) even if radiocarbon or other tool ages have uncertainties of few decades (Donnelly et al., 2001b). In this way, Donnelly et al (2001b) have shown that at least seven overwashing hurricanes have occurred in New England in the last 700 years. Historical archives have allowed Garnier (2014) to show graphically how marine floods are part of the coastal history in Europe. Comparing the French center-west shores and those of the North Sea, from 1500 to 2010, reveals some quiet periods (1st half of the 18th century, 2nd half of the 19th and 20th

centuries) and some stormy ones, but the historical science is unable to provide any explanation for this observation. Complementing this effort, Baart et al (2011) computed peak water levels for the greatest storm surges along the Northern Holland coast of the 18th century. Peak water levels were reconstructed from both paintings and geological records. From these peak levels and numerical modeling of coastal processes, a more confident estimate of low-probability storm surges was obtained. But, in areas where beach ridges are the result from marine inundation and not significantly reworked by wind, sandbodies have shown that both the magnitude and frequency of marine submersions have been largely underestimated (Nott, 2015).

Indeed, historical archives may be helpful to relate properties of storm surges sediment records to storm intensity. The relationship between storm intensity and the size of the overwash sand body deposited in a coastal backbarrier lagoon is complex. We have acknowledged some of the confounding factors, including the abundance of sand supply, and we highlight that in order to relate overwash layer thickness to event size, it must be assumed that the geomorphic setting remains roughly the same during the studied period and storm conditions (e.g., timing, duration, angle of approach) (Liu and Fearn, 1993; 2000a). However, recognizing these complexities, it is hypothesized that, in general, a positive relationship exists between storm intensity, storm-surge height, and the development of an overwash sand body for large events. Donnelly et al. (2001a, b) demonstrate that recent and historic major hurricanes on the U.S. Atlantic coast caused significantly higher storm surges than minor hurricanes and winter storms, and that over the past several centuries, only the major storms left a stratigraphically distinct and regionally consistent record of overwash sand layers in coastal marshes. A stratigraphic study of overwash deposits on the New Jersey coast (Donnelly et al., 2003) gives evidence of old overwash sediments, transported a considerably greater distance than more recent overwash fans correlated with recent strong storms (1821, 1938, 1944, 1950 and 1962). The greater distance of transport can be interpreted as resulting from prehistoric storms with much higher intensities than the most intense historical 1821 storm documented on this part of New Jersey coast.

Another example showing the relation between the size of overwash sand bodies and storm intensity is found on the French Mediterranean coast (Dezileau et al., 2011). During the past 50 years no catastrophic intense storm has directly struck the Pierre Blanche lagoon (Fig. 1), except maybe the 1982 storm of Category 2 wind intensity, but this event was not strong enough to deposit sand in the center of the lagoon. A coarse-grained event layer (1982 event) has been identified only in one sediment core, near the lagoon shore. However, three thin sand/silt layers have been observed in different cores collected in the center of the lagoon over 500 m landward from the sandy barrier. These three sand deposits have

interpolated ages of 1742, 1848 and 1893 A.D. (Fig.9). In communal archives, intense storm events were mentioned because they caused damage in the vicinity of the studied city. For the last 300 years, eighteen intense storms occurred in the Languedoc. Among all of these, some were apparently more intense, based on written accounts. The storm of December 4th, 1742, recorded in many city archives around the Aigues-Mortes Gulf, is considered to be the most catastrophic event during the last 300 years along the French Mediterranean coast. The lagoon was covered with a sand layer over 500 m in width. One of the main consequences was the creation of a large inlet, which remained open until 1761. The storm of 23 November 1848 had very strong SSE winds and induced the wreckage of a few ships in the Sète Harbor (Fig. 1). The sea completely submerged defense barriers in the harbor, and the conditions caused many casualties. Documented by many engraved illustrations, the storm of 21 September 1893 also resulted in the devastation of the Sète Harbor and the wreckage of a few ships. More recently, the winter storm of 1982, with 46 m/s maximum gusts caused the death of 15 people and caused a partial devastation of the new Palavas and Carnon Harbors. If the geomorphic setting of the Pierre Blanche Lagoon has not changed drastically during the last 300 years as suggested by ancient maps (see Fig. 3 in Dezileau et al., 2011) and if a positive relationship exists between storm intensity, storm-surge height, and the size of the overwash sand body, these three thin sand/silt layers recorded in the lagoon at more than 500 m from the sandy barrier, were probably formed by a stronger event, perhaps Category 3 wind intensity or more. To conclude, several studies illustrate how, such as for the Wadden Sea (Fruergaard et al., 2013), the recent coastal sedimentary record is in accord with historical archives.

Over the geological time scale (decades to more than millenia), stratigraphic data offer opportunities to reconstruct past intense events and extend insights well beyond the observational record. This can enable a better understanding of possible regional and local long-term trends of storm activity as they relate to past climatic conditions. From Europe to the northern part of Africa, sedimentary coastal archives of Holocene high storm activity periods have been retrieved from backshore environments, such as aeolian dune fields and cliffs (e.g., Hansom and Hall, 2009), back-barrier lagoons (e.g., Dezileau et al., 2011; Sabatier et al., 2012; Raji et al., 2015; Degeai et al., 2015), peat bogs (e.g., De Jong et al., 2006) or sedimentary archives collected from open-marine estuaries (e.g., Billeaud et al., 2009; Sorrel et al., 2009). The timing of storminess maxima for Europe and the northern part of Africa can be defined in five Holocene storm periods (HSPs) consisting of the most widespread stormy intervals during the mid- to late Holocene (Fig. 10 from Sorrel et al., 2012): HSP I (5,800-5,500 cal bp), HSP II (4,500-3,950 cal bp), HSP III (3,300-2,400 cal bp), HSP IV (1,900-1,050 cal bp) and HSP V (600-250 cal bp), the last one coinciding with the

early to mid-Little Ice Age (LIA). Interestingly, these HSP records are strikingly similar to those reported in a terrestrial palaeoclimate record south of Iceland and in sea-salt sodium proxies from Greenland ice cores. These data similarity suggest that the concurrent long-term climate deteriorations from northern Europe and the northern part of Africa respond coevally to a common mechanism. In particular, the time series of these storminess records exhibit peaks corresponding to the ice-rafted debris (IRD) maxima, which have also been tied to cooling events with a cycle of 1,500 years. Bond et al. (1997, 2001) associated this cycle to a solar forcing mechanism, which could have been amplified by the production of the North Atlantic Deep Water (NADW) in response to surface hydrographic changes. Since the pioneering studies of Bond et al. (1997, 2001), many studies have similarly provided evidence of millennial oscillations and have speculated on alternative origins to this climate cycle. By revisiting the IRD data and other well-known series in the North Atlantic by wavelet analysis, Debret et al. (2007, 2009) showed a cyclicity of 1500 yr since the Mid-Holocene potentially related to internal forcing due to the thermohaline circulation. Wanner et al. (2008) analyzed a compilation of worldwide paleoclimate proxies and found a clustering of spectral peaks around 1500 yrs with unclear origin. Later, Wanner et al. (2011) stated that different dynamical processes such as melt water flux into the North Atlantic, low solar activity, explosive eruptions, and fluctuations of the thermohaline circulation likely played a major role in the structure and origin of the millennial-scale Holocene Cold Events. It is noteworthy that Atlantic hurricane counts derived from both overwash sediments sampled on the East Coast of USA and proxy reconstructions of cyclone activity in Puerto Rico show a peak in cyclone activity during the Medieval time (Mann et al., 2009). These studies illustrate how coastal sedimentary systems are directly subjected to changes in storminess and thus can be used to reconstruct millennial-scale climate variability and climatic forcing factors (Sorrel et al., 2012). In this sense, they complement marine and terrestrial archives and offer valuable new insights to reconstruct and understand climate change.

### **3.2- Physical approaches improve the interpretation of historical and sedimentological archives**

One major limitation of both sedimentological and historical archives is that they rarely provide quantitative information, and they cannot solely explain the physical processes leading to marine flooding. In this section we show how oceanography and/or geomorphology and topography can strengthen historical and sedimentological archives by providing additional information about marine flooding. We first show how the historical data can be analysed and in turn how accuracy may be improved. Then, we highlight how

physical oceanography can help interpreting sedimentological records of storm-induced marine submersion.

An example of incomplete historical data enhanced by coastal oceanography and Lidar topographic measurements is provided by Breilh et al (2014). In their study area (southwest coast of France), wind and pressure measurements are available since the end of the 19th century, but tide gauge measurements are missing. So, wind and pressure measurements were used to hindcast historical storm surge using a numerical modeling system. Then, modeled water levels were compared against maximum water levels based on archives and available high-resolution topographic LiDAR data. Areas chosen for estimating past water levels included harbour docks or historical monuments because they are not likely to have changed over time while vertical land motions are not detectable in La Rochelle ([www.sonel.org](http://www.sonel.org)). Historical hindcast efforts revealed that three different meteo-oceanic mechanisms can lead to extreme water levels: a moderate storm surge (about 1 m) in phase with the highest astronomical high tide; a large storm surge in phase with moderate high tide level, and a large storm surge in phase with a moderate high tide level and associated with extremely high waves. Another important result of Breilh et al. (2014) was that water levels on six occasions exceeded 4 m NGF at La Rochelle harbour on the Atlantic coast of France and led to extensive floods. Such results question the return period of 100 years range for water levels ranging from 3.81 and 3.96 (Simon, 2008, Tomasin and Pirazzoli, 2008), as this seems to be an over-estimate (Bulteau et al., 2015).

Another example is given by the chronicle of marine submersions between 1500 and 2015 along the 400 km-long coastline between the Loire and the Gironde estuaries (central part of the Bay of Biscay, Fig. 1) (Athimon, in press). Within this database, 120 submersion events were reported, and 53 submersions may be associated with extreme sea levels. One major limitation of this database is related to the quality of sea-level references. Based on this critical information, the historical archives can be grouped in two main categories. In the first category (about one third of the reported submersions), the sea level is mentioned without any reference level. For this category of documents, further refinement of the inundation levels is impossible. In the second category (two thirds of the reported submersions), mentioned sea levels are relative to known landmarks, so further analysis was possible. Subsequent analysis had three steps: identification of marks mentioned in the archives during a flood, by the historian; characterisation of each mark (location, altitude, quality), and analysis of processes that may explain how the sea level reached the mark. The following description of the 1838 storm and related coastal flooding illustrates the analysis. From the night of 25 to 26 February 1838, a storm occurred associated with a very deep depression, measuring 975 hPa at the Hospital of the Navy in Rochefort (Fig.1), and a tidal prediction indicates that this storm occurred during a high spring tide (reaching 3.2 m NGF in

La Rochelle). The concomitance of this storm and a high spring tide resulted in extensive coastal flooding, along the coast from the Loire Estuary to the Oléron Island (Fig. 1). After this storm on the morning of 26 February 1838, an officer of the public maritime service estimated that the maximum water level exceeded 25 cm above the crest of a jetty located at the entrance of Boyard Harbour (Oléron Island, Fig. 1). This jetty still exists today and is in similar state as it was in 1838. Considering negligible vertical land motions in the area ([www.sonel.org](http://www.sonel.org)), it can be estimated that the height of the crest of this jetty was 4 m NGF. Consequently, the maximum sea level is estimated at 4.25 m NGF, suggesting the storm surge was on the order of 1 m. Similar sea level estimations have also been obtained when and where the inland flooding was accurately described for locations still identifiable today.

Additionally, sedimentological records of storm-induced marine submersion can be analyzed in conjunction with results from modeling of storms, storm surges, runup and overwash. A variety of efforts have used a combination of measurements and modeling of recent overwash processes and their stratigraphic and geomorphic consequences (e.g., Donnelly et al., 2006 and references therein). Nevertheless, there is still a lack of field data, partly due to difficulties of measurements during storm conditions, and more work is needed. The recent storm clustering of winter 2013-2014 caused massive beach and dune erosion in France (Castelle et al., 2015) and led to hazardous overwash, dune breaching and washover deposition (Fig. 11). Post-event surveys and trenches associated with modeling of storm surges and runup allowed correlation of sedimentary units within one washover fan produced by the storms (Fig.11). The fully-coupled tide-wave-surge modeling system of Bertin et al. (2015) was run for the entire winter 2013-2014; it was forced with wind fields from the Climate Forecast System Reanalysis reanalysis (Saha et al., 2010). Wave parameters and water levels were extracted for the study area to compute maximum still water (tide + surge + setup) and runup levels (tide + surge + setup + runup) using the empirical formula of Stockdon et al. (2006). Castelle et al. (2015) and other such studies on recent events show that washover fans may record several overwash areas and offer analogues to ancient storm deposits.

Another example comes from Australia where modeling of storm surge was conducted to reproduce marine inundation by tropical cyclone Larry at Cowley Beach (NE Australia). This modeling allowed the authors to estimate the parameters involved in beach ridge formation (Nott et al., 2009). From modeling results applied along 29 shore-parallel beach-ridge transects, Nott et al. (2009) concluded that extreme tropical cyclones occurred more frequently than that suggested by historical records for this region of NE Australia. As shown by Cheung et al. (2007), modeling results also can provide modern analogs for the interpretation of past storms that lack an instrumental record. This approach was used for

Hurricane Bob that hit New England and helps demonstrate the processes responsible for barrier overtopping and with interpretation of the sedimentary record. A similar approach was undertaken by Woodruff et al. (2008b) who generated a large number of synthetic storms and related overwash records for comparison with sediment archives sampled in Laguna Playa Grande (Puerto Rico, Fig. 1). This comparison allowed the assessment of trends observed within sediment records of paleo-storms and gave evidence for statistically significant changes in hurricane climatology over the last thousands years. Boldt et al., (2010) also compared between sediment records to modeling results with generally good agreement, although some storms were absent. The three previously mentioned studies used defined boundary conditions to produce an overwash signal for comparison with the stratigraphic record. Brandon et al. (2013) creatively employed the reverse approach by developing inverse modeling to constrain storm wind speed from deposits in Florida. Their method was performed using modern deposits and was consistent with historical hurricanes. They found that deposits throughout the last 2500 years are capable of being produced by hurricanes and they observed increased hurricane frequency between 1700 and 600 years BP. This effort and others can help test the notion of changes in frequency of intense hurricane in the Gulf of Mexico and elsewhere.

### **3.3- Combining historical data and numerical hindcast to determine extreme water level return periods**

While geological and historical records can provide information on the extent and frequency of past flooding events, few studies have combined estimates of storm activity from sedimentary records and from statistical model of proxies of past climate changes (Mann et al., 2009). Alternative sources of data can provide more continuous and rigorous information to determine the characteristics of the extreme events that hit the coast. At the simplest level, this characterization involves evaluating the probability associated to extreme sea levels at discrete points based on tide gauge measurements.

The probability of exceedance ( $P_x$ ) of a given threshold water level  $X$  in a given time interval (typically one year) is commonly expressed as the return period  $T_x$ , i.e., the average time interval between two consecutive occurrences. The two concepts are equivalent, and related as  $T_x = (1 - P_x)^{-1}$ . The return period is thus obtained by determining the probability  $P_x$ . For extreme sea levels,  $P_x$  is usually determined by performing statistical analyses on water level time series measured at tide gauges (e.g., Tawn, 1988; Coles, 2001; Bernardara *et al.*, 2011; Bardet *et al.*, 2011; Fortunato *et al.*, 2013). These probabilities can be determined using standard statistical methods. However, the simplest methods do not always provide

adequate results. Measured time series are usually short (typically a few decades) relative to the periods that need to be determined (typically 10 to 1000 years). This limitation can be slightly aggravated by gaps in the data, associated with instrument malfunctioning (Table 1). As a result, the tail of the empirical statistical distributions at the low-frequency (more rare and extreme) levels usually has very few data points. Thus uncertainties are very high for large return periods. In some cases, the strongest storms are outliers in an empirical statistical distribution, casting doubts on their return period (Bardet et al., 2011). These uncertainties are illustrated using data from Brest (Fig. 1), one of the world's oldest tide gauges (Wöppelmann et al., 2006). Excluding the years with significant gaps, there are 131 years of data available, between 1848 and 2011. The extreme sea levels associated with different return periods computed using 20 and 131 years of data display discrepancies on the order of 10 cm (Fig. 12) for both the empirical and an adjusted distribution.

Different methods have been proposed to determine the statistics of extreme sea levels (see Haigh et al., 2010 and Batstone et al., 2013 for recent reviews). Direct methods compute these statistics based on measured extremes. The simpler approach (AMAX) uses only the set of annual maxima, while more sophisticated approaches use several maxima per year (Tawn, 1988; Coles, 2001). In any case, the number of data points used to construct the statistical distribution remains small for most tidal records, and the uncertainty in the tail of the distribution is large. Indirect methods take advantage of the knowledge that tide gauge records combine signals from two different origins: tides and surges. The Joint Probability Method (JPM, Pugh and Vassie, 1980) splits the measured sea level signal into tidal and surge components, and statistically analyses each component independently. The probability distribution of extreme sea levels is then evaluated through the convolution of the probability distributions of the two components. However, the JPM has its own sources of errors (Haigh et al., 2010). In particular, it assumes that (1) the empirical distribution of the surge component is a sufficiently reliable estimate of the true distribution, which may not be valid near the extremes, the region of prime interest, and (2) consecutive hourly measurements of sea levels are independent, neglecting the strong temporal dependence of tides and surges. To address these limitations, several authors improved the JPM. For instance, the revised JPM adjusts an extreme value distribution to the tail of the extremes distribution (Tawn and Vassie, 1989; Tawn, 1992). The JPM is recommended by the U.S. Federal Emergency Management Agency (FEMA, 2012).

The uncertainty introduced by the small duration of the tidal records relative to the return periods that are of practical interest has motivated different approaches to increase the amount of data used in the statistical analyses. Bernardara et al. (2011) and Bardet et al. (2011) combined data from several tide gauges in the same region to increase the amount of



information used in the analysis. Fortunato et al. (2013) and Haigh et al. (2014) obtained smooth empirical distribution functions by generating a large number of synthetic yearly time series through the combination of different tide and surge series. Still, the highest water levels remain limited by the sum of the highest tide and surge levels. Lin et al. (2012) and Lin and Emanuel (2016) drastically increased the amount of data available for the statistical analyses by generating thousands of synthetic storm surge events with a general circulation model, a hurricane model and a circulation model. This approach allowed the simulation of events significantly more severe than any on record, and thus appears a promising avenue to determine extremes with very long return periods, although with large computational costs.

Since the analysis of tide gauge measurements only provides localized estimates of extreme sea levels, long-term numerical simulations of tides and surges are now used to provide the required time series for statistical analysis. This combination of atmospheric and ocean numerical model hindcasts with statistical methods can therefore provide a detailed spatial distribution of extreme sea levels, which was unavailable until recently (Batstone et al., 2013; Zhang and Sheng, 2013, 2015; Fortunato et al., 2016). Also, the availability of forecasts of future climates also provides the means to determine the future extreme sea levels for different climate change scenarios (Marcos et al., 2011, Lin and Emanuel, 2016, Vousdoukas et al., 2016).

Worst-case scenarios, which are often useful to define coastal management plans and strategies, can thus be obtained by extrapolating statistical functions for very large return periods. However, while this approach can provide extreme sea levels at different locations and for different return periods, it fails to provide the oceanographic and atmospheric conditions associated with these extreme sea levels. Since these conditions are necessary to determine the marine flooding condition using numerical models, alternative approaches are required to characterize worst-case scenarios. To illustrate one of these approaches, an ongoing project on marine submersions in the French Brittany (VIMERS-1) is summarized below. Once validated, archives, coming from atmospheric re-analyses (ERA-Intérim, Meteo-France), tidal and water levels measurements (SHOM) and waves and coastal damage (CEREMA) were collected to strengthen and refine statistical laws for computing highest sea level occurrence periods (return period). From these archives, 137 events were analyzed and classified into a typology, consisting of 25 families of storms (Goutx et al., 2014). Each family was characterized by similar criteria as atmospheric storm trajectory, pressure gradient, concomitance with large tidal amplitude. Then, real storms were combined with realistic tidal ranges, but higher than the ones during which they occurred, and the peak surge was synchronized with the high tide, in order to define a set of extreme events that did not occur but that are plausible. These plausible cases feed knowledge of the marine extreme event

hazard. An example of such plausible simulated event, is given in Figure 13 where the 100-year return period extreme sea level at Brest (8.33 m, SHOM-CETMEF, 2012) is exceeded as a result of a 7.68 m tide and 0.95 m storm surge). The highest simulated astronomic tidal sea level at Brest is 7.93 m (Fig.13). Comparison between modeled and measured surge sea level at Brest shows the good accuracy of the numerical model (HYCOM, Morel et al., 2008), in terms of amplitude and phase. Results were compared to the 25 reference events, in order to find similar cases of severe real and fictitious events. This approach also led to the determination of plausible worst-case scenarios of high sea level, waves and inundation risk in the future. At this step of the study, waves and tides have been simulated separately.

#### 4- From new knowledge to adaptation

In this section, we show how the management of future crises and the adaptation to sea level rise and marine submersions by policy makers, coastal managers, civil protection managers and the general public can be supported by new results or techniques from the research community whether of disciplinary or multi-disciplinary origin.

##### 4.1- Marine submersions forecast

Numerical modeling of storm surges and marine floods provides helpful information for marine submersion forecasts. There is two, conceptually very different, approaches to a storm surge forecast: the statistical approach and the dynamical-based deterministic approach (Lorentz, 1963). The statistical approach, which for example includes linear and non-linear regressions and neural networks, is based on the assumption that the storm surge in a specific location at a specific time is correlated to other known variables, usually called *predictors*, and can be estimated as a combination of these, weighted by coefficients, which must be calibrated. In the calibration process, long time series of predictors' values are used to form a cost function, which must be minimised by finding adequate values for the coefficients, which multiply the predictors. Different minimisation techniques can be used to find a minimum of the cost function and the values of the coefficients in the calibration.

The use of statistical methods in storm surge forecasting was probably tested for the first time by Harris (1962). These methods started to be used in Venice since the 70s (Goldmann and Tomasin, 1971; Mosetti 1971) and nowadays are still considered affordable and easy to implement (Canestrelli 1999; Canestrelli and Pastore, 2000; Canestrelli and Moretti, 2004a, b). In a simple linear regression model, if  $s_t$  is the storm surge in a given location at a time  $t$  in the future, it can be expressed as a combination of past and present

predictors (e.g., sea level, pressure gradients, wind), called *predictors*, correlated with it. With  $N$  predictors  $x_n$ , the surge  $s_t$  is:

$$s_t = \sum_{n=1}^N a_n x_{n,t} + \epsilon_t \quad (1)$$

where the coefficients  $a_n$  must be calibrated through the minimisation process and  $\epsilon_t$  the residual error of the minimisation. If  $s_o$  is the surge computed from the observations, corresponding to  $s_t$ , the cost function can be defined as:

$$J = \sum_{t=1}^T (s_o - s_t)^2 \quad (2)$$

Once the coefficients  $a_n$  are known, equation (1) can be used to forecast  $s_t$  using the latest values of the variables  $x_n$ . Good predictors for storm surge forecasting can be atmospheric pressure data from different stations, pressure gradients measured perpendicular to the main wind direction (thus correlated with the geostrophic wind) and tide-removed sea level data (i.e., residual level). In general, statistical models achieve good performance in short-term forecasts, but often they lack accuracy in long forecast and in case of extreme storm surges. This lack of accuracy can be explained considering that they are calibrated with a minimisation of the residual during a long time period, where calm meteorological conditions are statistically more frequent than storm conditions.

Deterministic methods are based on the use of hydrodynamic models which solve the hydrodynamic equations governing the sea dynamics. Many storm surge models use the *Saint-Venant* (or *shallow water*) equations (Eqs. 1-3). The bottom stress and, especially, the wind stress formulations are extremely important for a good forecast. Depending on the study area, an adequate spatial resolution and a good bathymetry can also be important. There are different methods to perform the numerical discretisation of the equations (Fletcher, 1996). The finite-difference method is very popular because of its simplicity and speed; this technique is normally used with regular structured grids. Finite-volume and finite-element methods, when formulated for unstructured meshes allow a better reproduction of the coastline and of the bathymetry, thanks to the possibility of varying the grid resolution. These features are often desirable in small to medium basins (Fig. 14).

Numerical formulations of the equations for storm surge forecasting were developed in the 60s (Welandar, 1961; Jelesnianski, 1965; Jelesnianski, 1966) and in the 70s, some operational systems were developed in the North and in the Irish Seas (e.g. Duun-Chriestensen, 1971; Heaps, 1973; Flather and Davies, 1975). Later also, in the Mediterranean Sea, some systems were developed in the 90s. A first comparison of five two-

dimensional storm surge models running in European seas was made by (De Vries et al., 1995). He concluded that for the accuracy of the forecast, a correct calibration of the model's parameters (mainly the wind drag coefficient and the bottom stress) is more important than the use of a specific model. Another error comes from the wind and pressure fields, which are the primary forcing of a storm surge model. These fields are forecast by some meteorological models and are always affected by forecast errors. Since the predictability of atmospheric variables decreases in case of extreme events and errors increase, the storm surge error increases as well (Horsburgh et al, 2011).

Satellite data can be used to improve both wind and sea level forecast. Recently, in two projects, eSurge and eSurge-Venice, funded by the European Space Agency (ESA), a database of storm surge events from different areas of the world, was created, containing satellite data recorded during the events (<http://www.storm-surge.info/data-access>). In these projects, scatterometer data was tested to improve the wind fields used in the storm surge models, while altimeter data assimilation was tested to improve the initial state of the sea. However, even hydrodynamic models can perform badly in some extreme events and an estimation of the forecast error is useful to help evaluate the hazard. This is why ensemble prediction systems (EPS), initially born for atmospheric weather forecasting, have been recently used also for the sea. Most EPS systems run a hydrodynamic model with different meteorological forcings, which are produced by an ensemble atmospheric model (Flowerdew et al., 2010; Bernier and Thompson, 2015). A different approach is the multi-modeling. In this case uses different hydrodynamic and/or statistical models, with different computational grids and parameters, provide an ensemble of forecasts. Recently, hydrodynamic storm surge models were set up in many sensible areas and several European operational centres deliver forecasts made by both hydrodynamical and statistical models (e.g., Vested et al., 1992; Verlaan et al., 2005; Bajo et al., 2007; Daniel et al., 2009; Werner et al., 2009; Bajo and Umgiesser, 2010).

Storm surges and the related flooding problems can be much more severe and dangerous when they are caused by hurricanes or typhoons (Blain et al., 1994; Dietsche et al., 2007; Graber et al., 2006). This is the case of the eastern coast of the United States, down to the Gulf of Mexico and to the Caribbean Sea, where particularly strong hurricanes happen every year, sometimes enhanced by the El Nino-Southern Oscillation (ENSO, Pielke, 1999). In this area, forecasts of surge and waves are provided by CERA - Coastal Emergency Risks Assessment. The system is based on the use of the ADCIRC finite element hydrodynamic model (Dietrich et al., 2010; Bunya et al., 2010) coupled to the SWAN wave model (Booij, 1999). Often, in case of hurricanes, the conventional atmospheric models do not use a spatial resolution fine enough to represent adequately the wind and pressure

gradients around the hurricane eye and simple parametric models are still used (Holland et al., 2010).

Fig. 14 shows a triangular computational grid, which can be used in a finite element model. The grid covers the Mediterranean Sea, but its resolution is higher in the Adriatic Sea, which is the area of interest in this case. The open boundary conditions are set quite far, in the Atlantic Ocean, in order to reduce the impact of the error in their assignment. Unstructured grids allow the use of a low resolution away from the zone of interest thus reducing the computational cost and to refine areas with a complex coastal morphology or bathymetry. The model is forced with 10 m wind and surface pressure forecast fields, so that the model sea level output represents the surge. The surge, added to the astronomical tide and to the seasonal mean sea level, provides an estimation of the total sea level. Fig. 15 shows the surge forecast in Venice, located in the northern part of the Adriatic Sea, some days before a storm, with (Ass) and without (Back) the use of the assimilation of tide gauge data. The reference surge (Obs) was obtained by removing the tide from the observations by means of a harmonic analysis (Foreman and Henry, 1989). The forecast starts on January 7, 2010, two days before a major storm surge event that happened on January 9, 2010. The forecast without data assimilation is shifted in time with respect to the observations and overestimates the maximum peak. The assimilation of the observations is made the day before the forecast, on January 6, and corrects the dynamic state used as initial condition by the model. On this day the error of the model is reduced drastically and the time shift error is completely corrected. In the forecast period the model always performs better with data assimilation than without, thus showing that errors in the initial state remain for several days.

#### **4.2- From the knowledge of flooding risk to the development decision support tool (The central French Atlantic coast example)**

Recent and/or well-documented floods bring valuable data for anticipating future storm-induced floods (Tavares et al., 2015). Indeed, a significant gap between predicted and observed flooded areas is often noticed. This gap was particularly obvious for the Xynthia Storm, which flooded the coastal zones located in the central part of the Bay of Biscay in 2010. The Bourgneuf Bay, located southward of the Loire Estuary (Figs. 1 and 16), gives an example where observed flooded areas after Xynthia strongly differed from a previously published hazard map (SOGREAH, 2002). Therefore the accurate mapping of flooded areas after recent storms is of key importance to improve the assessment of the coastal zone vulnerability. In this way, the feedback and lessons of the Xynthia Storm have been used, by the fire and rescue department of Charente-Maritime (SDIS 17), to improve the management

of such a crisis. The objectives of this initiative were to highlight the strengths and weaknesses of the operational organization, share them with other stakeholders, improve the safety of rescuers and residents, improve the understanding of the marine submersion and transmit historical knowledge on an exceptional event. To reach these goals, a mapping tool was developed for predicting marine flooding along the coastline from the characteristics of a weather forecast.

SDIS 17 has decided to conduct a study in two stages: first on modeling main storm surges scenarios, which allowed the identification of potentially flooded areas, secondly, on identifying issues present in these areas. Based on the storm surge model of Breilh et al. (2014), different storms surge modeling scenarios were simulated, combining three wind directions (NW, W, SW), three average wind speeds (25, 30, 35m/s) and two high tide levels (mean and extreme spring tides). This model relies on the 2DH implementation of the circulation model SELFE over the central part of the Bay of Biscay (Fig. 1), with a spatial resolution ranging from 10 km along the open boundary to 25 m along the coastline. Then, raster-based flood modeling methods (Breilh et al., 2013) were run and allowed to identify areas vulnerable to submersion. Those vulnerable areas were then merged into a single "envelope" scenario. Although the method includes many approximations (for further discussion about the method, please refer to Breilh et al., 2013), the comparison of modeling results with observations obtained during Xynthia Storm indicates that the method provide acceptable results. Based on the "envelope" scenario, the main human stakes threatened by submersion were identified. Within the 84 towns threatened by submersion, the main stakes include:

- Companies and among them, those subjected to the regulations on classified installations for environmental protection, like industries that use chemicals, gas stations (French law n°76-663 of the 19 July 1976).
- Public buildings, especially schools, retirement home, campsites.
- Residential or seasonal habitat.

A vulnerability index was defined, based on predicted water level, dikes levels, architectural characteristics including the presence or absence of storeys, window guards, electric curtain, etc... (Chevillot-Miot et al., 2013; Creach et al., 2015; Fig. 17).

Combining all these data, submersion consequences are better assessed, allowing the SDIS 17 to deploy the rescue teams as close as possible as submerged areas and to build an intervention map including expected water levels while targeting the vulnerabilities of the intervention area.

This scalable mapping, based on indexed scenarios should allow distributing the teams in the most judicious manner, on the field. This mapping is also helpful to prepare an evacuation zone or to identify retreat zones.

A more detailed version of this methodology (Figs.16 and 17) has been developed with the support of the SDIS 17 to be an integrated decision tool, the so-called VIE index (Flood Vulnerability Index, Creach et al., 2015). This index is based on works conducted for river floods, or tsunamis (Pistrika and Jonkman, 2010; Leone et al., 2011; Vinet et al., 2012; Chevillot-Miotet al. 2013), and aims at locating and identifying houses presenting life-threatening risk in case of coastal flooding. The VIE index is calculated for each house and depends on four criteria (Fig 17):

- Potential water level inside the house in case of coastal flood. The higher the potential water level in the house, the higher is the vulnerability. Vulnerability related to water level ranges from 0 (no water in the house) to 4 (more than the 2 m water level reached during Xynthia).
- Distance between the house and a flood defenses. The smaller the distance between the house and flood defenses, the higher the vulnerability. Vulnerability related to distance between the house and a flood defenses ranges from 0 (more than 600 m between the house and the flood defense) to 4 (less than 100 m).
- Architectural type (single-storey, single-storey with rescue level, multi-storey construction). A single-storey house is more dangerous than a multi-storey one in case of flooding because people cannot escape upstairs. Vulnerability related to architectural type ranges from 0 (multi-storey with unoccupied ground floor) to 4 (single-storey without roof evacuation). A house can be a trap for people in case of coastal flood if water level is important and rapidly rises in the house. In the specific case of houses close to flood-defenses or breaching of flood-defenses, people can be surprised how quickly the water level rises and may not be able to escape upstairs (in case of single-storey) or outside (in case of remoteness from a rescue point).
- Distance between the house and a rescue point. Short distance between a house and a rescue point facilitate the shelter of people before a flood. Vulnerability related to distance between the house and a rescue point ranges from 0 (house located in a rescue area) to 4 (house located at more than 200 m from a rescue area).

The formula of the VIE index has been tested through a statistical validation: a correlation matrix has confirmed the non-redundancy between the different criteria and a

Monte-Carlo analysis has demonstrated the robustness of the index (Creach et al., 2015). Results are divided in four classes, depending of the score of each house (Fig. 18). The green class concerns the less vulnerable houses that are constructions located outside potentially flooded area. The black class concerns the most vulnerable houses that are constructions where all people are exposed to injury and death in case of coastal flooding. These classes have been delineated using feedbacks and lessons from Storm Xynthia (Creach et al., 2015). Using this index, a vulnerability assessment of houses and adaptation solutions to protect lives in case of flooding can be proposed (Creach, 2015). This work was realized in a prospective view in order to answer to the question: how can we prevent a toll such the one of Storm Xynthia in future, in a context of sea level rise? Regarding the level of vulnerability identified with the VIE index, a Coast-Efficiency Analysis (CEA) was provided to compare the efficiency of different adaptation measures in regard of the number of life it could potentially save (using mortality functions, see Jonkman et al., 2008). The adaptation measures include:

- The upgrading offlood defences which is the most common measure for protection of urbanized area against floods (Klein et al., 2001).
- The architectural adaptation, which consists of building storeys on single storey houses and considering new architecture for future buildings (Nicholls, 2011).
- Warning and evacuation, which is the best way to prevent death in case of imminent flood (Parker et al., 2009). Evacuation could be facilitated with the installation of rescue point as proposed by IPCC (2014).
- Resettlement, which consist of destruction of the most vulnerable buildings.

This CEA shows that in most of the cases, the less expensive and the more efficient measure in order to save lives is warning and evacuation, which is achieved at a cost of around 200,000 € per life saved. Resettlement is a more expensive (around 10 millions € per life saved) but very efficient measure and therefore can be restricted to the most vulnerable areas. Architectural adaptation provide a compromise with an average cost of about 2 million € per life saved. To conclude, a mix between architectural adaptation and improvement in prevention and warning seems to be a good deal between cost and efficiency in protecting human life from a coastal flood such as Storm Xynthia.

#### **4.3- Managing realignment of coastal defenses**

In a context of sea-level rise and local increase in storminess related to global warming, the question of reinforcement or adaptation of coastal defences is critical. Mitigating storm surge risks by applying estuary-engineering solutions has already been



discussed (von Storch et al., 2008). Two options for estuary redesign include (1) adding obstacles, like sandbank or islands in order to dissipate tides and (2) flooding areas for tidal and surge dissipation and retention of water to reduce peak water levels.

Several studies based on numerical experiments have investigated the impact of coastal flooding on water levels in estuaries or (enclosed) bays bordered by flooded marshes. Townend and Pethick (2002) investigated the impacts of removing coastal defences in the Humber Estuary in case of storm surge scenario. The removal of coastal defences allowed the flooding of extensive marches resulting in a water level reduction locally exceeding 1 m. A similar water level reduction up to 1 m was highlighted by Bertin et al (2014) by comparing the results of a simulation of the flooding associated with Xynthia against a similar simulation where the flooding was disabled through increasing artificially the height of dikes and barriers. Comparable order of magnitude of water level reduction were obtained by Waeles et al. (2016) in two sites of the eastern English Channel: Authie Bay and Dives Estuary (Fig. 1) for which simulations of assessed future extreme events were run within the framework of risk mapping. Such results show that massive flooding of coastal marshes or uninhabited lowlands can significantly limit the high water levels seaward. Indeed, like expansion areas dedicated to minimize the risk on vulnerable areas during river flood events, the realignment of coastal defences may constitute a promising adaptation to flooding during storm surges and future sea level rise. The managed realignment, also called de-polderisation, has begun in Europe since the 1980s (Goeldner-Gianella, 2007) but only concerns 1% of the 15,000 km<sup>2</sup> of tidal polders in all of Europe. In the United States such schemes are more common and older (Titus, 1991). Indeed, beyond the limitation of water levels, and the role of barrier to surges, the temporary inundation and restoration of marches and lowlands in estuarine environments bring several advantages. First of all it reduces costs, as the price of coastal defences is of the order of 50 to 500 Euros per m coastline per year (van Rijn, 2011). When dikes are located further inland (i.e. not directly along the coastline), their design is less constraining as they can experience lower sea levels and significantly reduced wave energy. In addition, for specific configurations it provides nursing ground for many species of fish and shellfish, resting places for migratory birds, and natural cleaning of ground and surface waters. Compared to US or UK, depolderisation has rarely been used in France (Goeldner-Gianella et al., 2015). Following the recent marine floods of Xynthia (2010) and Martin (1999), risk management techniques for sea flooding mainly consist of raising or reinforcement of dikes. Nevertheless, given the very high dike repair and maintenance costs and the positive ecological impacts of depolderisation, the French Coastal Conservation Agency (Conservatoire du Littoral) and one national reserve (Belle Henriette near La Faute-sur-mer where 27 people passed away during Xynthia) decided to stop repairing the dikes bordering some protected natural coastal areas.

Further considerations have to be highlighted for coastal defences realignment strategy. An important feature is related to the non-stationarity of the sea level around high tide: the faster are the (tidal) level variations, the more efficient is the water level reduction related to marshes or lowlands flooding. Then, the realignment strategy is likely to be more efficient for larger tidal range areas. We have also to keep in mind that realignment planning and related hydrodynamic studies have to be carried out on the global scale of coastal systems (bays, estuaries, inlets...). Historically, borders between administrative areas were defined at the location of bays and estuaries. Then defence strategies and risk mapping are often managed at local scales and the consequences are unrealistic risk mapping and unsuitable coastal defence strategies.

#### **4.4- Sea flooding in the context of climate change: which legal perspectives for adaptation?**

Climate change implies reviewing the public policies implemented in areas that are particularly exposed to natural risks. From the legal perspective, only a few texts – international, European or national – pay specific attention to the risk of marine flooding. The main international instrument dealing with the subject of flood is related to the Convention on the Protection and Use of Transboundary Watercourses and International Lakes and then is not directly applicable for marine aspects. International guidelines and regulations for flood risk management have been given through the United Nations Economic Commission for Europe in 2009 (Transboundary Flood Risk Management Experiences from the UNECE Regions, United Nations, New York and Geneva, 2009) and are applicable to the river basin using a combination of measures.

The International Community has expressed three other preoccupations. First of all, the UN General Assembly has adopted a Resolution, the 22 December 1989, on Possible adverse effects of sea level rise in Islands and coastal areas, particularly low-lying coastal areas. Secondly, some international conventions such as 1971 Ramsar Convention on Wetlands, 1992 UN Framework Convention on Climate Change or Convention on Biodiversity have developed plans and actions on integrated coastal zone management that can include sea flood prevention. Thirdly, international cooperation can be developed to encourage systematic action to address disaster risk. Yokohama Strategy for a Safer World: “Guidelines for Natural Disaster Prevention Preparedness and Mitigation” and its Plan for Action (Yokohama Strategy) adopted in 1994 provides landmark guidance on reducing disaster risk and the impacts of disasters. The Hyogo Framework for Action 2005-2015 “Building the Resilience of Nations and Communities to Disasters” adopted by the World

Conference on Disaster Reduction held in Kobe in 2005 gives international guidelines and regulations for floods management. One of the main objectives is to ensure that Disaster Risk Reduction is the national and local priority with strong institutional basis for its implementation.

At the European level, the EU Directive 2007/60/CE on the assessment and management of flood risks implemented in coordination with the EU Water Directive 2000/60/EC has given a global approach about how to prevent and manage the impacts of climate change on the occurrence of floods. The EU Directive has also clarified the definition of flood (article 2.1 Directive 2007/60/CE), for a more in-depth definition see Wisner, et al. (2012). Three major requirements for Member States are given in the Directive: assessment of the risk from flooding, mapping the flood extent and assets and humans at risk in these areas, and adoption of adequate and coordinated measures to reduce flood risk. A white paper introducing “An EU Strategy on adaptation to climate change” supports an integrated and coordinated approach at the Community level (EU Strategy on Adaptation to Climate Change, 16/04/2013). This paper also refers to the vulnerability of Europe with regards to climate change, and it points to the absence of an exhaustive evaluation of that vulnerability, as well as the lack of indicators and studies at the Member States level. The objective of the paper is to improve resilience in the European territory, and several principles for action are recommended: the precautionary principle, according to a long-term approach; an adaptive risk management, taking into consideration the diversity and specificity of local situations, the principle of respect of the ecosystems capacity, and the management efforts regarding natural processes. The study on risk prevention in European States establishes both structural measures of adaptation and prevention (flood defence works, dikes), as well as non-structural measures (alert systems, regular information made available to the citizenship). Nevertheless, each State attributes a different importance to these measures. The Netherlands has focused its adaptation strategy on expensive flood defence works, financed by individual and collective contributions. Considering the cluster of flooding events, the United Kingdom is very much exposed and has focused on the management of territorial occupation, by making populations aware of their responsibilities. The main objective is making the location of housing durable, by working on urban planning. The Department for Environment, Food and Rural Affairs (DEFRA) through its Environment Agency plays a central role regarding the coordination of risk prevention, as well as in the management of defence works; which allows for coherent and efficient actions. In parallel, no financing has been envisaged for the compensation of the populations who would like to leave the risk zones, and the private insurance system is not efficient enough. Another interesting example of a non-European system of risk prevention and management is the one of the USA. The consequences of hurricane Katrina unveiled all the weaknesses of the system of natural risk

prevention in the country, even though the authorities had announced the storm 56 hours prior to its occurrence (Sobel and Leeson, 2006). Differing from the English case, the US protection mechanism (mainly through dikes) is disconnected from the units of natural risk management. The failure of federal authorities when it came to coordinating all the mechanisms of intervention raises questions concerning the need of a global response that will also count on local governments. The National Incident Management System (NIMS) was created, in order to allow local and federal authorities to coordinate their means and actions. In parallel, a National Response Plan (NRP) was elaborated in collaboration with the NIMS, with operational procedures for crisis management. However, urban planning was not re-evaluated, when it came to risk exposure.

At the French national level, the fight against the intensification of the greenhouse effect and the prevention of risks linked to global warming is considered a “national priority” by a law of 19 February 2001 (Loi n°2001-153 du 19 février 2001 tendant à conférer à la lutte contre l'effet de serre et à la prévention des risques liés au réchauffement climatique la qualité de priorité nationale et portant création d'un Observatoire national sur les effets du réchauffement climatique en France métropolitaine et dans les départements et territoires d'outre-mer). The national adaptation plan (Plan National d'Adaptation au Changement Climatique, PNACC), in agreement with article 42 of the law of 3 August 2009 on environmental programming, has the objective of introducing concrete operational measures to prepare the country to face the new climatic conditions. On their side, the regional schemes “State-region” focus on territorial policies in the area of adaptation to climate change. This territorial approach to adaptation is based on the regional schemes climate-air-energy (Schéma Régional du Climat, de l'Air et de l'Energie, SRCAE) and the regional schemes on ecologic coherence (Schéma Régional de Cohérence Ecologique, SRCE). In the specific domain of flooding, a plan concerning fast flooding (2011-2016) was elaborated after Xynthia storm and the flooding of the Var region in June 2010. The plan, which includes a section on coastal areas risks, was validated on 17 February 2011. It is divided in four types of actions concerning the relevant public authorities:

(1) Urban management and adaptation of buildings. Each region affected by the “post-Xynthia context” must adopt a plan on coastal natural risks prevention and elaborate a national reference document for the adaptation of housing in the zones liable to flooding by 2012.

(2) Improving the knowledge of hazards. Surveillance, alert and crisis management mechanisms must be developed. The creation of a national observatory for natural risks in 2012 by the State, local authorities and insurance companies, among others, constitutes a step forward in this direction.

(3) Improving the reliability of defence works and protection systems. This refers to the specification of competences on dikes restoration and management. The law for the modernisation of public action and cities of 2013 gives the municipalities competence over the management of aquatic environments and the prevention of flooding. Thus, it strengthens the local competences in this area of risk prevention.

(4) Improving the resilience of populations in zones prone to flooding. This plan aims at strengthening the consideration given to sea flooding risks in public information documents (“Documents d’Information Communaux sur les Risques Majeurs” and “Dossiers Départementaux sur les Risques Majeurs”).

After examination of these law instruments mainly conceived at the national level, it appears clear that the quest for adaptation to climate change encourages the development of public policies that are more engaged with the prevention and management of flooding risks. It seems important to promote a “culture of risk”, by paying attention to reference climate projections in specific territories, and create climate services that tackle all the potential impacts of climate change. The reference scenarios could be conceived at different territorial levels, taking into consideration their geographic particularities. They should guide the planning of adaptation policies and put in place more efficient regional schemes of ecologic coherence, open to the prevention of future risks –notably, when it comes to flooding. Local urban planning should be developed with a cartography that constantly updates future risks (Bonduelle and Jouzel, 2014). But, most of all, the preservation and restoration of ecosystems must remain a priority, in order to limit the risks and decrease the impacts beforehand. The conservation of coastal ecosystems is still the best guarantee against natural risks (Beck and Shepard, 2012; Mirza et al., 2005, Millennium Ecosystem Assessment, 2005), and this means that environmental law must become a priority among other branches of law. The approach and instruments proposed by integrated coastal zone management and used by local communities should contribute to the anticipation of flooding risks.

Improved adaptation of societies to coastal flooding is also possible today by the effectiveness of preventive evacuations. Evacuation in the case of flooding related to storm surges is much easier than in the case of flooding by tsunamis. Thus India has averted a humanitarian disaster in October 2013 during the passage of Hurricane Phailin classified as category 5 (Murty et al., 2014), thanks to the perfect control of the displacement of over 860,000 people in the single state of Orissa, where only 22 victims were recorded (Orissa Cyclone Appeal No. 28/1999 Final Report). Fourteen years ago, in 1999, a super-cyclone of the same magnitude had resulted in about 10,000 victims along the eastern coast of India (Chhotray and Few, 2012), during an episode marked by inadequate preparation for flooding.

The strategic retreat is another category of adaptation to the risk of flooding. It is increasing in some exposed regions, where a socio-political context is unfavourable to the anticipation by the authorities. It is notably what reveals the study conducted by Zaninetti (2013) on Mississippi coasts, several years after Katrina. The population density has decreased along this coastline as it has increased inland (at distances over 5 km from the coastline) in higher areas, which were not affected by the flooding associated with Katrina. This rapid population migration related to increase in costs for maintenance of coastal defence systems and insurance premiums has been called "second-order" adaptation (Birkmann, 2011), because it encompasses processes of adjustment to consequences of first-order measures and structures developed to adapt to floods (mainly coastal defences). This case study shows that insurance market is therefore a more effective lever than public planning to boost the strategic retreat of coastal urbanization. Moreover, the strategic retreat can be a political choice.

## 5- Conclusions

This synthesis of storm-induced marine flooding relies on recent studies that span several scientific disciplines. This review highlights some key-points that are useful for the management of future crises and for the planning efforts to adapt to sea-level rise and marine flooding.

Significant progress has been made in numerical modeling and in-situ measurements. Furthermore the increasing accuracy of bathymetry and topography data makes it possible to better understand the physical processes involved in storm-induced marine flooding and to better reproduce them by means of numerical models. The forecast of these models is getting more and more accurate in the estimate of the flood's extension. Provided that the nearshore bathymetry/topography is accurately known, the main issue in storm surge reproduction is the accuracy of the atmospheric forcing, mainly the surface wind over the sea, and of the roughness of the sea surface, which influences the wind stress, especially for cyclonic systems.

Detailed chronologies of past marine flooding events have been locally compiled from both historical archives and sediment records and revealed forgotten and pre-historic major events. Such chronologies, together with numerical model results, validation data from recent events and statistical analyses can be used to define local storm surge thresholds and return periods of extreme events. Similar multidisciplinary studies are used to predict worst-case scenarios and anticipate future flooding. In addition to the physical hazard risk assessment, the vulnerability parameters of coasts can be identified from well-documented events. Therefore, in some coastal areas, the level of knowledge is sufficient to predict the geographical extension of a flooding for different storm scenarios and also to define a vulnerability index. This vulnerability index coupled with a cost-benefit analysis allows comparing the effectiveness of different adaptation in minimizing damages and saving lives. Numerical experiments are also helpful to explore the efficiency of different coastal defense strategies. In particular they show that the realignment of coastal defences (e.g., dykes) may constitute a promising adaptation to storm surge flooding and future sea level rise.

However, while there is much new knowledge, it may have not been made available to managers and the public, or it may not be being used for policy decisions or in development planning. Indeed, only some literatures address the risk of marine flooding locally, regionally or globally. At the international level, a resolution on possible adverse effects of sea-level rise in coastal areas was adopted and some international conventions have developed plans and actions including sea flood prevention. In Europe, there is a directive on the assessment and management of flood risks. Recent catastrophic events and their unintended consequences in terms of casualties and damages have triggered political

actions and investments particularly after Hurricane Katrina in United States and the catastrophic coastal flood of 2010 in France.

From this review we suggest some specific areas that should be targeted for future research:

- (1) Improving the understanding of the physical processes controlling storm surges and their representation in numerical models.
  - (1.1) While the role of atmospheric pressure gradients is now well understood and taken into account in storm surge models, the parameterization of the surface stress, its dependence on the sea state under multi-modal spectra and extreme wind patterns are all issues topics required more research and debate in the scientific community.
  - (1.2) Several studies have shown that, in some locations, the wave setup could propagate outside surf zones and therefore contribute to storm surges significantly. Accounting for this process in operational modeling system requires a higher spatial resolution, which poses a computational challenge. Finally, short wave runup and infra-gravity waves can produce intermittent but significant flooding, but accounting for these processes at large scale would be also very challenging.
  - (1.3) Although flooding due to wave overtopping can be represented using phase-resolving models like the one shown in section 2.1.2.2, the heavy computational resources required still prevent widespread application at regional scales. Better and faster models are needed.
  - (1.4) Data assimilation is another major issue to improve storm surge forecasts. Two types of sea level observations can be assimilated in a storm surge model: satellite altimetry and tide gauges. Blending methods and combining high temporal-resolution and real-time tide-gauge data and the broad spatial coverage of satellite altimetry, could significantly reduce the error for storm surge forecasting (e.g. Madsen et al., 2015).
  - (1.5) Recent and future improvements in the understanding physical processes will in turn allow improvements in data assimilation techniques, e.g., parameterization of the wind drag coefficient as a control variable of the assimilation scheme, specific approach for shelf surge resonance.
- (2) Pursuing research on past marine floods on unexplored coastal areas. Many historical archives and sediment records are still not analyzed and many coasts where historical archives are absent left unexplored. One of the hardest obstacles in analysis of sedimentological records of past marine floods is related to absolute chronology of events that occurred during the last centuries.



- (3) Vulnerability parameters are greatly variable from one coast to another and it is necessary in most cases to refine vulnerabilities diagnosis to better anticipate crisis management (warning, prevention, evacuation). Vulnerability indicators should especially be developed taking into account social aspects. The lack of adequate legal instruments to prevent the management of flooding risks can participate to the vulnerability. New legal indicators of vulnerability (such as level of legitimacy of the rule, level of the prevention rules in the hierarchy of norms, level of the integration of risks prevention in public policies...) should be created.
- (4) Meanwhile, adaptation measures (adapted buildings, installation of easily accessible refuges, relocation/retreatment) should be developed, to create more resilient territories, with strong institutional basis.
- (5) Performing comprehensive sensitivity analysis on coastal realignment configurations, on both schematic and realistic coastal systems. Tests carried out with numerical models could be related, among others, to the relevancy and, when appropriate, to the height of a first row of submersible dikes along the coastline. Realignment configurations should also be tested with regards to the characteristics (topography, roughness...) of the expansion area between the first row of dikes and non-submersible dikes protecting vulnerable areas behind. Guidelines for realignment strategies, addressed to the managing authorities and coastal engineering companies, could be achieved.
- (6) Finally, it seems essential to develop or strengthen the risk culture, including evacuation simulations, in order to keep alive the awareness of exposed populations, which represents a very sensitive factor to reduce the potential death toll in case of disaster.

**Acknowledgments:** This synthesis article is the result of the exchanges and discussions that occurred during the meeting, « Marine submersions: Past, Present and Future », organized by the University of La Rochelle, during a period of three days (19, 20 and 21 June 2014) in Rochefort, La Faute-sur-Mer and La Rochelle. The choice of these three towns was justified because they were severely hit by two recent storm-related marine submersions: Martin (December 1999) and Xynthia (February 2010) and they represent various examples of coastal vulnerable areas. The main objective of this meeting was to bring together researchers from different disciplines, coastal managers, managers of civil security and policy makers in order to exchange recent knowledge about marine submersions, in particular, their physical processes, their forecast, the vulnerability of the coasts and their inhabitants, the past marine submersions and the management and the adaptation to future marine submersions. This meeting was funded by Région Poitou-Charentes, Conseil général de Charente-Maritime, Communauté d'agglomérations de La Rochelle, Communauté d'agglomérations de l'île de Ré, Corderie Royale de Rochefort, Parc Naturel Interrégional du Marais Poitevin, Université de La Rochelle. X. Bertin was partly funded by the European FP7 project Risc-Kit (Grant Agreement n° 603458). We thank Sam Bentley and one anonymous reviewer for their useful comments, which help us to greatly improve this article.

## References

- Aigner, T., 1985. Storm Depositional Systems – Dynamic Stratigraphy in Modern and Ancient Shallow-Marine Sequences. In: Friedman, G.M., Neugebauer, H.J., Seilacher, A. (Eds.), *Lecture Notes in Earth Sciences* 3, 174 p., Springer Verlag Berlin.
- Alcántara-Ayala, I., 2002. Geomorphology, natural hazards, vulnerability and prevention of natural disasters in developing countries. *Geomorphology* 47, 107–124.
- Allison, M.A., Sheremet, A., Goñi, M.A., Stone, G.W., 2005. Storm layer deposition on the Mississippi–Atchafalaya subaqueous delta generated by Hurricane Lili in 2002. *Continental Shelf Research* 25, 2213–2232.
- Allison, M.A., Dellapenna, T.M., Gordon, E.S., Mitra, S., Petsch S.T., 2010. Impact of Hurricane Katrina (2005) on shelf organic carbon burial and deltaic evolution, *Geophys. Res. Lett.*, 37, L21605, doi:10.1029/2010GL044547.
- Andrade, C., Freitas, M.C., Moreno, J., Craveiro, S.C., 2004. Stratigraphical evidence of Late Holocene barrier breaching and extreme storms in lagoonal sediments of Ria Formosa, Algarve, Portugal. *Marine Geology* 210, 339–362.
- Apotsos, A., Raubenheimer, B., Elgar, S., Guza, R.T., Smith, J.A., 2007. Effects of wave rollers and bottom stress on wave setup. *Journal of Geophysical Research* 112, C02003, doi:10.1029/2006JC003549.
- Arakawa, H., Ishida, Y., Ito, T., 1961. *Nihon takashio shiryō*. Meteorological Research Institute (in Japanese).
- Athimon, E., in press. Adversités météo-marines : reconstruction historique, impacts et résilience en Anjou, Poitou, Bretagne méridionale (xive-début xvie siècles) », 10 p., Laget, Rabot, Josserand (dir.), *Entre terre et mer. Hommes, paysages et sociétés dans l'Ouest atlantique, Moyen Âge et Temps modernes*, PUR Editions, Rennes.
- Aucan, J., Hoeke, R., Merrifield, M.A., 2012. Wave-driven sea level anomalies at the Midway tide gauge as an index of North Pacific storminess over the past 60 years. *Geophysical Research Letters* 39 (17), L17603.
- Baart, F. Bakker, M.A.J., van Dongeren, A., den Heijer, C., van Heteren, S., Smit, M.W.J., van Koningsveld, M., Pool, A., 2011. Using 18th century storm-surge data from the Dutch Coast to improve the confidence in flood-risk estimates. *Natural Hazards and Earth System Sciences* 11, 2791–2801.
- Baines, G. B. K., McLean, R. F., 1976. "Sequential studies of hurricane deposit evolution at Funafuti Atoll". *Marine Geology* 21, M1–M8.
- Bajo M., Zampato L., Umgiesser G., Cucco A., Canestrelli P., 2007. A finite element operational model for storm surge prediction in Venice. *Estuarine, Coastal and Shelf Science* 75 (1), 236–249.
- Bajo M., Umgiesser G., 2010. Storm surge forecast through a combination of dynamic and neural network models. *Ocean Modelling* 33 (1), 1–9.
- Bardet, L., Duluc, C.-M., Rebour, V., L'Her, J., 2011. Regional frequency analysis of extreme storm surges along the French coast. *Natural Hazards and Earth System Sciences* 11, 1627–1639.

- Barriendos, M., 2010. Les variations climatiques dans la péninsule ibérique : l'indicateur des processions. *Revue d'Histoire Moderne et Contemporaine* 57 (3), 131–159.
- Barousseau, J., Akouango, E., Bâ, M., Descamps, C., Golf, A., 1996. Evidence for short term retreat of the barrier shorelines. *Quarterly Science Reviews* 15, 763–771.
- Batstone, C., Lawless, M., Tawn, J., Horsburgh, K., Blackman, D., McMillan, A., Worth, D., Laeger, S., Hunt, T., 2013. A UK best-practice approach for extreme sea-level analysis along complex topographic coastlines. *Ocean Engineering* 71, 28–39.
- Beck, M. W., Shepard, C., 2012. Coastal Habitats and Risk Reduction: World at Risk Report, Alliance Development Works.
- Bentley, S.J., Keen, T.R., Blain, C.A., Vaughan, W.C., 2002. The origin and preservation of a major hurricane bed in the northern Gulf of Mexico: Hurricane Camille, 1969. *Marine Geology* 186, 423–446.
- Bentley, S.J., Nittrouer, C.A., 2003. Emplacement, modification, and preservation of event strata on a flood-dominated continental shelf: Eel shelf, Northern California. *Continental Shelf Research* 23, 1465–1493.
- Bentley, S.J., Sheremet, A., 2003. New model for the emplacement, bioturbation, and preservation of fine-scaled sedimentary strata. *Geology* 31 (8), 725–728.
- Bentley, S.J., Sheremet, A., Jaeger, J.M., 2006. Event sedimentation, bioturbation, and preserved sedimentary fabric: Field and model comparisons in three contrasting marine settings. *Continental Shelf Research* 26 (17–18), 2108–2112.
- Bernardara, P., Andreewsky, M., Benoit M., 2011. Application of regional frequency analysis to the estimation of extreme storm surges. *Journal of Geophysical Research* 116, C02008, doi:10.1029/2010JC006229.
- Bernier, N.B., Thompson, K.R., 2015. Deterministic and ensemble storm surge prediction for Atlantic Canada with lead times of hours to ten days. *Ocean Modelling* 86, 114–127.
- Bertin, X., Fortunato, A.B., Oliveira, A., 2009. A modeling-based analysis of processes driving wave-dominated inlets. *Continental Shelf Research* 29, 819–834.
- Bertin, X., Bruneau, N., Breilh, J.F., Fortunato, A.B., Karpytchev, M., 2012. Importance of wave age and resonance in storm surges: The case Xynthia, Bay of Biscay. *Ocean Modelling* 42, 16–30.
- Bertin, X., Li, K., Roland, A., Zhang, Y. J., Breilh, J.F., Chaumillon, E., 2014. A modeling-based analysis of the flooding associated with Xynthia, central Bay of Biscay. Submitted to *Coastal Engineering*.
- Bertin, X., Li, K., Roland, A., Bidlot, J.R., 2015. The contributions of short-waves in storm surges: two case studies in the Bay of Biscay. *Continental Shelf Research* 96, 1–15.
- Beucher, S., Reghezza-Zitt, M. (Dir. Veyret, Y.), 2004. Les risques. Ed. Bréal, *Amphi Géographie*. 208 p.
- Billeaud, I., Tessier, B., Lesueur, P., 2009. Impacts of late Holocene rapid climate changes as recorded in a macrotidal coastal setting (Mont Saint-Michel Bay, France). *Geology* 37, 1031–1034.

- Birkmann J., 2011. First- and second-order adaptation to natural hazards and extreme events in the context of climate change. *Natural Hazards* 58, 811–840.
- Blain, C., Westerink, J., Luettich, R., 1994. Domain and grid sensitivity studies for hurricane storm surge predictions. In: Peters, X.A. et al. (Eds.), *Computational Methods in Water Resources*, Heidelberg, 1994.
- Blake, E.S., 2007. The deadliest, costliest and most intense United States tropical cyclones from 1851 to 2006 (and other frequently requested hurricane facts). NOAA Technical Memorandum NWS TPC 5, 43 p.
- Blumenstock, D.I., 1958. Typhoon effects at Jaluit Atoll in the Marshall Islands, *Nature* 182, 1267–1269, doi: 10.1038/1821267a0.
- Boldt, K.V., Lane, P., Woodruff, J.D., Donnelly, J.P., 2010. Calibrating a sedimentary record of overwash from Southeastern New England using modeled historic hurricane surges. *Marine Geology* 275, 127–139.
- Bond, G., Showers, W., Cheseby, M., Lotti, R., Almasi, P., deMenocal, P., Priore, P., Cullen, H., Hajdas, I., Bonani, G., 1997. A Pervasive Millennial-Scale Cycle in North Atlantic Holocene and Glacial Climates. *Science* 278 (5341) 1257–1266.
- Bond, G., Kromer, B., Beer, J., Muscheler, R., Evans, M.N., Showers, W., Hoffmann, S., Lotti-Bond, R., Hajdas, I., Bonani, G., 2001. Persistent Solar Influence on North Atlantic Climate During the Holocene. *Science* 294 (5549), 2130–2136.
- Bonduelle, A., Juzel, J., 2014. L'adaptation de la France au changement climatique mondial, Avis du Conseil économique, social et environnemental, mai 2014, Les éditions des journaux officiels.
- Bonnot-Courtois, C., Feiss-Jehel, C., de Saint-Léger, E., 2008. Vulnérabilité des rivages en Côtes d'Armor (Bretagne Nord, France): aléas et enjeux. *Actes des Xe Journées Nationales Génie Côtier – Génie Civil*, 14-16 octobre 2008, Sophia Antipolis, 191–200.
- Booij, N., Ris, R.C., Holthuijsen, L.H., 1999. A third-generation wave model for coastal regions, Part I, Model description and validation. *Journal of Geophysical Research* C4 (104), 7649–7666.
- Boose, E.R., Chamberlin, K.E., Foster, D.R., 2001. Landscape and regional impacts of hurricanes in New England. *Ecological Monographs* 71, 27-48.
- Brandon, C.M., Woodruff, J.D., Lane, D.P., Donnelly, J.P., 2013. Tropical cyclone wind speed constraints from resultant storm surge deposition: A 2500 year reconstruction of hurricane activity from St. Marks, FL. *Geochemistry, Geophysics Geosystems* 14 (8), 2993–3008.
- Breilh, J.-F., Chaumillon, E., Bertin, X., Gravelle, M., 2013. Assessment of static flood modeling techniques: application to contrasting marshes flooded during Xynthia (western France). *Natural Hazards and Earth System Sciences* 13, 1595–1612.
- Breilh, J.-F., Bertin, X., Chaumillon, E., Giloy, N., Sauzeau, T., 2014. How frequent is storm-induced flooding in the central part of the Bay of Biscay?". *Global and Planetary Change* 122, 161–175.

- Brown, J.M., Wolf, J., 2009. Coupled wave and surge modelling for the eastern Irish Sea and implications for model wind-stress. *Continental Shelf Research* 29 (10), 1329–1342.
- Brown, S., Nicholls, R.J., 2015. Subsidence and human influences in mega deltas: The case of the Ganges–Brahmaputra–Meghna. *Science of the Total Environment* 527–528, 362–374.
- Buckley, M.L., Wei, Y., Jaffe, B.E., Watt, S.G., 2012. Inverse modeling of velocities and inferred cause of overwash that emplaced inland fields of boulders at Anagada, British Virgin Islands. *Natural Hazards* 63, 133–149.
- Bulteau, T., Idier, D., Lambert, J., Garcin, M., 2015. How historical information can improve estimation and prediction of extreme coastal water levels: application to the Xynthia event at La Rochelle (France). *Natural Hazards and Earth System Sciences*, 15, 1135–1147.
- Bunya, S., Dietrich, J.C., Westerink, J.J., Ebersole, B.A., Smith, J.M., Atkinson, J.H., et al., 2010. A high resolution coupled riverine flow, tide, wind, wind wave and storm surge model for southern Louisiana and Mississippi: Part I — model development and validation. *Monthly Weather Review* 138, 345–377.
- Buynevich, I.V., FitzGerald, D.M., van Heteren, S., 2004. Sedimentary records of intense storms in Holocene barrier sequences, Maine, USA. *Marine Geology* 210, 135–148.
- Buynevich, I.V., Donnelly, J.P., 2006. Geological signatures of barrier breaching and overwash, southern Massachusetts, USA. *Journal of Coastal Research* SI 39, 112–116.
- Buynevich, I.V., FitzGerald, D.M., Goble, R.J., 2007. A 1500 yr record of North Atlantic storm activity based on optically dated relict beach scarps. *Geology* 35 (6), 543–546.
- Camuffo, D., Secco, C., Brimblecombe, P. and Martin-Vide, J., 2000. Sea storms in the Adriatic Sea and the Western Mediterranean during the last millennium. *Climatic Change* 46, 209–223.
- Canestrelli, P., 1999. Il sistema statistico del Comune di Venezia per la previsione del livello della marea in città. Risultati teorici e in fase di operatività, Comune di Venezia - C.P.S.M.
- Canestrelli, P., Pastore, F., 2000. Modelli stocastici per la previsione del livello di marea a Venezia. In: Commissione di studio dei provvedimenti per la conservazione e difesa della laguna e della città di Venezia, Rapporti e Studi, Venezia, Istituto Veneto di Scienze, Lettere e Arti 2(2), Venezia, 635–663.
- Canestrelli, P. and Moretti, F., 2004a. I modelli statistici del comune di Venezia per la previsione della marea: valutazioni e confronti sul quinquennio 1997-2001. *Atti Istituto Veneto Scienze, Lettere ed Arti* 167 (2003-2004), Venezia.
- Canestrelli P., Moretti F., 2004b. Una prima applicazione di modello statistico di tipo esparto. Comune di Venezia, Centro Previsioni e Segnalazioni Maree.
- Carter, R.W.G., Orford, J.D., 1981. Overwash processes along a gravel beach in South-East Ireland. *Earth Surface Processes and Landforms* 6 (5), 413–426.

- Castelle, B., Marieu, V., Bujan, S., Splinter, K.D., Robinet, A., Sénéchal, N., Ferreira, S., 2015. Impact of the winter 2013–2014 series of severe Western Europe storms on a double-barred sandy coast: Beach and dune erosion and megacusp embayments. *Geomorphology* 238, 135–148.
- Castaigns, J., Dezileau L., Fiandrino, A., Verney, R., 2011. Recent morphological evolution of a Mediterranean lagoon complex: the Palavasian lakes system (France) *Revue Paralia* 4, 7.1–7.12.
- CETMEF and western CETEs, 2009. *Vulnérabilité du territoire National aux risques littoraux - France métropolitaine*. CETMEF / DLCE. 163 p.
- Chadenas, C., Creach, A., Mercier, D., 2013. The impact of storm Xynthia in 2010 on coastal flood prevention policy in France. *Journal of Coastal Conservation* 18, 529–538.
- Charnock, H., 1955. Wind stress on a water surface. *Quarterly Journal of the Royal Meteorological Society* 81, 639–640.
- Chaumillon, E., Tessier, B., Weber, N., Tesson, M., Bertin, X., 2004. Buried sand bodies within present-day estuaries (Atlantic Coast of France) revealed by very high resolution seismic surveys. *Marine Geology* 211, 189–214.
- Chauveau E., Chadenas C., Comentale B., Pottier P., Blancœil A., Feuillet T., Mercier D., Pourinet L., Rollo N., Tillier I., Trouillet B., 2011. Xynthia: leçons d'une catastrophe. *Cybergeo: European Journal of Geography*, <http://cybergeo.revues.org/23763>; doi:10.4000/cybergeo.23763.
- Cheung, K.F., Tang, L., Donnelly, J.P., Scileppi, E.M., Liu, K.-B., Mao, X.-Z., Houston, S.H. and Murnane, R.J., 2007. Numerical modeling and field evidence of coastal overwash in southern New England from Hurricane Bob and implications for paleotempestology. *Journal of Geophysical Research*, 112, 1–24.
- Chevillot-Miot, E., Creach, A., Mercier, D., 2013. La vulnérabilité du bâti face au risque de submersion marine: premiers essais de quantification sur l'île de Noirmoutier (Vendée). *Les Cahiers Nantais* 1, 5–14.
- Chhotray, V., Few, R., 2012. Post-disaster recovery and ongoing vulnerability: Ten years after the super-cyclone of 1999 in Orissa, India. *Global Environmental Change* 22, 695–702.
- Ciavola, P., Organo, C., León Vintrolá, L., Mitchell, P. I., 2002. Sedimentation processes on intertidal areas of the lagoon of Venice: identification of exceptional flood events (Acqua Alta) using Radionuclides, *Journal of Coastal Research* 139–147, SI 36139147.
- Clemmensen, L.B., Bendixen, M., Hede, M.U., Kroon, A., Nielsen, L., Murray, A.S., 2013. Morphological records of storm floods exemplified by the impact of the 1872 Baltic storm on a sandy spit system in south-eastern Denmark. *Earth Surface Processes and Landforms* 2013, doi:10.1002/esp.3466.
- Coch, N.K., 1994. Geologic effects of hurricanes. *Geomorphology* 10, 37–63.
- Coles, S., 2001. *An Introduction to Statistical Modeling of Extreme Values*. Springer, Berlin, 210 p.

- Collins, E.S., Scott, D.B., Gayes, P.T., 1999. Hurricane records on the South Carolina coast: can they be detected in the sediment record? *Quaternary International* 56, 15–26.
- Corbett, D.R., Walsh, J.P., Harris, C.K., Ogston, A.S., Orpin, A.R., 2014. Formation and preservation of sedimentary strata from coastal events: Insights from measurements and modeling. *Continental Shelf Research* 86, 1–5.
- Corbett, D.R. and Walsh, J.P., 2015. <sup>210</sup>Pb and <sup>137</sup>Cs – Establishing a Chronology for the Last Century. In: *Handbook of Sea-Level Research*, eds. Editors: I. Shennan, A. Long and B. Horton. John Wiley & Sons. West Sussex, UK., 361–372.
- Creach, A., Pardo, S., Guillotreau, P., Mercier, D., 2015. The use of a micro-scale index to identify potential death risk areas due to coastal flood surges: lessons from Storm Xynthia on the French Atlantic coast. *Natural Hazards* 77, 1679–1710.
- Cunningham, A.C., Bakker, M.A.J., van Heteren, S., van der Valk, B., van der Spek, A.J.F., Schaart, D.R., Wallinga, J., 2011. Extracting storm-surge data from coastal dunes for improved assessment of flood risk. *Geology* 39 (11), 1063–1066.
- Daniel, P., Haie, B., Aubail, X., 2009. Operational forecasting of tropical cyclones storm surges at Météo-France. *Marine Geodesy* 32, 233–242.
- Das, P. K., 1972. Prediction Model for Storm Surges in the Bay of Bengal. *Nature* 239, 211–213, doi:10.1038/239211a0.
- Das, O., Wang, Y., Donoghue, J., Xu, X., Coor, J., Elsner, J., Xu, Y., 2013. Reconstruction of paleostorms and paleoenvironment using geochemical proxies archived in the sediments of two coastal lakes in northerwest Florida. *Quaternary Science Reviews* 68, 142–153.
- Debret, M., Bout-Roumazielles, V., Grousset, F., Desmet, M., Mcmanus, J.F., Massei, N., Sebag, D., Petit, J.-R., Copard, Y., Trentesaux, A., 2007. The origin of the 1500-year climate cycles in Holocene North-Atlantic records. *Climate of the Past Discussions*, European Geosciences Union (EGU) 3 (2), 679–692.
- Debret, M., Sebag, D., Crosta, X., Massei, N., Petit, J.-R., Chapron, E., Bout-Roumazielles, V., 2009. Evidence from wavelet analysis for a mid-Holocene transition in global climate forcing. *Quaternary Science Reviews* 28, 2675–2688.
- Degeai J.P., Devillers B., Dezileau L., Oueslati H., Bony G., 2015. Major storm periods and climate forcing in Western Mediterranean during the Late Holocene. *Quaternary Science Reviews* 129, 37–56.
- de Groot, A.V., Veeneklaas, R.M., Bakker, J.P., 2011. Sand in the salt marsh: Contribution of high-energy conditions to salt-marsh accretion. *Marine Geology* 282, 240–254.
- De Jong, R., Björck, S., Björkman, L., Clemmensen, L.B., 2006. Storminess variation during the last 6500 years as reconstructed from an ombrotrophic peat bog in Halland, southwest Sweden. *Journal of Quaternary Science* 21 (8), 905–919.
- de Kraker, A.M.J., 1999. A method to assess the impact of high tides, storms and storm surges as vital elements in climatic history, the case of stormy weather and dikes in the northern part of Flanders, 1488 to 1609. *Climatic Change* 43, 287–302.
- Denommee, K.C., Bentley, S.J., Droxler, A.W., 2014. Climatic controls on hurricane patterns: a 1200-y near-annual record from Lighthouse Reef, Belize. *Nature Scientific Reports* 4 (3876), 1–7.



- De Vries, H., Breton, M., De Mulder, T., Krestenitis, Y., Ozer, J., Proctor, R., Ruddick, K., Salomon, J.C., Voorrips, A., 1995. A Comparison of 2D storm surge models applied to three shallow European Seas. *Environmental Software* 10 (1), 23–42.
- Desarthe, J., 2011. Les caprices du bon vieux temps. Climat et sociétés dans l'Ouest de la France (XVIe-XIXe siècle). PhD thesis, Univ. Caen, 439 pp.
- Dezileau, L., Bordelais, S., Condomines, M., Bouchette, F., Briquieu, L., 2005. Evolution des lagunes du Golfed'Aigues-Mortes à partir de l'étude de carottes sédimentaires courtes (étude géochronologique, sédimentologique et géochimique des sédiments récents). *Association des Sedimentologues Français* 51, p. 91.
- Dezileau, L., Sabatier, P., Blanchemanche, P., Joly, P., Swingedouw, D., Cassou, C., Castaings, J., Martinez, P., von Grafenstein, U., 2011. Intense storm activity during the Little Ice Age on the French Mediterranean coast. *Palaeogeography, Palaeoclimatology, Palaeoecology* 299, 289–297.
- Dezileau, L., Castaings, J., 2014. Extreme storms during the last 500 years from lagoonal sedimentary archives in Languedoc (SE France). *Mediterranean Journal of Geography* 122, 113–120.
- Dezileau, L., Perez-Ruzafa, A., Blanchemanche, P., Martinez, P., Marcos, C., Raji O., Van Grafenstein, U., 2016. Extreme storms during the last 6,500 years from lagoonal sedimentary archives in Mar Menor (SE Spain). *Climate of the Past* 12, 1389–1400.
- Dietrich, J.C., Bunya, S., Westerink, J.J., Ebersole, B.A., Smith, J.M., Atkinson, J.H., Jensen, R. D., Resio, T., Luettich, R.A., Dawson, C., Cardone, V.J., Cox, A.T., Powell, M. D., Westerink, H. J., Roberts, H. J., 2010. A high resolution coupled riverine flow, tide, wind, wind wave and storm surge model for southern Louisiana and Mississippi: Part II — synoptic description and analyses of Hurricanes Katrina and Rita. *Monthly Weather Review* 138, 378–404.
- Dietsche, D., Hagen, S., Bacopoulos, P., 2007. Storm surge simulations for Hurricane Hugo (1989): On the significance of inundation areas. *Journal of Waterway, Port, Coastal, and Ocean Engineering* 133 (3), 183–191.
- Dodet, G., Bertin, X., Bruneau, N., Fortunato, A.B., Nahon, A., Roland, A., 2013. Wave-current interactions in a wave-dominated tidal inlet. *Journal of Geophysical Research Ocean* 118 (3), 1587–1605.
- Donnelly, J.P., Roll, S., Wengren, M., Butler, J., Lederer, R., Webb, T., III, 2001a. Sedimentary evidence of intense hurricane strikes from New Jersey. *Geology* 29 (7), 615–618.
- Donnelly, J.P., Smith Bryan, S., Butler, J., Dowling, J., Fan, L., Hausmann, N., Newby, P., Shuman, B., Stern, J., Westover, K., Webb, T., III, 2001b. 700 yr sedimentary record of intense hurricane landfalls in southern New England. *Geological Society of America Bulletin* 113 (6), 714–727.
- Donnelly, J.P., Butler, J., Roll, S., Wengren, M., Webb, T., 2004. A backbarrier overwash record of intense storms from Brigantine, New Jersey. *Marine Geology* 210, 107–121.
- Donnelly, C., Kraus, N., Larson, M., 2006. State of knowledge on measurement and modeling of coastal overwash. *Journal of Coastal Research* 22 (4), 965–991.

- Donnelly, J.P., Woodruff, J.D., 2007. Intense hurricane activity over the past 5,000 years controlled by El Niño and the West African monsoon. *Nature* 447 (7143), 465–468, doi:10.1038/nature05834.
- Donnelly, J. P., A. D. Hawkes, P. Lane, D. MacDonald, B. N. Shuman, M. R. Toomey, P. J. van Hengstum, Woodruff, J.D., 2015. Climate forcing of unprecedented intense-hurricane activity in the last 5000 years. *Earth's Future* 3, 49–65, doi:10.1002/2014EF000274.
- Doodson, A.T., 1924. Meteorological perturbations of sea-level and tides. *Geophysical Journal International* 1, 124–147.
- Dott, R.H., Jr., 1983. Episodic sedimentation – how normal is average? How rare is rare? Does it matter? *Journal of Sedimentary Petrology* 53, 5–23.
- Douglas, J., 2007. Physical vulnerability modelling in natural hazard risk assessment. *Natural Hazards and Earth System Science* 7 (2), 283–288.
- Duller, G.A.T., 2004. Luminescence dating of Quaternary sediments: recent advances. *Journal of Quaternary Science* 19 (2), 183–192
- Dumas, S., Arnott, R.W.C., 2006. Origin of hummocky and swaley cross-stratification—The controlling influence of unidirectional current strength and aggradation rate. *Geological Society of America* 34 (12), 1073–1076.
- Duun-Chriestensen, J.T., 1971. Investigations on the practical use of a hydrodynamic numeric method for calculation of sea level variations in the North Sea, the Skagerrak and the Kattegat. *Ocean Dynamics* 24 (5), 210–227.
- Einsele, G., Chough, S.K., Shiki, T., 1996. Depositional events and their records – an introduction. *Sedimentary Geology* 104, 1–9.
- Eipert, A.A., 2007. Sand and mud deposited by Hurricane Katrina on Deer Island, Biloxi Bay, Mississippi. M.S. thesis, University of Washington, 31 pp.
- EPRI, 2011. [www.eptb-loire.fr/PDF/EVAL\\_PRELIM\\_INOND](http://www.eptb-loire.fr/PDF/EVAL_PRELIM_INOND).
- EU Strategy on Adaptation to Climate Change, 16/04/2013 - COM (2013) (216).
- Fan, S., Swift, D.J.P., Traykovski, P., Bentley, S., Borgeld, J.C., Reed, C.W., Niedoroda, A.W., 2004. River flooding, storm resuspension, and event stratigraphy on the northern California shelf: observations compared with simulations. *Marine Geology* 210, 17–41.
- Fanthou, Th., Kaiser, B., 1990. Évaluation des risques naturels dans les Hautes-Alpes et la Savoie. Le recours aux documents d'archives et aux enquêtes. *Bulletin de l'Association des Géographes Français* 4, 323–339.
- FEMA, 2012. Operating guidance 8 – 12. Joint probability – Optimal sampling method for tropical storm surge frequency analysis. Federal Emergency Management Agency, 40 pp.
- Fisher, J.S., Stauble, D.K., 1977. Impact of Hurricane Belle on Assateague Island washover. *Geology* 5 (12), 765–768.
- FitzGerald, D.M., Fenster, M.S., Argow, B.A., Buynevich, I.V. 2008. Coastal impacts due to sea-level rise. *Annual Review of Earth and Planetary Sciences* 36, 601–647.

- Flather, R.A., Davies, A.M., 1975. The application of numerical models to storm surge prediction. Natural Environmental Research Council, Technical Report 16, 37 pp.
- Fletcher, C.A.J., 1996. Computational Techniques for Fluid Dynamics. Second Edition, Springer-Verlag, 401 pp.
- Flowerdew, J., Horsburgh, K., Wilson, C., Mylne, K., 2010. Development and evaluation of an ensemble forecasting system for coastal storm surges. Quarterly Journal of the Royal Meteorological Society 136, 1444–1456.
- Foreman, M.G.G., Henry, R.F., 1989. The harmonic analysis of tidal model time series. Advances in Water Resources 12 (3), 109–120.
- Fortunato, A.B., Rodrigues, M., Dias, J.M., Lopes, C., Oliveira, A., 2013. Generating inundation maps for a coastal lagoon: A case study in the Ria de Aveiro (Portugal). Ocean Engineering 64, 60–71.
- Fortunato, A.B., Li, K., Bertin, X., Rodrigues, M., Miguez, B.M., 2016. Determination of extreme sea levels along the Iberian Atlantic Coast. Ocean Engineering 111, 471–482.
- Fritz, H.M., Blount, C., Sokoloski, R., Singleton, J., Fuggle, A., McAdoo, B.G., Moore, A., Grass, C., Tate, B., 2007. Hurricane Katrina storm surge distribution and field observations on the Mississippi Barrier Islands. Estuarine, Coastal and Shelf Science 74 (1–2), 12–20.
- Froede, C.R., Jr., 2006. A Hurricane Frederic-generated storm-surge deposit exposed along a surf-zone foredune scarp on Dauphin Island, Alabama, U.S.A. Journal of Coastal Research 22 (2), 371–376.
- Fruergaard, M., Andersen, T.J., Johannesse, P.N., Nielsen, L.H., Pejrup, M., 2013. Major coastal impact induced by a 1000-year storm event. Nature, Scientific Reports 3, 1051, doi: 10.1038/srep01051.
- Garnier, E., 2010. Submersions et sociétés sur les littoraux français et européens (1500-2010). In: Chaumillon, E. et al. (Coord.), Les littoraux à l'heure des changements climatiques. Rivage des Xantons, pp. 59–74.
- Garnier, E., Surville, F., 2010. La tempête Xynthia face à l'histoire des submersions et tsunamis sur les littoraux français du Moyen Âge à nos jours. Le Croît Vif, Saintes, 176 pp.
- Garnier, E., Henry, N., Desarthe, J., 2012. Visions croisées de l'historien et du courtier en réassurance sur les submersions. Recrudescence de l'aléa ou vulnérabilisation croissante? Gestion des risques naturels, leçons de la tempête Xynthia, Ed. Quae, Versailles, pp. 105–128.
- Garnier, E., 2014. Histoire des tempêtes. Risques, Les cahiers de l'assurance 91, 2–9, <http://www.ffsa.fr/Risques>.
- Gill, A.E., 1982. Atmosphere-Ocean Dynamics, Volume 30. Academic Press. 1st Edition.
- Giosan, L., Syvitski, J., Constantinescu, S., 2014. Protect the world's deltas. Nature 516, 31–33.
- Gischler, E., Shinn, E.A., Oschmann, W., Fiebig, J., Buster, N.A., 2008. A 1500-Year Holocene Caribbean Climate Archive from the Blue Hole, Lighthouse Reef, Belize. Journal of Coastal Research 24, 1495–1505.

- Goeldner-Gianella, L., 2007. Perceptions and attitudes towards de-polderisation in Europe: A comparison of five opinion surveys (F, U.K.). *Journal of Coastal Research* 23 (5), 1218–1230.
- Goeldner-Gianella, L., Bertrand, F., Oiry, F., Grancher, D., 2015. Depolderisation policy against coastal flooding and social acceptability on the French Atlantic coast: The case of the Arcachon Bay. *Ocean and Coastal Management* 116, 98–107.
- Goff, J.A., Wheatcroft, R.A., Lee, H., Drake, D.E., Swift, J.P., Fan, S., 2002. Spatial variability of shelf sediments in the STRATAFORM natural laboratory, Northern California. *Continental Shelf Research* 22, 1199–1223.
- Goff, J.A., Allison, M.A., Gulick, S.P.S., 2010. Offshore transport of sediment during cyclonic storms: Hurricane Ike (2008), Texas Gulf Coast, USA. *Geology* 38 (4), 351–354.
- Goldberg, E.D., 1963. Geochronology with Pb-210 in radioactive dating. *International Atomic Energy Contribution* 1510, 121–131.
- Goldmann, A., Tomasin, A., 1971. Model for the Adriatic sea. *Colloque international sur l'exploitation des océans, II, Bordeaux (France), abstracts volume*.
- Goni, M.A., Alleau, Y., Corbett, D., Walsh, J.P., Mallinson, D., Allison, M.A., Gordon, E., Petsch, S., Dellapena, T.M., 2007. The effects of Hurricanes Katrina and Rita on the seabed of the Louisiana shelf. *The Sedimentary Record* 5, 4–9.
- Gönnert, G., Dube, S.K., M, T., Siefert, W., 2001. Global storm surges. In: *Die Küste* 63, 623 pp.
- Goodbred, S.L., Hine, A.C., 1995. Coastal storm deposition: saltmarsh response to a severe extratropical storm, March 1993, west-central Florida. *Geology* 23, 679–682.
- Goutx, D., Baraer, F., Roche, A., Jan, G., 2014. Ces tempêtes extrêmes que l'histoire ne nous a pas encore dévoilées. *La Houille Blanche* 2, 27–33; doi 10.1051/lhb/2014013.
- Graber, H., Cardone, V., Jensen, R., Slinn, D., Hagen, S., Cox, A., Powell, M., Grassl, C., 2006. Coastal forecasts and storm surge predictions for tropical cyclones: a timely partnership program. *Oceanography* 19 (1), 130–141.
- Grande Ordonnance de la Marine, 1681. Livre Premier, Titre II, in Jean-Marie Pardessus (1772-1853), *Collection de lois, maritimes antérieures au XVIIIe siècle*, Paris, Imprimerie royale, 1828-1845, 6 vol., in-4, tome IV, pp. 15–32.
- Gratiot, N., Anthony, E.J., Garedl, A., Gaucherel, C., Proisy, C., Wells, J.T., 2008. Significant contribution of the 18.6 year tidal cycle to regional coastal changes. *Nature Geoscience* 1, 169–172.
- Haigh, I.D., Nicholls, R., Wells, N., 2010. A comparison of the main methods for estimating probabilities of extreme still water levels. *Coastal Engineering* 57, 838–849.
- Haigh, I.D., Wijeratne, E.M.S., MacPherson, L.R., Pattiaratchi, C.B., Mason, M.S., Crompton, R.P., George, S., 2014. Estimating present day extreme total water level exceedance probabilities around the coastline of Australia: tides, extra-tropical storm surges and mean sea level. *Climate Dynamics*, 42 (1–2), 121–138.

- Hanson, J.D., Hall, A.M., 2009. Magnitude and frequency of extra-tropical North Atlantic cyclones: A chronology from cliff-top storm deposits. *Quaternary International* 195 (1–2), 42–52.
- Harris, D.L., 1962. The equivalence between certain statistical prediction methods and linearized dynamical methods. *Monthly Weather Reviews* 90, 331–340.
- Haslett, S.K., Bryant, E.A., 2007. Reconnaissance of historic (post-AD 1000) high-energy deposits along the Atlantic coasts of southwest Britain, Ireland and Brittany, France. *Marine Geology* 242, 207–220.
- Hayes, M.O., 1967a. Hurricanes as geologic agents, south Texas coast. *A.A.P.G. Bulletin* 51, 937–942.
- Hayes, M.O., 1967b. Hurricanes as geological agents; case studies of Hurricane Carla, 1961 and Cindy, 1963. University of Texas Bureau of Economic Geology Report 61, Austin, 56 pp.
- Haynes, M., Chappell, J., 2001. Cyclone frequency during the last 5,000 years from Curacao Island, Queensland. *Palaeogeography, Palaeoclimatology, Palaeoecology* 168, 201–219.
- Heaps, N.S., 1973. Three-dimensional numerical model of the Irish Sea. *Geophysical Journal of the Royal Astronomical Society* 35 (1-3), 99–120.
- Hesp, P.A., 2006. Beach-ridges – Definition and re-definition. *Journal of Coastal Research* SI39, 72–75.
- Hippensteel, S.P., Eastin, M.D., Garcia, W.J., 2013. The geological legacy of Hurricane Irene: Implications for the fidelity of the paleo-storm record. *GSA Today* 23 (12), 4–10.
- Holland, G.J., Belanger, J.I., Fritz, A., 2010. A revised model for radial profiles of hurricane winds. *Monthly Weather Review* 138, 4393–4401.
- Horsburgh, K.J., Wilson, C., 2007. Tide–surge interaction and its role in the distribution of surge residuals in the North Sea. *Journal of Geophysical Research (Oceans)* 112, C08003.
- Horsburgh, K., de Vries, J., Etala, M., Murty, T., Seo, J., Dube, S., Lavrenov, I., Holt, M., Daniel, P., Higaki, M., Warren, G., Cabrera, R., Nirupama, N., Paradis, D., Dandin, P., 2011. Guide to Storm Surge Forecasting. WMO-No. 1076, 117 p.
- Horton, B.P., Rossi, V., Hawkes, A.D., 2009. The sedimentary record of the 2005 hurricane season from the Mississippi and Alabama coastlines. *Quaternary International* 195, 15–30.
- Hudock, J.W., Flaig, P.P., Wood, L.J., 2014. Washover fans: a modern geomorphologic analysis and proposed classification scheme to improve reservoir models. *Journal of Sedimentary Research* 84, 854–865.
- Idier, D., Dumas, F., Muller, H., 2012. Tide-surge interaction in the English Channel. *Natural Hazards and Earth System Sciences*, 12, 3709–3718.
- INSEE, 2014, Recensement général de la population 2011. <http://www.insee.fr/fr/ppp/bases-de-donnees/recensement/populations-legales/france-departements.asp?annee=2011>

- IPCC, 2014. Climate Change, 2014. Synthesis Report. Contribution of Working Groups I, II and III to the Fifth Assessment Report of the Intergovernmental Panel on Climate Change [Core Writing Team, edited by Pachauri, R.K., and Meyer, L.A.]. IPCC, Geneva, Switzerland, 151 pp.
- Jelesnianski, C.P., 1965. Numerical calculation of storm tides induced by a tropical storm impinging on a continental shelf. *Monthly Weather Review* 93, 343–358.
- Jelesnianski, C.P., 1966. Numerical computations of storm surges without bottom stress. *Monthly Weather Review* 94 (6), 379–394.
- Jonasson, K.E., Patterson, R.T., 1992. Preservation potential of salt marsh foraminifera from the Fraser River delta, British Columbia. *Micropaleontology* 38, 289–301.
- Jonkman, S.N., Vrijling, J.K., Vrouwenvelder, A.C.W.M., 2008. Methods for the estimation of loss of life due to floods: a literature review and a proposal for a new method. *Natural Hazards* 46, 353–389.
- Jonkman, S.N., Kelman, I., 2005. An analysis of causes and circumstances of flood disaster deaths. *Disasters* 29 (1), 75–97.
- Karim, M., Mimura, N., 2008. Impacts of climate change and sea-level rise on cyclonic storm surge floods in Bangladesh. *Global Environmental Change* 18, 490–500.
- Keen, T.R., Bentley, S.J., Vaughan, W.C., Blain, C.A., 2004. The generation and preservation of multiple hurricane beds in the northern Gulf of Mexico. *Marine Geology* 210, 79–105.
- Kennedy, A.B., Gravois, U., Zachry, B.C., Westerink, J.J., Hope, M.E., Dietrich, J.C., Powell, M.D., Cox, A.T., Luettich Jr., R.A., Dean, R.G., 2011. Origin of the Hurricane Ike forerunner surge. *Geophysical Research Letters* 28 (8), L08608.
- Kennedy, A.B., Westerink, J.J., Smith, J.M., Hope, M.E., Hartman, M., Taflanidis, A.A., Tanaka, S., Westerink, H., Cheung, K.F., Smith, T., Hamann, M., Minamide, M., Ota, A., Dawson, C., 2012. Tropical cyclone inundation potential on the Hawaiian Islands of Oahu and Kauai. *Ocean Modelling* 52–53, 54–68.
- Kiage, L.M., Deocampo, D., McCloskey, T.A., Bianchette, T.A., Hursey, M., 2011. A 1900-year paleohurricane record from Wassaw Island, Georgia, USA. *Journal of Quaternary Science* 26 (7), 714–722.
- Klein, R. J.T., Nicholls, R.J., Ragoonaden, S., Capobianco, M., Aston, J., Buckley, E.N., 2001. Technological options for adaptation to climate change in coastal zones. *Journal of Coastal Research* 17 (3), 531–543.
- Kolen, B., Slomp, R., Jonkman, S.N., 2013. The impacts of storm Xynthia February 27–28, 2010 in France: lessons for flood risk management. *Journal of Flood Risk Management* 13, 261–278.
- Lagomasino, D., Corbett, D.R., Walsh, J.P., 2013. Influence of wind-driven inundation and coastal geomorphology on sedimentation in two microtidal marshes, Pamlico River Estuary, NC. *Estuaries and Coasts* 36 (6), 1–16.
- Lapidez, J.P., Tablazon, J., Dasallas, L., Gonzalo, L.A., Cabacaba, K.M., Ramos, M.M.A., Suarez, J.K., Santiago, J., Lagmay, A.M.F., Malano, V., 2015. Identification of storm surge vulnerable areas in the Philippines through the simulation of Typhoon

- Haiyan-induced storm surge levels over historical storm tracks. *Natural Hazards and Earth System Sciences* 15, 1473–1481.
- Leatherman, S.P., 1976. Barrier island dynamics: overwash processes and eolian transport. *Coastal Engineering* 15, 1958–1974.
- Leatherman, S.P., Williams, A.T., Fisher, J.S., 1977. Overwash sedimentation associated with a large-scale northeaster. *Marine Geology* 24, 109–121.
- Leatherman, S.P., 1979. Barrier dune systems: a reassessment. *Sedimentary Geology* 24, 1–16.
- Leone, F., Lavigne, F., Paris, R., Denain, J.-C., Vinet, F., 2011. A spatial analysis of the December 26th, 2004 tsunami-induced damages: Lessons learned for a better risk assessment integrating buildings vulnerability. *Applied Geography* 31 (1), 363–375.
- Lee, K., and S. I. Hsu. 1989. Typhoon records from ancient chronicles of Guangdong Province (in Chinese). Department of Geography Occasional Paper 98. Hong Kong: Department of Geography, The Chinese University of Hong Kong.
- Le Roy, S., Pedreros, R., André, C., Paris, F., Lecacheux, S., Marche, F., Vinchon, C., 2015. Coastal flooding of urban areas by overtopping: Dynamic modelling application to the Johanna storm (2008) in Gâvres (France). *Natural Hazards and Earth System Sciences* 15 (11), 2497–2510.
- Lin, N., Emanuel, K., 2016. Grey swan tropical cyclones. *Nature Climate Change* 6, 106–111.
- Lin, N., Emanuel, K., Oppenheimer, M., Vanmarcke, E., 2012. Physically based assessment of hurricane surge threat under climate change. *Nature Climate Change* 2, 1–6.
- Liu, K.-b. 2004. Palaeotempestology: principles, methods and examples from Gulf coast lake sediments. In: Murnane, R., Liu, K.-b. (Eds.), *Hurricanes and Typhoons: Past, Present and Future*. Columbia University Press, New York, pp. 13–57.
- Liu, K.-b., Fearn, M.L., 1993. Lake-sediment record of late Holocene hurricane activities from coastal Alabama. *Geology* 21 (9), 793–796.
- Liu, K.-b., Fearn, M.L., 2000a. Reconstruction of prehistoric landfall frequencies of catastrophic hurricanes in northwestern Florida from lake sediment records. *Quaternary Research* 54, 238–245.
- Liu, K.-b., Fearn, M.L., 2000b. Holocene history of catastrophic hurricane landfalls along the Gulf of Mexico coast reconstructed from coastal lake and marsh sediments. In: Ning, Z.H., Abdollahi, K.K. (Eds.), *Current Stresses and Potential Vulnerabilities: Implications of Global Change for the Gulf Coast Region of the United States*. Franklin Press, Baton Rouge, LA, pp. 38–47.
- Liu, K.-b., Shen, C., Louie, K. 2001. A 1,000-Year History of Typhoon Landfalls in Guangdong, Southern China, Reconstructed from Chinese Historical Documentary Records. *Annals of the Association of American Geographers*, 91 (3), 453–464.
- Longuet-Higgins, M.S., Stewart, R.W., 1964. Radiation stresses in water waves; physical discussion, with applications. *Deep-Sea Research* 11, 529–562.
- Lorenz, E.N., 1963. The predictability of hydrodynamic flow. *Transactions of the New York Academy of Sciences Ser. II* 25 (4), 409–432.

- Ludlum, D.M., 1963. Early American hurricanes: Boston. American Meteorological Society, 198pp.
- Lumbroso, D.M., Vinet, F., 2011. A comparison of the causes, effects and aftermaths of the coastal flooding of England in 1953 and France in 2010. *Natural Hazards and Earth System Sciences* 11, 2321–2333.
- Lutz, W., Samir, K.C., 2010. Dimensions of global population projections: what do we know about future population trends and structures? *Philosophical Transactions of the Royal Society B* 365, 2779–2791.
- Madsen, K.S., Høyer, J.L., Fu, W., Donlon, C., 2015. Blending of satellite and tide gauge sea level observations and its assimilation in a storm surge model of the North Sea and Baltic Sea. *Journal of Geophysical Research (Oceans)*.
- Mann, M.E., Woodruff, J.D., Donnelly, J.P., Zhang, Z., 2009. Atlantic hurricanes and climate over the past 1,500 years. *Nature* 460, 880–883.
- Maragos, J., G. Baines, Beveridge, P., 1973. Tropical cyclone Bebe creates a new land formation on Funafuti Atoll. *Science*, 181, 1161–1164.
- Marche, F., Bonneton, P., Fabrie, P., Seguin, N., 2007. Evaluation of well-balanced bore-capturing schemes for 2D wetting and drying processes. *International Journal for Numerical Methods in Fluids* 53 (5), 867–894.
- Marcos, M., Jorda, G., Gomis, D., Perez, B., 2011. Changes in storm surges in southern Europe from a regional model under climate change scenarios. *Global and Planetary Change* 77 (3-4), 116–128, doi: 10.1016/j.gloplacha.2011.04.002.
- Mason, O.K., Jordan, J.W., 1993. Heightened North Pacific storminess during synchronous Late Holocene erosion of Northwest Alaska beach ridges. *Quaternary Research* 40, 55–69.
- Mastenbroek, C., Burgers, G., Janssen, P.A.E.M., 1993. The dynamical coupling of a wave model and a storm surge model through the Atmospheric Boundary Layer. *Journal of Physical Oceanography* 23, 1856–1866.
- Matias, A., Ferreira, Ó., Vila-Concejo, A., Morris, B., Dias, J.A., 2010. Short-term morphodynamics of non-storm overwash. *Marine Geology* 274, 69–84.
- McCall, R., Van Thiel de Vries, J., Plant, N., Van Dongeren, A., Roelvink, J.A., Thompson, D., Reniers A., 2010. Two-dimensional time dependent hurricane overwash and erosion modeling at Santa Rosa Island. *Coastal Engineering* 57 (7), 668–683.
- Mikami, T., Esteban, M., Shibayama, T., 2015. Chapter 7 – Storm surge in New York City caused by Hurricane Sandy in 2012. In: Esteban, M., Takagi, H., Shibayama, T. (Eds.), *Handbook of Coastal Disaster Mitigation for Engineers and Planners*, pp. 115–131.
- Millennium Ecosystem Assessment, 2005. *Ecosystems and Human Well-being: Synthesis*. Island Press, Washington, DC.
- Mirza, M.Q., Patwardhan, A., Attz, M., Marchand, M., Ghimire, M., Hanson, R., Norgaard, R., 2005. Assessment report outline, chapter 11, Flood and Storm Control, *Millennium Ecosystem Assessment*, 335–352.
- Moon, I.J., 2005. Impact of a coupled ocean wave-tide-circulation system on coastal modeling. *Ocean Modelling* 8, 203–236.



- Morel A., Baraille R., Pichon A., 2008. Time splitting and linear stability of the slow part of the barotropic component. *Ocean Modelling* 23, 73–81.
- Morton, R.A., Sallenger, A.H., 2003. Morphological Impacts of Extreme Storms on Sandy Beaches and Barriers. *Journal of Coastal Research* 19 (3), 560–573.
- Mosetti, F., 1971. *Sulle cause dell'acqua alta a Venezia e sui sistemi di previsione*. Osservatorio Geofisico Sperimentale, Trieste.
- Mulligan, R.P., Walsh, J.P., Wadman, H., 2014. Wind-generated storm surge and surface waves in North Carolina Estuaries during Hurricane Irene, 2011, *Journal of Waterway, Port, Coastal and Ocean Engineering*.
- Murty, P.L.N., Sandhya, K.G., Bhaskaran, P.K., Jose, F., Gayathri, R., Balakrishnan Nair, T.M., Srinivasa Kumar, T., Shenoi, S.S.C., 2014. A coupled hydrodynamic modeling system for PHAILIN cyclone in the Bay of Bengal. *Coastal Engineering* 93, 71–81.
- Nelson, S.A., Leclair, S.F., 2006. Katrina's unique splay deposits in a New Orleans neighborhood. *GSA Today* 16 (9), doi: 10.1130/GSAT01609A.1.
- Neumann, C.J., Jarvinen, B.R., McAdie, C.J., Elms, J.D., 1993. Tropical cyclones of North Atlantic Ocean, 1871-1992. National Climatic Data Center / National Hurricane Center Historical Climatology Series 6-2, 193 pp.
- Nicholls, R.J., 2011. Planning for the impacts of sea level rise. *Oceanography* 24 (2), 144–157.
- Nittrouer, C.A., Austin, J.A., Field, M.E., Kravitz, J.H., Syvitski, J.M.P., Wiberg, P.I., 2007. *Writing a Rosetta Stone: Insights into Continental-Margin Sedimentary Processes and Strata*. International Association of Sedimentologists. Special Publication 37, Blackwell Publishing Ltd., Oxford, 549 pp.
- Nott, J., 1997. Extremely high-energy wave deposits inside the Great Barrier Reef, Australia: determining the cause – tsunami of tropical cyclone. *Marine Geology* 141, 193–207.
- Nott, J., Hayne, M., 2001. High-frequency of 'super-cyclones' along the Great Barrier over the past 5,000 years. *Nature* 413, 508–511.
- Nott, J., 2003. Intensity of prehistoric tropical cyclones. *Journal of Geophysical Research* 108 (D7), 4012, doi:10.1029/2002JD002726.
- Nott, J., 2004a. Palaeotempestology: the study of prehistoric tropical cyclones—a review and implications for hazard assessment. *Environment International* 30, 433–447.
- Nott, J., 2004b. The tsunami hypothesis – comparisons of the field evidence against the effects, on the Western Australian coast, of some of the most powerful storms on Earth. *Marine Geology* 208, 1–12.
- Nott J, Smithers S, Walsh K, Rhodes Ed, 2009. Sand beach ridges record 6000 years history of extreme tropical cyclone activity in northeastern Australia. *Quaternary Science Reviews* 28, 1511–1520.
- Nott, J., Chagué-Goff, C., Goff, J., Sloss, C., Riggs, N., 2013. Anatomy of sand beach ridges: Evidence from severe Tropical Cyclone Yasi and its predecessors, northeast Queensland, Australia. *Journal of Geophysical Research* 118, 1710–1719.

- Nott, J., 2015. A rapid, economical, and accurate method to determining the physical risk of storm marine inundations using sedimentary evidence. *Geophysical Research Letters* 42 (7), 2426–2433.
- Olabarrieta, M., Warner, J.C., Armstrong, B., Zambon, J.B., He, R., 2012. Ocean-atmosphere dynamics during Hurricane Ida and Nor'Ida: an application of the coupled ocean-atmosphere wave sediment transport (COAWST) modeling system. *Ocean Modelling* 43–44, 112–137.
- ONML (Observatoire National de la Mer et du Littoral), 2013. Densité de population des communes littorales en 2010 et évolution depuis 1961-1962. MEDDE et SOeS, 4 pp.
- Orissa Cyclone Appeal No. 28/1999 Final Report, International Federation of Red Cross and Red Crescent Societies.
- Otvos, E.G., Price, W.A., 1979. Problems of chenier genesis and terminology - an overview. *Marine Geology* 31, 251–263.
- Otvos, E.G., 2000. Beach ridges — definitions and significance. *Geomorphology* 32, 83–108.
- Otvos, E.G., 2011. Hurricane signatures and landforms—toward improved interpretations and global storm climate chronology. *Sedimentary Geology* 239, 10–22.
- Parker, D.J., Priest, S.J., Tapsell, S.M., 2009. Understanding and enhancing the public's behavioural response to flood warning information. *Meteorological Applications* 16 (1), 103–114.
- Pawlowicz, R., Beardsley, B., Lentz, S., 2002. Classical tidal harmonic analysis including error estimates in MATLAB using T\_Tide. *Computer & Geosciences* 28, 929–937.
- Peeters, P., Schoorens, J., Le Cornec, E., Michard, B., Lechat, M., 2009. Définition de l'aléa submersion marine sur le site de la Grande Plage de Gâvres (Morbihan). *La Houille Blanche*, 1 (Mars), 45-51.
- Pelling, M., Dill, K., 2010. Disaster politics: tipping points for change in the adaptation of sociopolitical regimes. *Progress in Human Geography* 34 (1), 21–37.
- Perillo, G.M.E., 1995. Definitions and geomorphologic classifications of estuaries. In: Perillo, G.M.E. (Ed.), *Geomorphology and Sedimentology of Estuaries, Developments in Sedimentology* 53, Elsevier, Science, Amsterdam, pp. 17-47.
- Péret, J., Sauzeau, T., 2014. Xynthia ou la mémoire réveillée. Des villages charentais et vendéens face à l'océan (XVIIIe-XXIe siècles). *La Crèche, Geste*, 296 pp.
- Pielke Jr, Roger A, 1999. La Nina, El Nino and Atlantic hurricane damages in the United States. *Bulletin of the American Meteorological Society* 80 (10), 0003–0007.
- Pierce, J.W., 1970. Tidal inlets and washover fans. *Journal of Geology* 78, 230–234.
- Pistrika, A.K., Jonkman, S.N., 2010. Damage to residential buildings due to flooding of New Orleans after hurricane Katrina. *Natural Hazards* 54 (2), 413–434.
- Powell, M.D., Vickery, P.J., Reinhold, T.A., 2003. Reduced drag coefficient for high wind speeds in tropical cyclones. *Nature* 422, 279–283.
- Pugh, D., Vassie, J., 1980. Applications of the joint probability method for extreme sea-level computations. *Proceedings of the ICE* 69 (4), 959–975.

- Pugh, D.T., 1987. Tides, Surges and Mean Sea Level. United States: John Wiley and Sons Inc., New York, NY.
- Rabien, K.A, Culver, S.J., Buzas, M.A., Corbett, D.R., Walsh, J.P., Tichenor, H.R., in press. The foraminiferal signature of recent Gulf of Mexico hurricanes. *Journal of Foraminiferal Research*.
- Radakovitch, O., Charmasson, S., M., A., Bouisset, P., 1999.  $^{210}\text{Pb}$  and caesium accumulation in the Rhône Delta sediments. *Estuarine and Coastal Shelf Science* 48, 77–92.
- Rahman, S., Rahman, M.A., 2015. Climate extremes and challenges to infrastructure development in coastal cities in Bangladesh. *Weather and Climate Extremes* 7, 96–108.
- Raji, O., Dezileau, L., Snoussi, M., Niazi, S., 2015. Extreme sea events during the last millennium in North-East of Morocco. *Natural Hazards and Earth System Sciences* 15, 203–211.
- Rego, J.L., Li, C., 2010. Nonlinear terms in storm surge predictions: effect of tide and shelf geometry with case study from Hurricane Rita. *Journal of Geophysical Research* 115, C06020.
- Reineck, H.E., Singh, I.B., 1972. Genesis of laminated sand and graded rhythmites in storm-sand layers of shelf mud. *Sedimentology* 18, 123–128.
- Reineck, H.-E., Singh, I.B., 1978. *Depositional Sedimentary Environments*. Springer Verlag, New York, 439 pp.
- Rilo, A., Freire, P., Tavares, A.O., Santos, P.P., Sá, L., 2015. Historical flood events in the Tagus estuary: contribution to risk assessment and management tools. In: *Safety and Reliability of Complex Engineered Systems – Podofillini et al. (Eds)*, Taylor & Francis Group, London, ISBN 978-1-138-02879-1, 4281-4286.
- Robbins, J.A., Edgington, D.N., 1975. Determination of recent sedimentation rates in Lake Michigan using Pb-210 and Cs-137. *Geochemica et Cosmochimica Acta* 39, 285–304.
- Rodriguez, A.B., Fegley, S.R., Ridge, J.T., VanDusen, B.M., Anderson, N., 2013. Contribution of aeolian sand to backbarrier marsh sedimentation. *Estuarine, Coastal and Shelf Science* 117, 248–259.
- Roeber, V., Bricker, J.D., 2015. Destructive tsunami-like wave generated by surf beat over a coral reef during Typhoon Haiyan. *Nature Communications* 6, 7854.
- Roelvink, J.A., Reniers, A., Van Dongeren, J., Van Thiel de Vries, R., McCall, J. Lescinski, 2009. Modeling storm impacts on beaches, dunes and barrier islands. *Coastal Engineering* 56 (11-12), 1133–1152.
- Rogers, L.J., Moore, L.J., Goldstein, E.B., Hein, C.J., Lorenzo-Trueba, J., Ashton, A.D., 2015. Anthropogenic controls on overwash deposition: Evidence and consequences. *Journal of Geophysical Research, Earth Surface* 120 (12), 2609-2624.
- Roland, A., Cucco, A., Ferrarin, C., Hsu, T.W., Liau, J.M., Ou, S.H., Umgiesser, G., Zanke, U., 2009. On the development and verification of a 2-D coupled wave-current model on unstructured meshes. *Journal of Marine Systems* 78, S244–S254

- Roland, A., Zhang, Y., Wang, H.V., Meng, Y., Teng, Y.C., Maderich, V., Brovchenko, I., Dutour-Sikiric, M. and Zanke, U., 2012. A fully coupled 3D wave-current interaction model on unstructured grids. *Journal of Geophysical Research* 117 (C11), doi:10.1029/2012JC007952.
- Sabatier, P., Dezileau, L., Condomines, M., Briquieu, L., Colin, C., Bouchette, F., Le Duff, M., Blanchemanche, P., 2008. Reconstruction of paleostorm events in a coastal lagoon (Hérault, South of France). *Marine Geology* 251, 224–232.
- Sabatier, P., Dezileau, L., Blanchemanche, P., Siani, G., Condomines, M., Bentaleb, I., Piquès, G., 2010. Holocene variations of radiocarbon reservoir ages in a Mediterranean lagoonal system. *Radiocarbon*, 52 (1), 91–102.
- Sabatier, P., Dezileau, L., Colin, C., Briquieu, L., Bouchette, F., Martinez, P., Siani, G., Raynal, O., von Grafenstein, U., 2012. 7000 years of paleostorm activity in the NW Mediterranean Sea in response to Holocene climate events. *Quaternary Research* 77 (1), 1–11.
- Saha S., Moorthi S., Pan H.-L., Wu X., Wang J., Nadiga S., Goldberg M. et al., 2010. The NCEP Climate Forecast System Reanalysis. *Bulletin of the American Meteorological Society* 91 (8), 1015–1057, doi.org/10.1175/2010BAMS3001.1.
- Sakuna-Schwartz, D., Feldens, P., Schwarzer, K., Khokiattiwong, S., Stattedder, K., 2015. Internal structure of event layers preserved on the Andaman Sea continental shelf, Thailand: tsunami vs. storm and flash-flood deposits. *Natural Hazards and Earth System Sciences* 15, 1181–119.
- Sallenger, A.H., 2000. Storm Impact Scale for Barrier Islands. *Journal of Coastal Research* 16 (3), 890–895.
- Sawai, Y., Fujii, Y., Fujiwara, O., Kamataki, T., Komatsubara, J., Okamura, Y., Satake, K., Shishikura, M., 2008. Marine incursions of the past 1500 years and evidence of tsunamis at Suijin-numa, a coastal lake facing the Japan Trench. *The Holocene* 18 (4), 517–528.
- Schwartz, R.K., 1975. Nature and genesis of some washover deposits. United States Army Coastal Engineering Research Center, Technical Memorandum 61, 69 pp.
- Schwartz, R.K., 1982. Bedform and stratification characteristics of some modern small-scale washover sand bodies. *Sedimentology* 29, 835–849.
- Scott, D.B., Collins, E.S., Gayes, P.T., Wright, E., 2003. Records of prehistoric hurricanes on the South Carolina coast based on microplaeontological and sedimentological evidence, with comparison to other Atlantic Coast record. *Geological Society of America Bulletin* 115 (9), 1027–1039.
- Sedgwick, P.E., Davis, R.A., Jr., 2003. Stratigraphy of washover deposits in Florida: implications for recognition in the stratigraphic record. *Marine Geology* 200, 31–48.
- Shah-Hosseini, M., Morhange, C., Naderi Beni, A., Marriner, N., Lahijani, H., Hamzeh, M., Sabatier, F., 2011. Coastal boulders as evidence for high-energy waves on the Iranian coast of Makran. *Marine Geology* 290, 17–28
- Shearman, P., Bryan, J., Walsh, J.P., 2013. Trends in deltaic change over three decades in the Asia-Pacific region. *Journal of Coastal Research* 29 (5) 1169–1183.

- Shiki, T., 1996. Reading of the trigger records of sedimentary events – a problem for future studies. *Sedimentary Geology* 104, 249–255.
- Shimozono, T., Tajima, Y., Kennedy, A.B., Nobuoka, H., Sasaki, J., Sato, S., 2015. Combined infragravity wave and sea-swell runup over fringing reefs by super typhoon Haiyan. *Journal of Geophysical Research (Oceans)* 120, 4463–4486, doi:10.1002/2015JC010760.
- Simon, B., 2008. Statistiques des niveaux marins extrêmes de pleine mer en Manche et Atlantique. In: SHOM, CETMEF (Eds.), CD-Rom (in French).
- Sobel, R., Leeson, P.T., 2006. Government's response to Hurricane Katrina: A public choice analysis. *Public Choice* 126, 55–73.
- SOGREAH, 2004. Atlas de l'aléa submersion marine sur le littoral vendéen, 53 maps, 86 pp.
- Solomon, S., et al., 2007. *Climate Change 2007. The physical science basis: contribution of Working Group I to the Fourth Assessment Report of the Intergovernmental Panel on Climate Change*, viii, Cambridge University Press. Cambridge, New York, 996 pp.
- Sorrel, P., Tessier, B., Demory, F., Delsonne, N., Mouazé, D., 2009. Evidence for millennial-scale climatic events in the sedimentary infilling of a macrotidal estuarine system, the Seine estuary (NW France). *Quaternary Science Reviews* 28, 499–516.
- Sorrel, P., Debret, M., Billeaud, I., Jaccard, S.L., McManus, J.F., Tessier, B., 2012. Persistent non-solar forcing of Holocene storm dynamics in coastal sedimentary archives. *Nature Geoscience* 5, 892–896.
- Stewart, R.W., 1974. The air-sea momentum exchange. *Boundary Layer Meteorology* 6, 151–167.
- Stockdon, H.F., Holman, R.A., Howd, P.A., Sallenger, A.H., 2006. Empirical parameterization of setup, swash, and runup. *Coastal Engineering* 53 (7), 573–588.
- Switzer, A.D., Jones, B.G., 2008. Large-scale washover sedimentation in a freshwater lagoon from the southeast Australian coast: sea-level change, tsunami or exceptionally large storm? *The Holocene* 18 (5), 787–803.
- Syvitski, J.P.M., Vörösmarty, C.J., Kettner, A.J., Green, P., 2005. Impact of humans on the flux of terrestrial sediment to the global coastal ocean. *Science* 308, 376–380.
- Syvitski, J.P.M., Saito, Y., 2007. Morphodynamics of deltas under the Influence of humans. *Global and Planetary Changes* 57, 161–182.
- Syvitski, J.P.M., Kettner, A.J., Overeem, I., Hutton, E.W.H., Hannon, M.T., Brakenridge, G.R., Day, J., Vörösmarty, C., Saito, Y., Giosan, L., Nicholls, R.J., 2009. Sinking deltas due to human activities. *Nature Geoscience* 2, 681–686.
- Syvitski, J.P.M., Overeem, I., Brakenridge, G.R., Hannon, M.D., 2012. Floods, floodplains, delta plains – A satellite imaging approach. *Sedimentary Geology* 267–268, 1–14.
- Takagaki, N., Komori, S., Suzuki, N., Iwano, K., Kuramoto, T., Shimada, S., Kurose, R., Takahashi, K., 2012. Strong correlation between the drag coefficient and the shape of the wind sea spectrum over a broad range of wind. *Geophysical Research Letters* 39, L23604.

- Tavares, A.O., dos Santos, P.P., Freire, P., Fortunato, A.B., Rilo, A., Sá, L., 2015. Flooding hazard in the Tagus estuarine area: The challenge of scale in vulnerability assessments. *Environmental Science and Policy* 51, 238–255.
- Tawn, J.A., 1988. An extreme value theory model for dependent observations. *Journal of Hydrology* 101, 227–250.
- Tawn, J.A., Vassie, J.M., 1989. Extreme sea levels: the joint probability method revisited and revised. *Proceedings of the Institution of Civil Engineers Part 2*, 87, 429–442.
- Tawn, J., 1992. Estimating probabilities of extreme sea levels. *Applied Statistics* 41, 77–93.
- Taylor, R.E., Long, A., Kra, R.S., 1992. *Radiocarbon after Four Decades*. Springer, New York, 596 pp.
- Taylor, M., Stone, G.W., 1996. Beach ridges: a review. *Journal of Coastal Research* 12, 612–621.
- Tesi, T., Langone, L. Goñi, M. Wheatcroft, R.A., Miserocchi, S., Bertotti, L., 2012. Early diagenesis of recently deposited organic matter: A 9-yr time-series study of a flood deposit. *Geochimica et Cosmochimica Acta* 83, 19–36.
- Theuerkauf, E.J., Rodriguez, A.B., Fegley, S.R., Luettich, R.A., Jr, 2014. Sea level anomalies exacerbate beach erosion. *Geophysical Research Letters* 41 (14), 5139–5147.
- Tillmann, T., Wunderlich, J., 2013. Barrier rollover and spit accretion due to the combined action of storm surge induced washover events and progradation: Insights from ground-penetrating radar surveys and sedimentological data. *Journal of Coastal Research* 29, 600–605.
- Titus, J.G., 1991. Greenhouse effect and coastal wetland policy: How Americans could abandon an area the size of Massachusetts at minimum cost. *Environmental Management* 15 (1), 39–58.
- Tomasin, A., Pirazzoli, P.A., 2008. Extreme Sea Levels in the English Channel: Calibration of the Joint Probability Method. *Journal of Coastal Research* 24 (4A), 1–13.
- Toomey, M.R., Donnelly, J.P., Woodruff, J.D., 2013. Reconstructing mid-late Holocene cyclone variability in the Central Pacific using sedimentary records from Tahaa, French Polynesia. *Quaternary Science Reviews* 77, 181–189.
- Townend, I., Pethick, J., 2002. Estuarine flooding and managed retreat. In: *Proceedings of “Flood risk in a changing climate”*. *Philosophical Transactions of the Royal Society of London A* 360 (1796), p. 1477.
- Tsuchiya, Y., Kawata, Y., 1986. Historical study of changes in storm surge disasters in the Osaka Area. *Natural Disaster Science* 8 (2) 1-18.
- Turner, R.E., Baustian, J.J., Swenson, E.M., Spicer, J.S., 2006. Wetland Sedimentation from Hurricanes Katrina and Rita. *Science* 314, 449–452.
- Valle-Levinson, A., Olabarrieta, M., Valle, A., 2013. Semidiurnal perturbations to the surge of Hurricane Sandy. *Geophysical Research Letters* 40, 2211–2217, doi:10.1002/grl.50461

- van Rijn, L.C., 2011. Coastal erosion and control. *Ocean and Coastal Management* 54, 867–887.
- Verlaan, M., Zijderveld, A., de Vries, H., Kroos, J., 2005. Operational storm surge forecasting in the Netherlands: developments in the last decade. *Philosophical Transactions of the Royal Society* 363, 1441–1453.
- Vested, H.J., Jensen, H.R., Petersen, H.M., Jørgensen, A.-M., Machenhauer, B., 1992. An operational hydrographic warning system for the North Sea and the Danish Belts. *Continental Shelf Research* 12 (1), 65–81.
- Vinet, F., Lumbroso, D., Defossez, S., Boissier, L., 2012. A comparative analysis of the loss of life during two recent floods in France: the sea surge caused by the storm Xynthia and the flash flood in Var. *Natural Hazards* 61, 1179–1201.
- von Storch, H., Gönner, G., Meine M., 2008. Storm surges – An option for Hamburg, Germany, to mitigate expected future aggravation of risk. *Environmental Science & Policy* II, 735–742.
- von Storch, H., Reichardt, H., 1997. A scenario of storm surge statistics for the German Bight at the expected time of doubled atmospheric carbon dioxide concentration. *Journal of Climate* 10, 2653–2662.
- Vousdoukas, M.I., Voukouvalas, E., Annunziato, A., Giardino, A., Feyen, L., 2016. Projections of extreme storm surge levels along Europe. *Climate Dynamics*, DOI 10.1007/s00382-016-3019-5
- Waeles, B., Bertin, X., Chevaillier, D., Breilh, J.-F., Li, K., Le Mauff, B., 2016. Limitation of high water levels in bays and estuaries during storm flood events. In: Gourbesville, P., Cunge, J.A., Caignaert, G. (Eds.), *Advances in Hydroinformatics, SIMHYDRO 2014*, pp. 439–449.
- Wahl, T., Jain, S., Bender, J., Meyers, S.D., Luther, M.E., 2015. Increasing risk of compound flooding from storm surge and rainfall for major US cities. *Nature Climate Change*, 5 (12), 1093–1097.
- Walsh, J.P., Corbett, R., Mallinson, D., Goni, M., Dail, C., Loewy, K., Marciniak, K., Ryan, C., Smith, A., Stevens, B., Sumners, Tesi, T., 2006. Mississippi delta mudflow activity and 2005 Gulf hurricanes. *EOS Transactions AGU* 87 (44), 477–478.
- Walsh, J.P., Corbett, D.R., Kiker, J., Orpin A., Hale, R., Ogston, A., 2014. Spatial and temporal variability in sediment deposition and seabed character on the Waipaoa River margin, New Zealand. *Continental Shelf Research* 34, 85–102.
- Wang, P., Horwitz, M.H., 2007. Erosional and depositional characteristics of regional overwash deposits caused by multiple hurricanes. *Sedimentology* 54, 545–564.
- Wanner, H., Beer, J., Bütikofer, J., Crowley, T.J., Cubasch, U., Flückiger, J., Goosse, H., Grosjean, M., Joos, F., Kaplan, J.O., Küttel, M., Müller, S.A., Prentice, I.C., Solomina, O., Stocker, T.F., Tarasov, P., Wagner, M., Widmann, M., 2008. Mid- to Late Holocene climate change: an overview. *Quaternary Science Reviews* 27 (19–20), 1791–1828.
- Wanner, H., Solomina, O., Grosjean, M., Ritz, S.P., Jetel, M., 2011. Structure and origin of Holocene cold events, *Quaternary Science Reviews* 30 (21–22), 3109–3123.

- Wheatcroft, R.A., Drake, D.E., 2003. Post-depositional alteration and preservation of sedimentary event layers on continental margins, I. The role of episodic sedimentation. *Marine Geology* 199, 123–137.
- Wheatcroft, R.A., Wiberg, P.L., Alexander, C.R., Bentley, S.J., Drake, D.E., Harris, C.K., Ogston, A.S., 2007. Post-depositional alteration and preservation of sedimentary strata. In: Nittrouer, C., Austin, J., Field, M., Kravitz, J. & Wiberg, P. (eds.), *Continental Margin Sedimentation: From Sediment Transport to Sequence Stratigraphy*. Blackwell Publishing, Boston, pp. 101-156.
- Weber, N., Chaumillon, E., Tesson, M., Garland, T., 2004a. Architecture and morphology of the outer segment of a mixed tide and wave-dominated incised valley, revealed by HR seismic reflection profiling: The paleo-Charente River, France. *Marine Geology* 207, 17–38.
- Weber, N., Chaumillon, E., Tesson, M., 2004b. Enregistrement de la dernière remontée du niveau marin dans l'architecture interne d'une vallée incisée : Le Pertuis Breton (Charente-Maritime). *C.R. Geoscience* 336, 1273–1282.
- Welander, P., 1961. Numerical Prediction of Storm Surges, *Advances in Geophysics*, 8 (C), 315-379.
- Weill, P., Tessier, B., Mouazé, D., Bonnot-Courtois, C., Norgeot, C., 2012. Shelly cheniers on a modern macrotidal flat (Mont-Saint-Michel bay, France). Internal architecture revealed by ground-penetrating radar. *Sedimentary Geology* 279, 173–186.
- Weill, P., Mouazé, D., Tessier, B., 2013. Internal architecture and evolution of bioclastic beach ridges in a megatidal chenier plain: Field data and wave flume experiment. *Sedimentology* 60, 1213–1230.
- Werner, M., Cranston, M., Harrison, T., Whitfield, D., Schellekens, J., 2009. Recent developments in operational flood forecasting in England, Wales and Scotland. *Meteorological Applications* 16 (1), 13–22.
- Wheeler, A.J., Oldfield, F., Orford, J.D., 1999. Depositional and post-depositional controls on magnetic signals from saltmarshes on the north-west coast of Ireland. *Sedimentology* 46 (3), 545-558.
- Williams, H.F.L., Flanagan, W.M., 2009. Contribution of Hurricane Rita storm surge deposition to long-term sedimentation in Louisiana coastal woodlands and marshes; *Journal of Coastal Research* SI56, 1671–1675.
- Williams, H.F.L., 2011a. Stratigraphic record of Hurricanes Audrey, Rita and Ike in the Chenier Plain of Southwest Louisiana. *Journal of Coastal Research* SI64, 1921–1926.
- Williams, H.F.L., 2011b. Shell bed tempestites in the Chenier Plain of Louisiana: late Holocene example and modern analogue. *Journal of Quaternary Science* 36 (2), 199–206.
- Wisner, B., Gaillard, J.C., Kelman, I., 2012. Framing disaster: Theories and stories seeking to understand hazards, vulnerability and risk. In: Wisner, B., Gaillard, J.C., Kelman, I. (Eds.), *The Routledge Handbook of Hazards and Disaster Risk Reduction*, Routledge, London, pp. 18-34.



- Wolf, J., 1978. Interaction of tide and surge in a semi-infinite uniform channel, with application to surge propagation down the east coast of Britain. *Applied Mathematical Modelling* 2, 245–253.
- Wolf, J., Flather, R.A., 2005. Modelling waves and surges during the 1953 storm. *Philosophical Transactions of the Royal Society A: Mathematical, Physical and Engineering Sciences* 363, 1359–1375.
- Woodruff, J., Donnelly, J.P., Mohrig, D., Geyer, W.R., 2008a. Reconstructing relative flooding intensities responsible for hurricane-induced deposits from Laguna Playa Grande, Vieques, Puerto Rico. *Geology* 36 (5), 391–394.
- Woodruff, J.D., Donnelly, J.P., Emanuel, K., Lane P., 2008b. Assessing sedimentary records of paleohurricane activity using modeled hurricane climatology. *Geochemistry Geophysics Geosystems* 9 (9), 1–12.
- Wöppelmann, G., Pouvreau, N., Simon, B., 2006. Brest sea level record: a time series construction back to the early eighteenth century. *Ocean Dynamics* 56, 487–497.
- Xu, K.H., Mickey, R.C., Chen, Q.J., Harris, C.K., Hetland, D., Hu, K., Wang, J., 2016. Shelf Sediment Transport during Hurricanes Katrina and Rita. *Computers & Geosciences* 90, 24–39.
- Zaninetti, J.M., 2013. Catastrophe et adaptation sur le littoral du Mississipi. *Annales de géographie* 692, 445–465.
- Zhang, Y., Baptista, A.M., 2008. SELFE: A semi-implicit Eulerian-Lagrangian finite-element model for cross-scale ocean circulation. *Ocean Modelling* 21(3-4), 71–96.
- Zhang, H., Sheng, J., 2013. Estimation of extreme sea levels over the eastern continental shelf of North America. *Journal Geophysical Research: Ocean* 118, 6253–6273.
- Zhao, C., Ge, J., Ding, P., 2014. Impact of sea level rise on storm surges around the Changjiang Estuary. *Journal of Coastal Research* 68, 27–34.

Figure captions-

Fig. 1- Locations maps of places mentioned in the text. The seaward boundary of the continental shelf is indicated thanks to the 200 m isobaths.

Fig. 2- Maximum water levels (as indicated in the color bar) computed during Xynthia (colorscale), showing that the model reasonably reproduces the observed extension of the flooding (red line), with the notable exception of several small areas located along the shoreline (modified from Bertin et al., 2014).

Fig. 3 - Snapshots of the simulation of overtopping and flooding in Gâvres during the Johanna storm (situations at 04h00 and 6h30 UTC, March 11 2008) with the reported flooded buildings and stagnation area according to the municipality (modified from Le Roy et al. 2015).

Fig. 4 - Snapshot of the free-surface elevation and barrier topography at Santa Rosa Island simulated with X-Beach during hurricane Ivan (adapted from McCall et al., 2010).

Fig. 5 – Number of damages per year (damages definition is given in the text) due to marine floods from 1800 to 2010 (in red) compared to the number of tide levels higher than 7,25 m at Brest tide-gauge (in blue), with reference to the lowest astronomical tide (0 m). High tide level variations are related to the 18.6-year tidal cycle. Years with highest tidal range are characterized by an increasing number of flood-induced damages.

Fig. 6 - The various types of storm surge sedimentation processes and contexts.

Fig. 7 - Synthetic sequences of various sequences of storm surge-related depositional intervals in various settings (from data of the literature). See text for explanations.

Fig. 8 - An example of washover deposits (Gatseau Spit, southern Oléron Island, location in Figure 1). A. Photograph of the deposits. Note the presence of a general planar lamination with rippled intervals (oblique foresets, arrow) and bent plants at the base of the deposit. Visibly pronounced laminations are underlined with concentrations of heavy minerals. B. Core OW2 from the same location. Left: lithologic section; middle: photograph of the core section; right: X-radiograph of the core. X-ray examination allows the reconnaissance of more detailed structures that are not visible by direct observation of the core.

Fig. 9 – Modified from Dezileau et al., 2011. Location of cores in Pierre Blanche and Prevost lagoons (upper panel). Grain-size distribution of the eight cores, sampled in the Pierre Blanche and Prevost lagoons, showing three storm-related sand deposits (Coarse grained event layers – CGE) with interpolated ages of 1742, 1848 and 1893 A.D.

Fig. 10 – Modified from Sorrel et al., 2012: North Atlantic climate records, the solar forcing and the HSPs during the late Holocene. (a) HSPs. (d) IRD stack series of four drillings (MC52; MD29191CMC21; GGC22; ref. 1; grey) and the 1,500-year period (red). (e) Water density difference (stratification increases upwards) between *Globorotalia bulloides* and *G. inflata* (grey) with three-point running means (black) and the 1,500-year period (red; ref. 21). (f) Detrended temperature anomalies from core ODP 658C (grey) and the 1,500-year period (red; ref. 23). (g) Smectite/(illite-chlorite) ratio in the northwest Mediterranean Sea<sup>25</sup>. Grey shading highlights the match between the HSPs and North Atlantic climate and TSI records across the key intervals.

Fig. 11 – Sediment record of the recent storm clustering of winter 2013-2014. The two upper panels show the morphological evolution of the Gatseau Spit (southern part of the Oléron Island, French Atlantic Coast) from 2010 to 2014. The fast erosion rate is associated with washovers, emplaced during the winter 2013-2014. The lower left panel shows a post-event trench in the northern washover (red star in upper right panel), where three main sedimentary units can be observed. Those 3 units are interpreted as

recording three main overwashes, related to three storms that occurred during high spring tides (06/01/2014, 02/02/2014, 03/03/2014). The lower right panel shows the modeled maximum runup for the entire winter 2013-2014 using the empirical formula of Stockdon et al., (2006). Three main overwashes are evidenced with water levels higher than the barrier elevation at the location of the orange star (in upper right panel).

Fig. 12 - Illustration of the uncertainties associated to the evaluation of return periods using short data records. The return periods were computed using 20 and 131 years of data from the Brest tide gauge (location in Fig. 1). Data were previously detrended to remove the sea level rise signal. The adjustment of "Generalized Extreme Value" distributions to different years of data shows discrepancies of the order of 10 cm.

Figure 13 – Comparison between plausible storm surges obtained from numerical simulations (red curve) and storm surges recorded from tide gauge at Brest (black dashed curve). The observed storm surge peak occurred on the 23 December of 2013. The plausible storm surges have been obtained after synchronizing the storm surge peak that occurred on the 23 December of 2013 with the high spring tide that occurred on the 3 January of 2014 (lower blue dotted curves); the high tide was at 05:06 UTC.

Fig. 14 - Finite element computational grid covering the Mediterranean Sea. This grid is used to forecast the sea level along the Italian Adriatic coast.

Fig. 15 - Surge obtained from observations (OBS) near Venice, compared with the model's forecast without (BACK) and with data assimilation (ASS). The data assimilation window is displayed with two vertical red lines. This severe storm happened on January 2010.

Fig. 16 – Comparison between predicted potential flooding zones (red and pink, from the Atlas of Flood Zones, SOGREAH, 2002) and observed flooding areas caused by the Xynthia storm (blue hatched) in the Bay of Bourgneuf (Location in Fig. 1).

Fig. 17 - Vulnerability index used by the fire and rescue department of Charente-Maritime (SDIS 17) taking into account the type of construction (above) and the potential water level inside the constructions in case of Marine flooding (below). Modified from Chevillot-Millot et al., 2013.

Fig. 18 – Sketch showing the V.I.E. Index methodology. The V.I.E. Index (FloodVulnerability Index) depends on four criteria, including the water level, the sea-flood protections, the architectural typology, the proximity of a refuge place (Cr1 to Cr4). The four criteria and the score are listed in the upper part of the figure, the formula of the index and the vulnerability score are presented in the lower of the figure (modified from Creach et al., 2015).

Table 1 - Effect of data gaps on the evaluation of return periods of extreme sea levels. Water levels associated with different return periods were evaluated following the approach of Fortunato et al. (2013) using 116 years of hourly data from the Brest tide gauge. Different fractions of random daily gaps were artificially introduced in the data, and the procedure was repeated 10 times for each fraction. Results show how the extreme sea level decreases and the uncertainty increases with the fraction of gaps.

| Return period (years) | Sea levels (cm, relative to Hydrographic Zero) and standard deviations (cm) |          |          |          |          |          |          |
|-----------------------|---|----------|----------|----------|----------|----------|----------|
|                       | No gaps   | 10% gaps |          | 20% gaps |          | 30% gaps |          |
|                       |   | Mean     | St. dev. | Mean     | St. dev. | Mean     | St. dev. |
| 20                    | 809   | 808      | 0.2      | 807      | 0.4      | 806      | 0.2      |
| 50                    | 818   | 817      | 0.3      | 816      | 0.5      | 815      | 0.3      |
| 100                   | 825   | 823      | 0.5      | 822      | 0.8      | 821      | 0.4      |
| 1000                  | 847   | 846      | 1.1      | 844      | 2.1      | 843      | 1.7      |

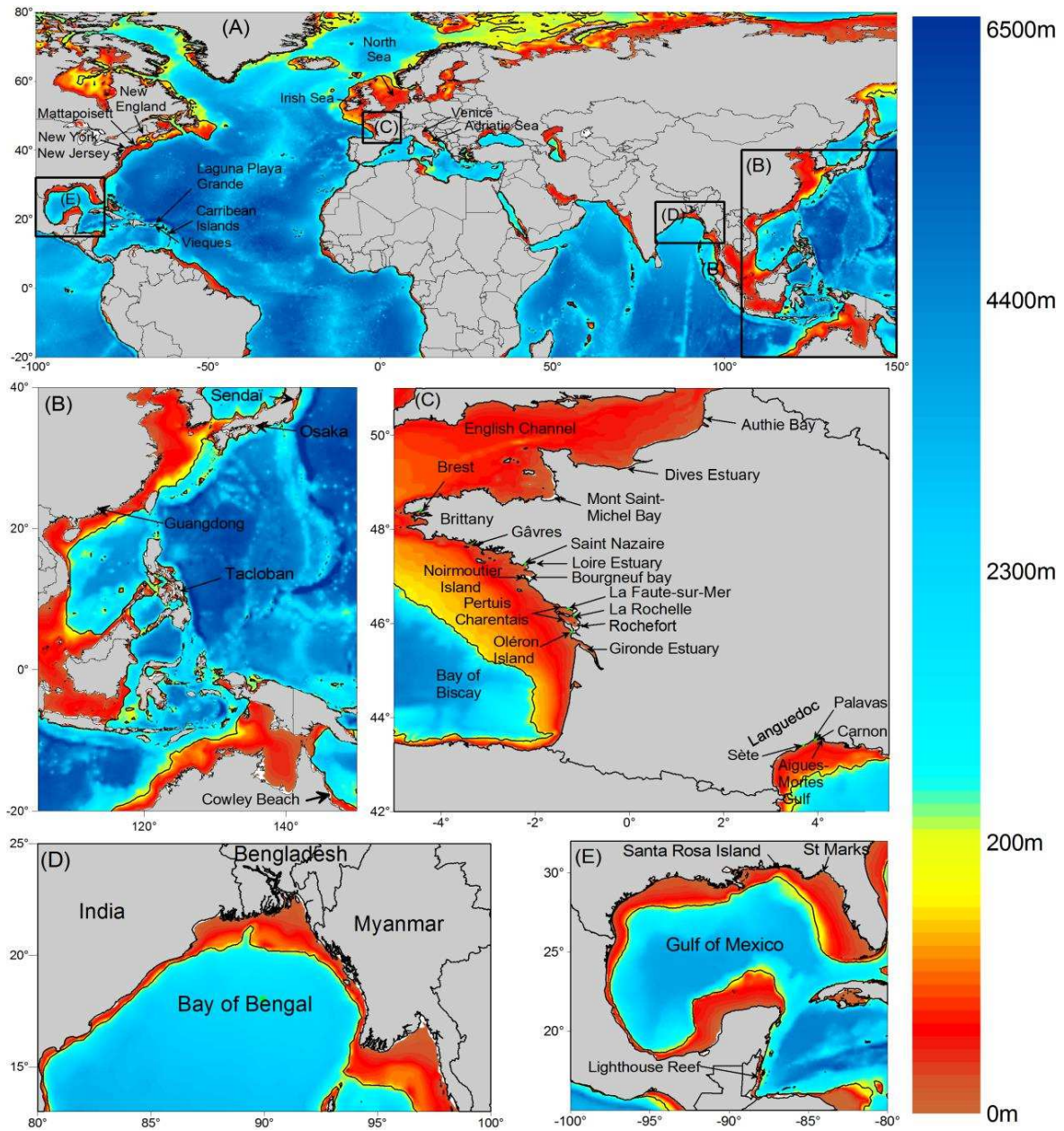


Fig. 1

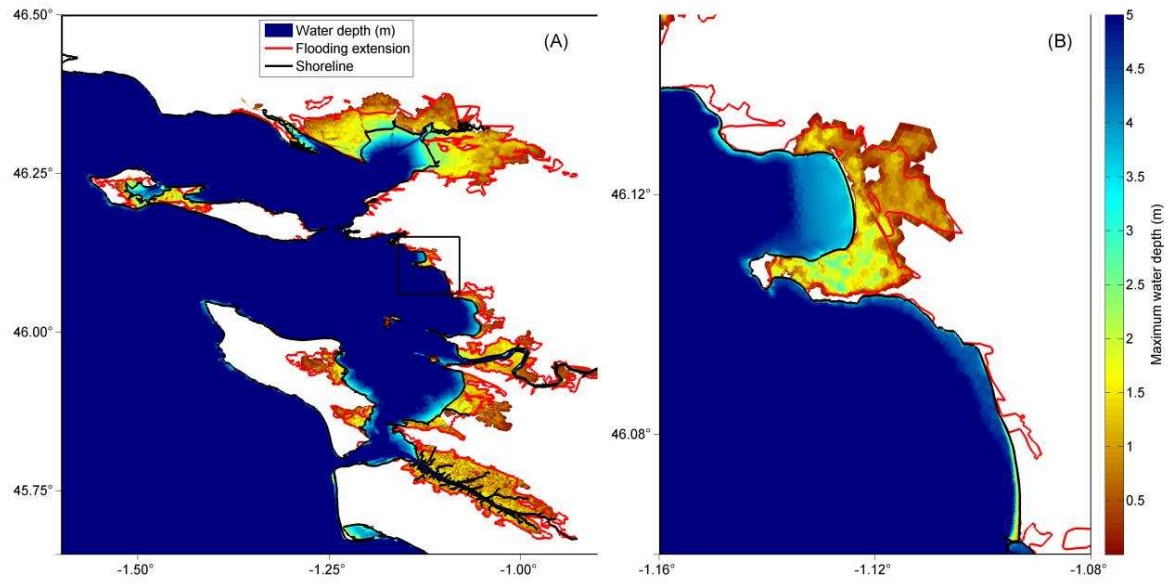


Fig. 2



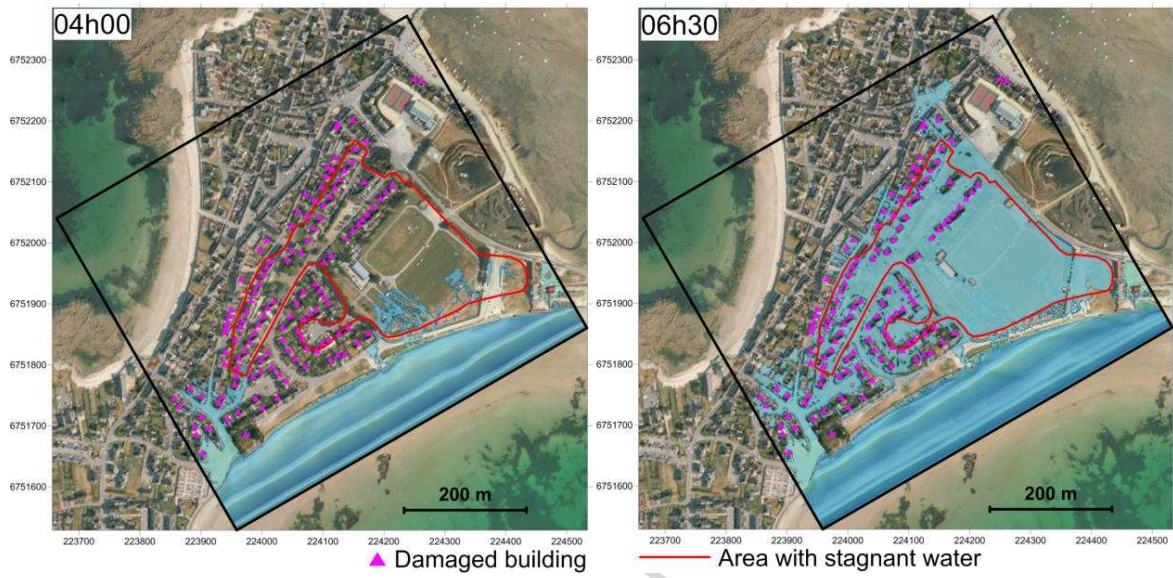


Fig. 3



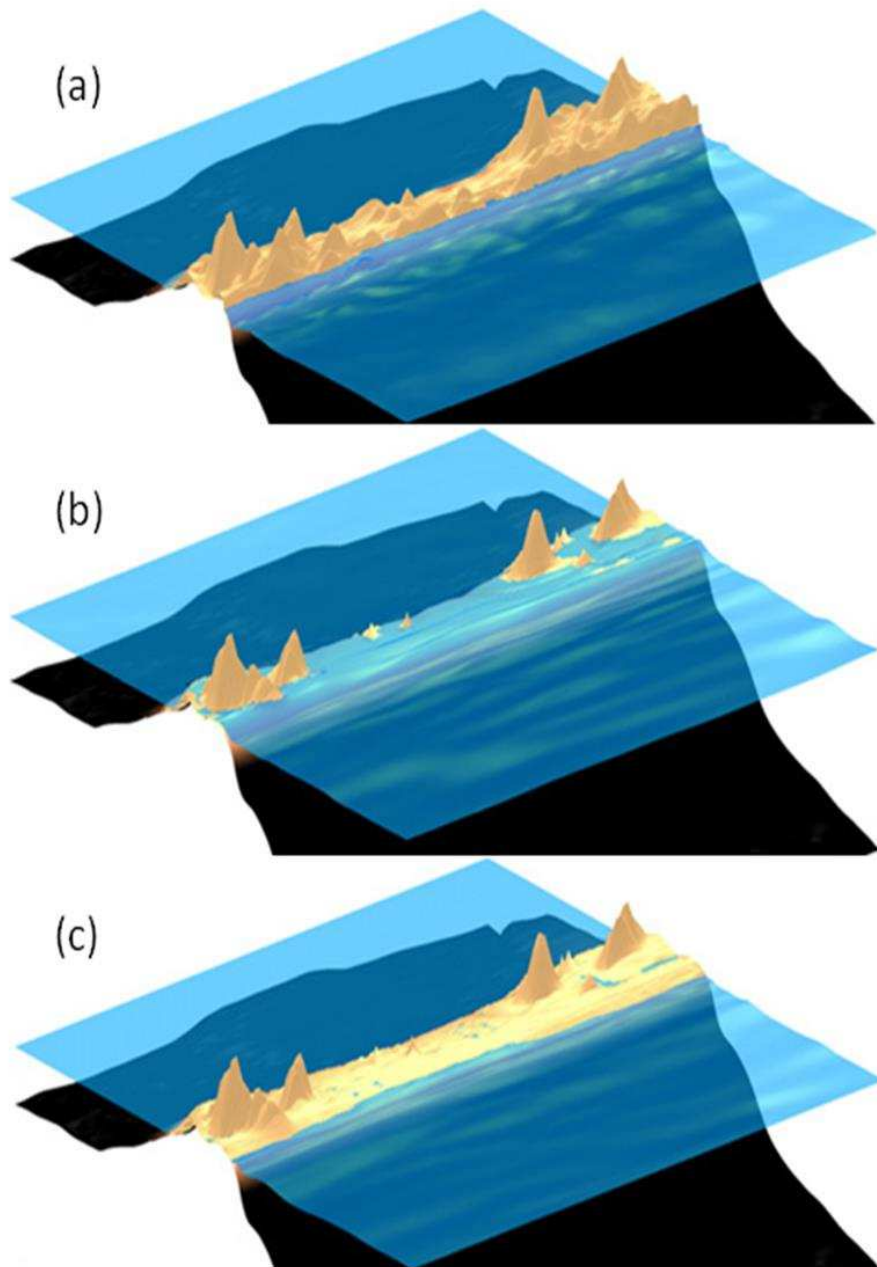


Fig. 4

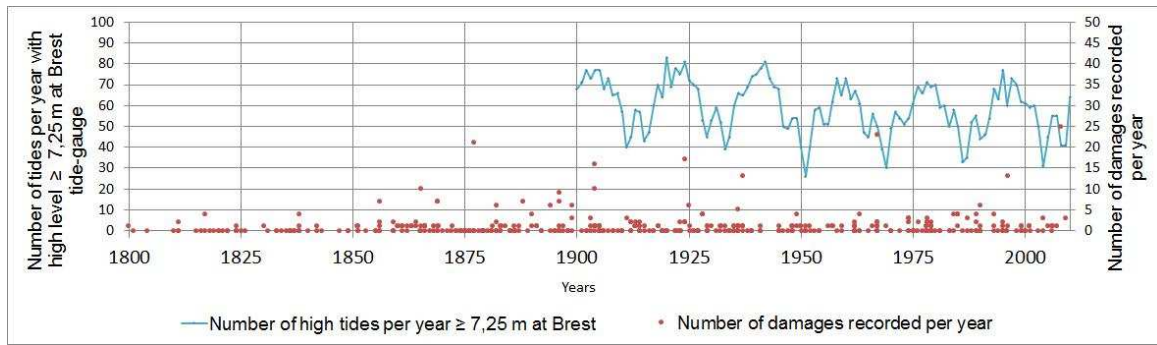


Fig. 5

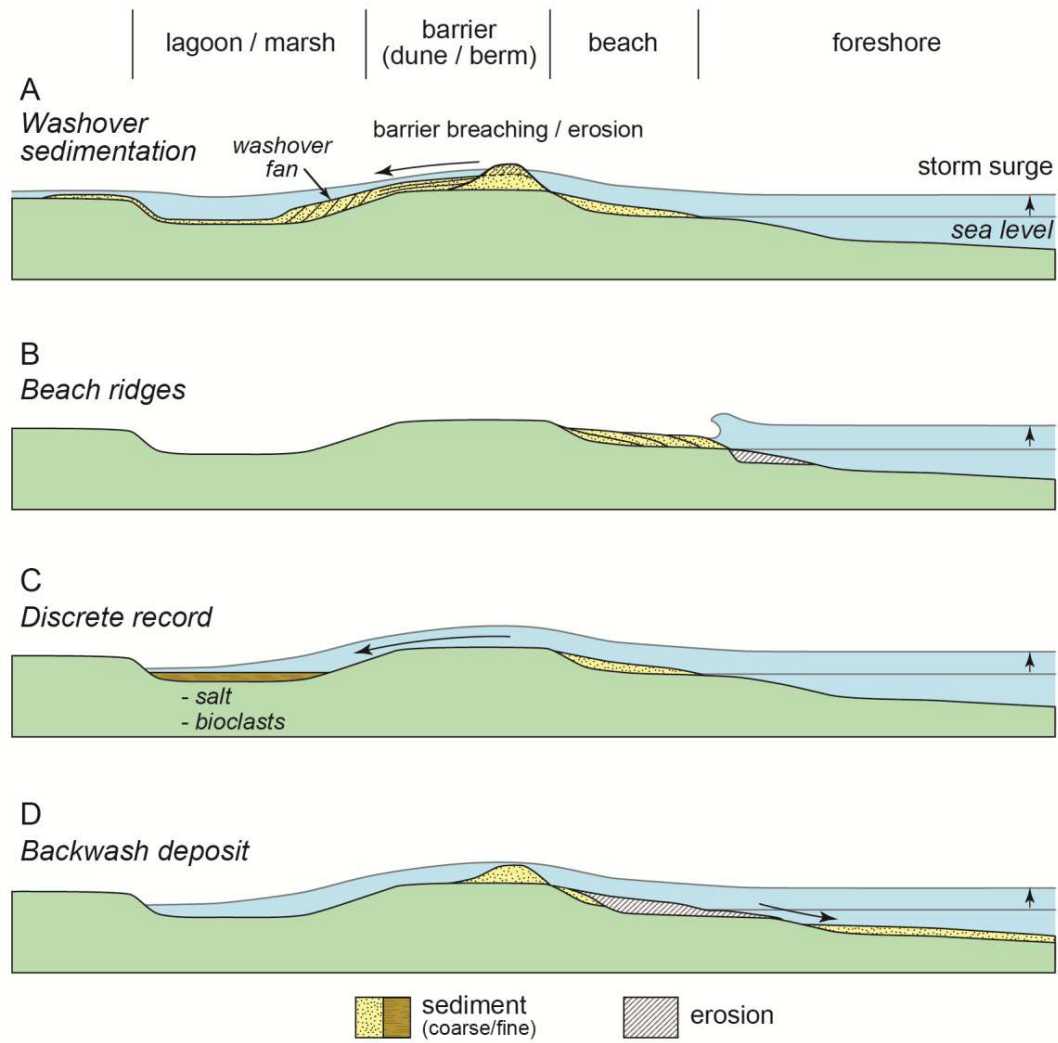


Fig. 6

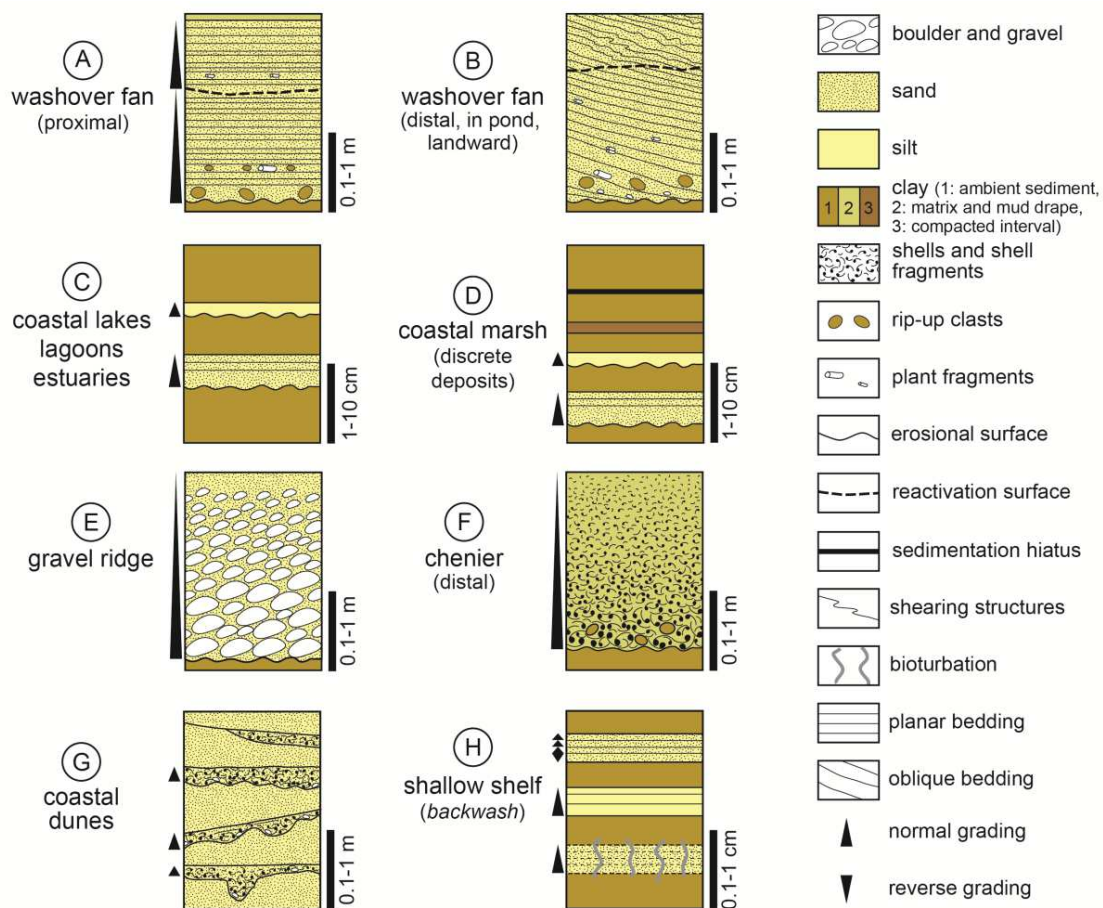


Fig. 7

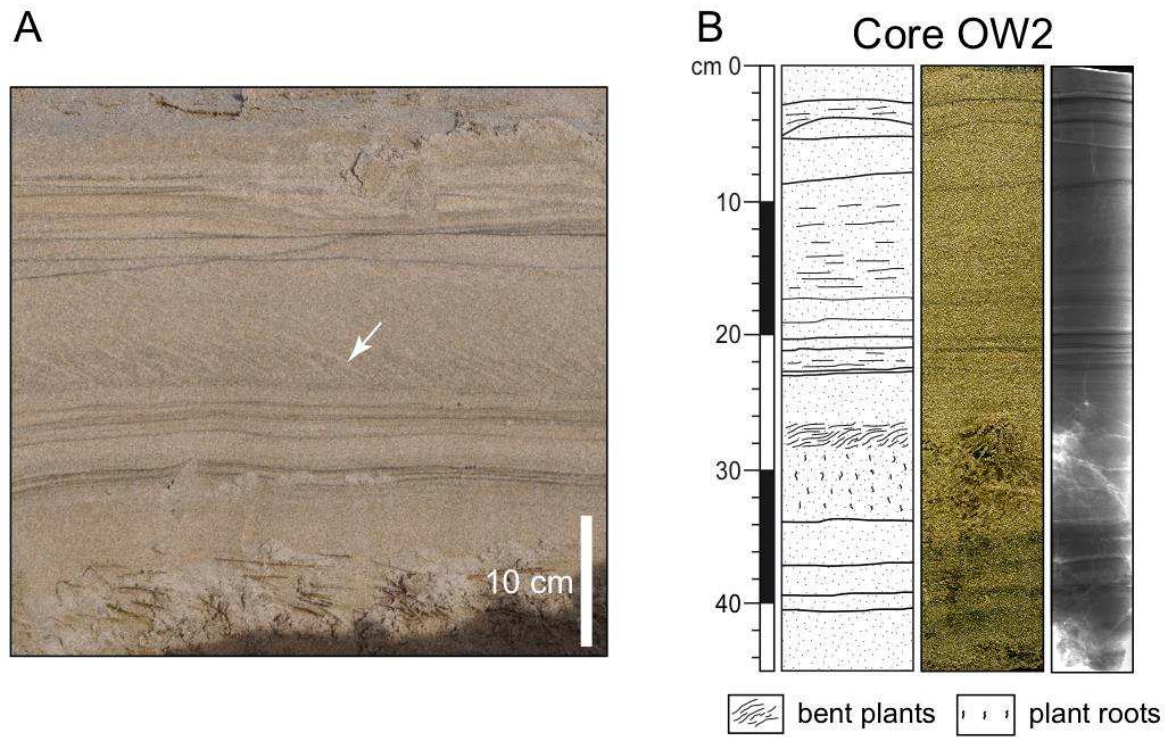


Fig. 8



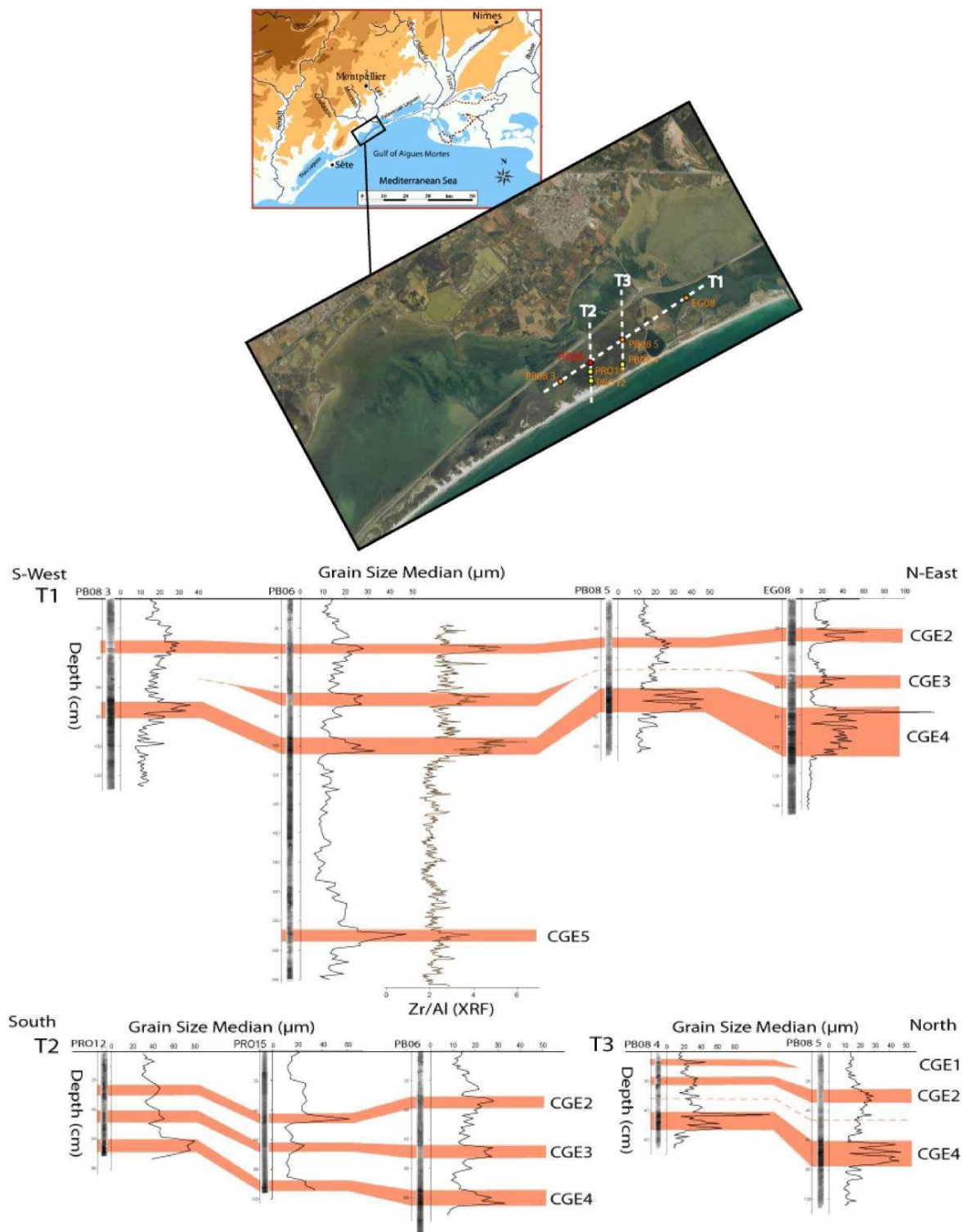


Fig. 9

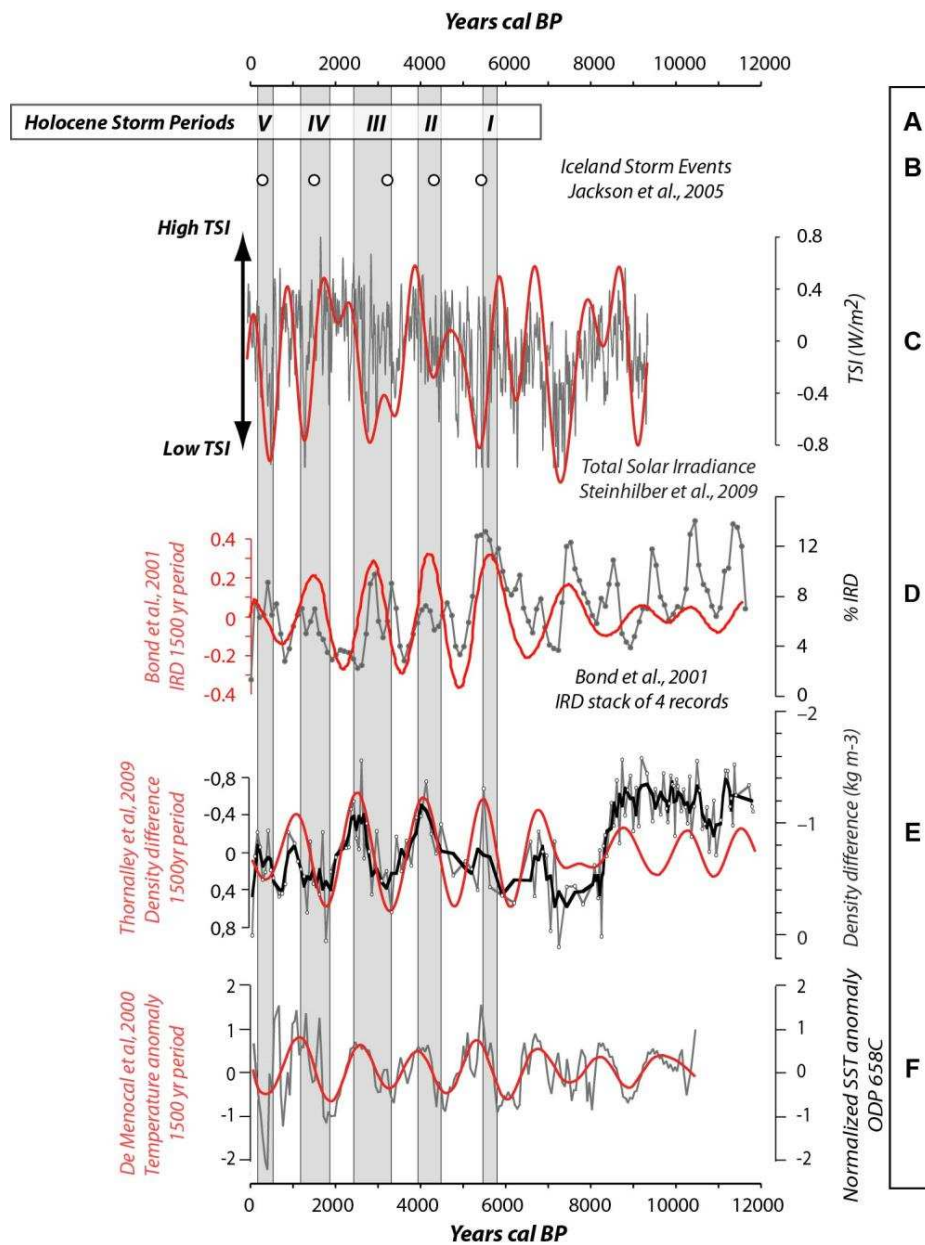


Fig. 10

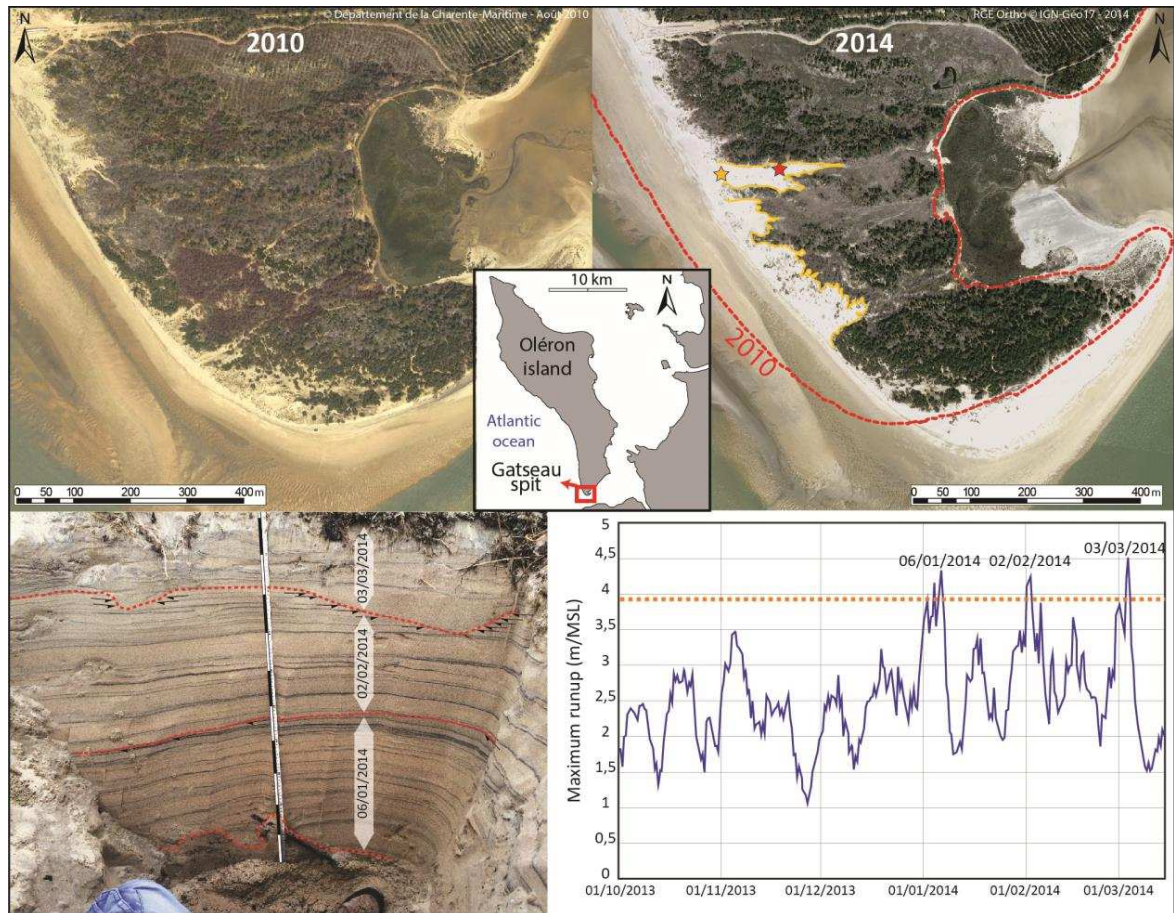


Fig. 11



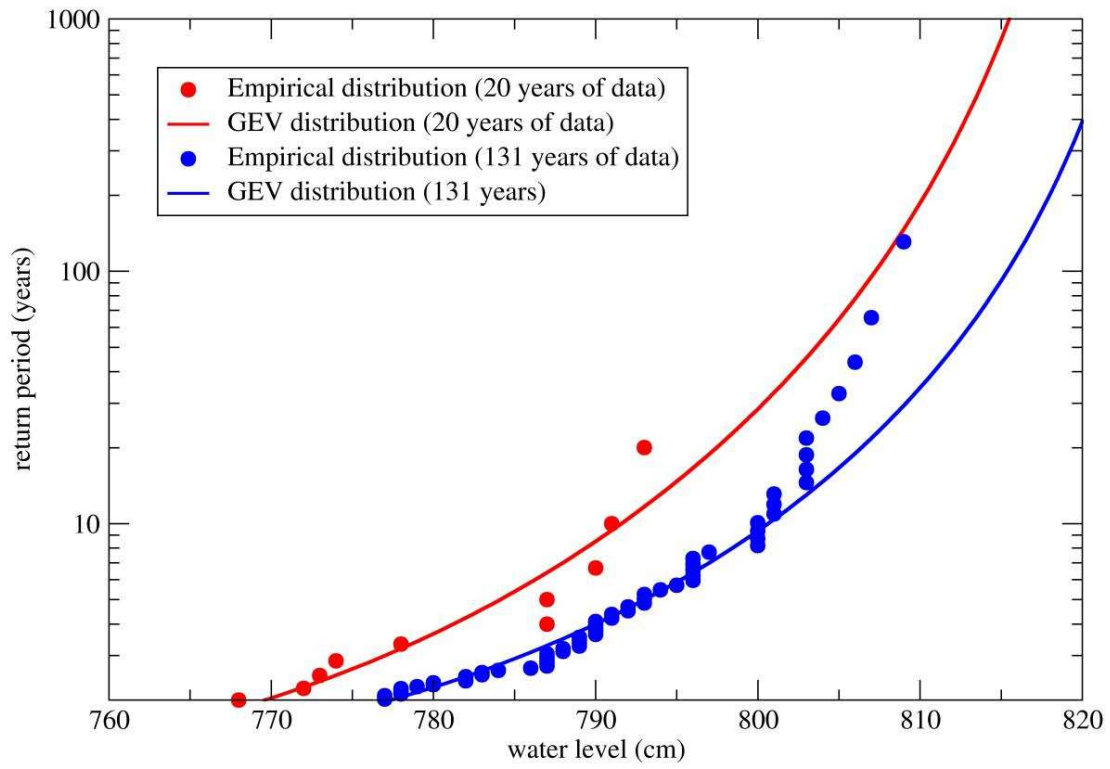


Fig. 12

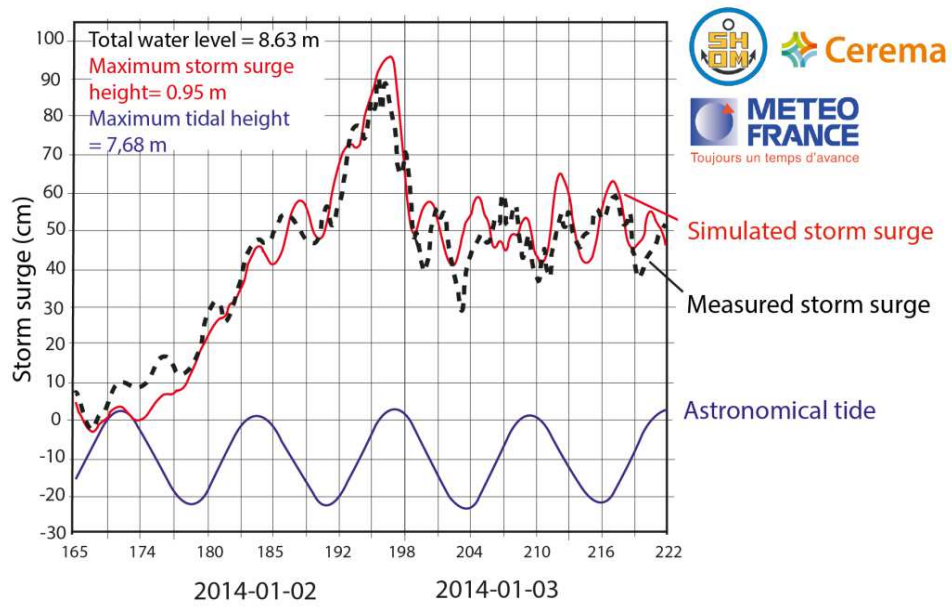


Fig. 13

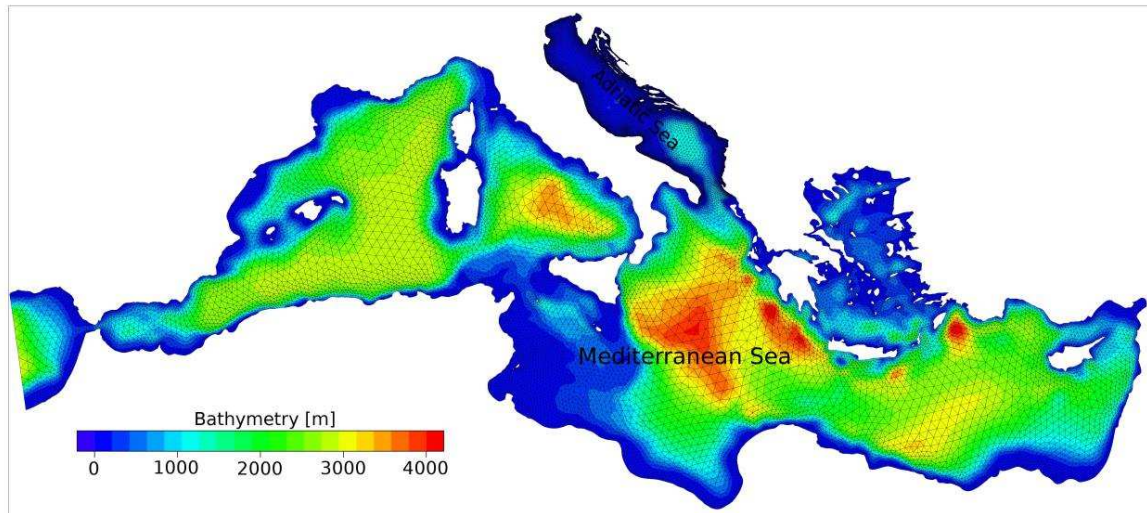


Fig. 14

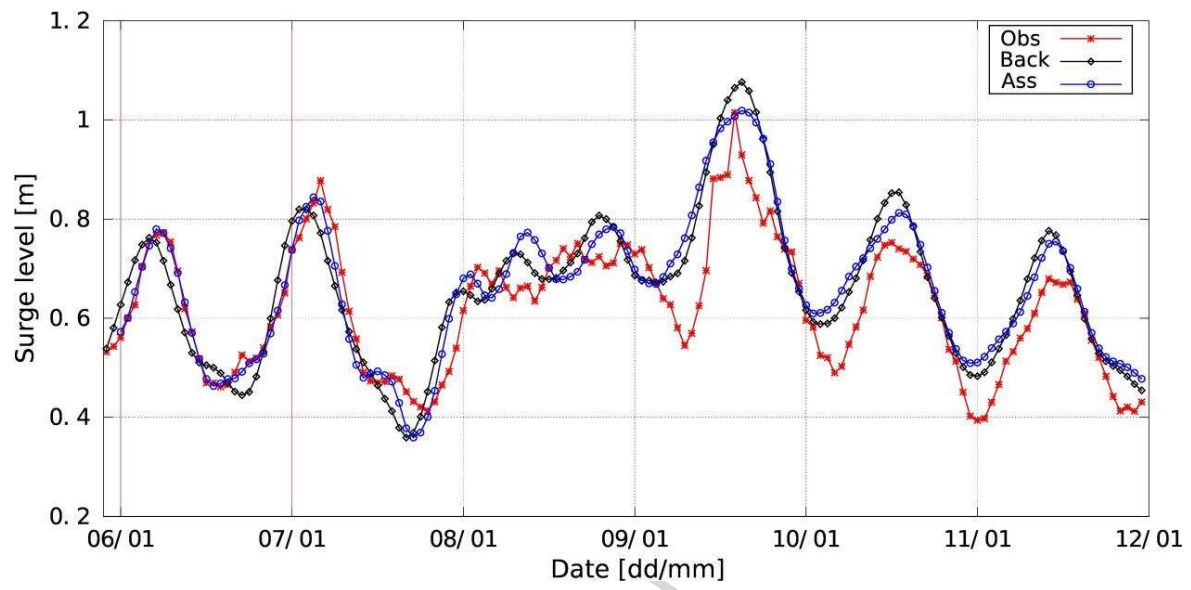


Fig. 15

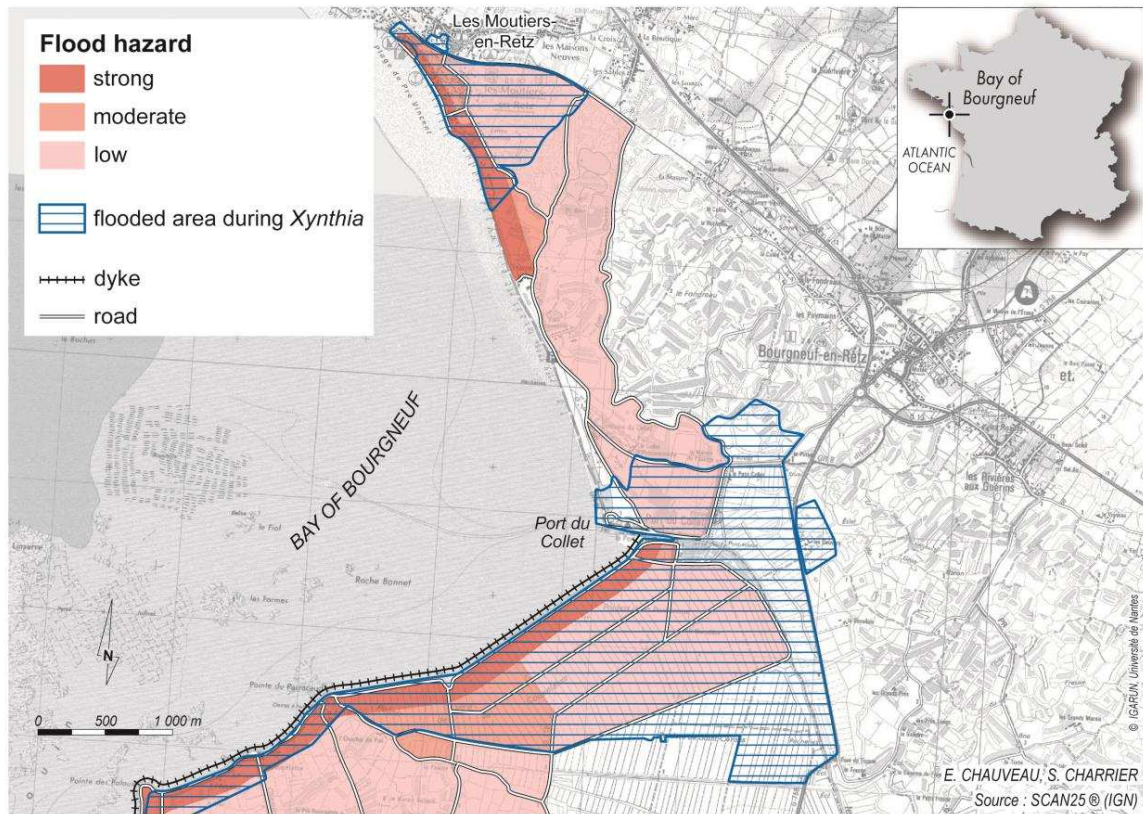


Fig. 16

## Vulnerability Index

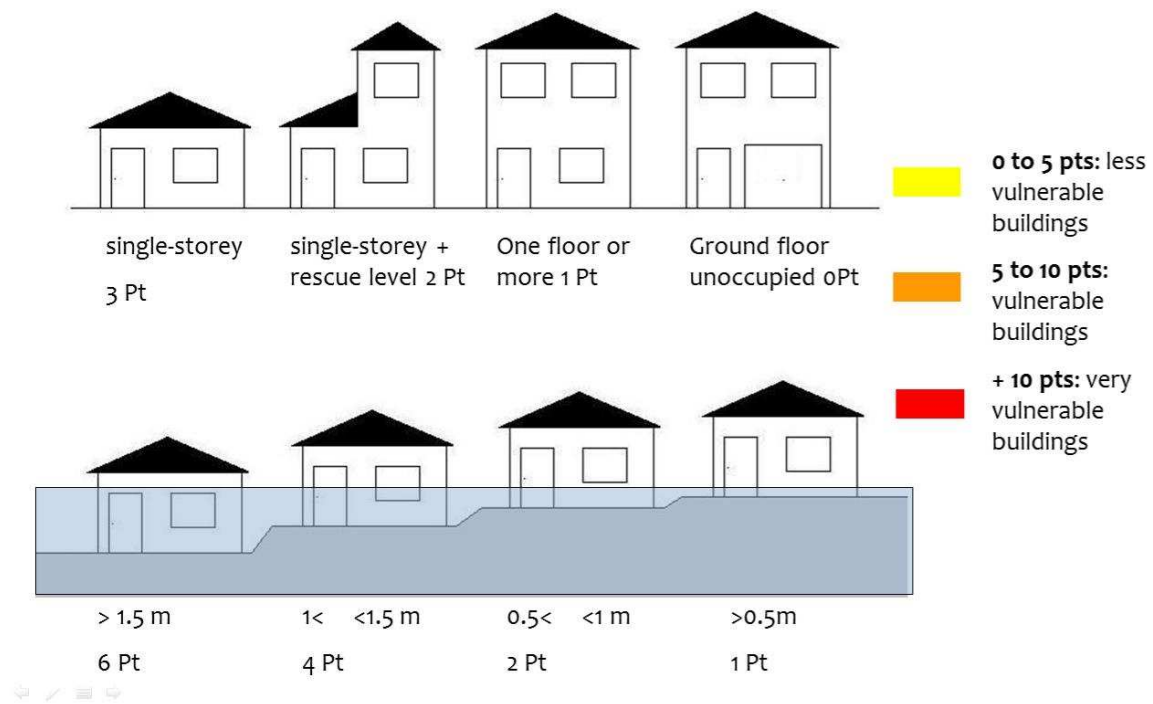


Fig. 17



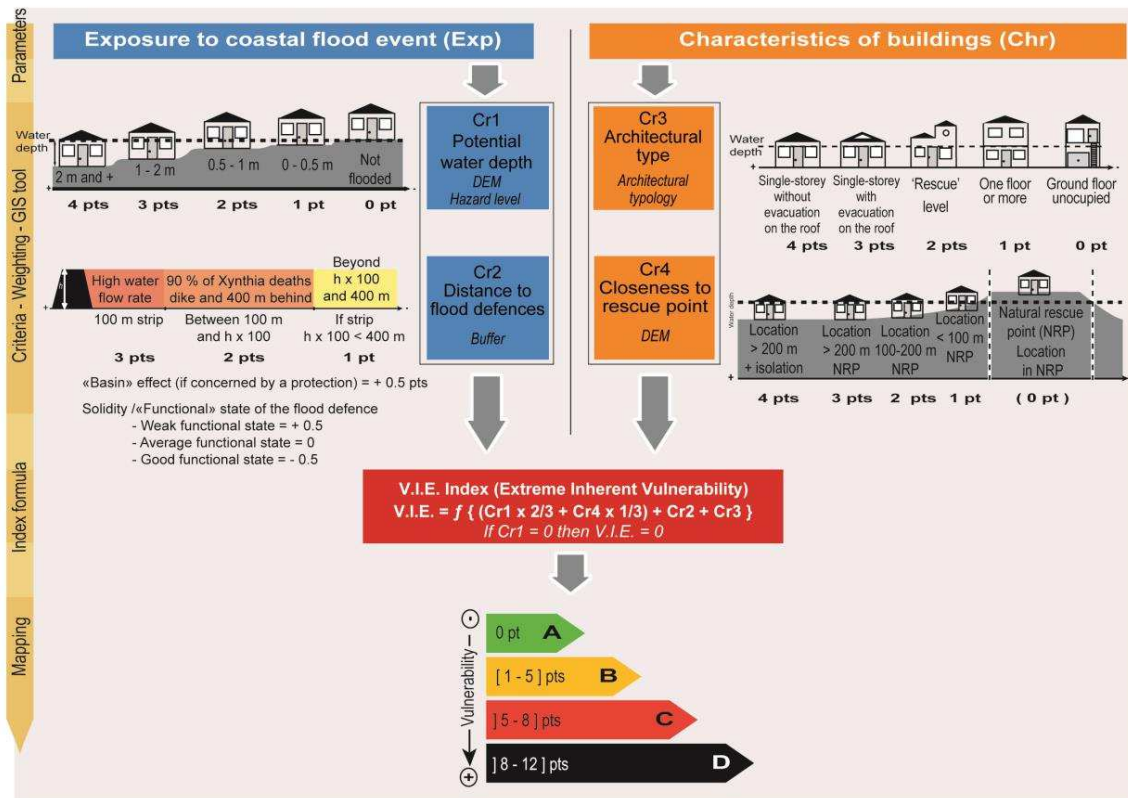


Fig. 18

Table 2 - Effect of data gaps on the evaluation of return periods of extreme sea levels. Water levels associated with different return periods were evaluated following the approach of Fortunato et al. (2013) using 116 years of hourly data from the Brest tide gauge. Different fractions of random daily gaps were artificially introduced in the data, and the procedure was repeated 10 times for each fraction. Results show how the extreme sea level decreases and the uncertainty increases with the fraction of gaps.

| Return period (years) | Sea levels (cm, relative to Hydrographic Zero) and standard deviations (cm) |          |          |          |          |          |          |
|-----------------------|---|----------|----------|----------|----------|----------|----------|
|                       | No gaps   | 10% gaps |          | 20% gaps |          | 30% gaps |          |
|                       |   | Mean     | St. dev. | Mean     | St. dev. | Mean     | St. dev. |
| 20                    | 809   | 808      | 0.2      | 807      | 0.4      | 806      | 0.2      |
| 50                    | 818   | 817      | 0.3      | 816      | 0.5      | 815      | 0.3      |
| 100                   | 825   | 823      | 0.5      | 822      | 0.8      | 821      | 0.4      |
| 1000                  | 847   | 846      | 1.1      | 844      | 2.1      | 843      | 1.7      |